THE FORMATION OF GOLD-BEARING QUARTZ VEINS IN NOVA SCOTIA: HYDRAULIC FRACTURING UNDER CONDITIONS OF GREENSCHIST REGIONAL METAMORPHISM DURING EARLY STAGES OF DEFORMATION

by

Milton C. Graves

Submitted in partial fulfilment of the requirements for the degree of Master of Science at Dalhousie University, Halifax, Nova Scotia, June, 1976.

DALHOUSIE UNIVERSITY

Date September 21, 1976

Author Milton Charles Graves

Title The formation of gold-bearing quartz veins in Nova Scotia: hydraulic fracturing under conditions of greenschist regional metamorphism during early stages of deformation

Department or School Geology

Degree M.Sc. Convocation Fall Year 1976

Permission is herewith granted to Dalhousie University to circulate and to have copied for non-commercial purposes, at its discretion, the above title upon the request of individuals or institutions.

Signature of Author

TABLE OF CONTENTS

ABSTRACT

The study of fluid inclusions and the analyses of mineral phases in the Fe-As-S system allow temperatures and pressures to be estimated at 432° ± 60°C and 2.3 ± 1.0 kilobars for the crystallization of groups of quartz-carbonate-arsenopyrite veins which are concordant with the bedding of the flyschoid Meguma Group (Cambro-Ordovician) of Southern Nova Scotia. The bedding and the enclosed veins are deformed by upright folds with northeast-trending axial-plane slaty cleavage defined by greenschist-grade regional metamorphic minerals. The vein mineral assemblages were in equilibrium with the greenschist assemblages. The formation of veins by "open-space" filling followed by regional F_1 folding ending with the fixing of slaty cleavage appear to have occurred during the regional metamorphism to greenschist grade and under a relatively homogeneous strain regime. Emplacement of Devonian plutons, small-scale kink folding, and faulting occurred later and under a different strain regime.

Microprobe analysis of arsenopyrites (32.1 ± 0.9 mean atomic percent arsenic) from seventeen groups of veins indicate a temperature of crystallization of 432° ± 60°C. No trends of composition can be ascertained within grains, across or along veins, or between groups of veins. Although the present resolution of the arsenopyrite geothermometer only allows broad temperature estimates, the data obtained in this work may indicate that arsenopyrite crystallization in the veins took place under conditions of relatively constant temperature.

Fluid inclusions in quartz of the veins are two-phase (water as a liquid and carbon dioxide as a vapour). No solid phases were observed. They fall into two populations: one with a very constant vapour-to-liquid ratio (pseudosecondary), which homogenize at 262 ± 10°C and a second population which mainly occur in groups and along planes with varying vapour-to-liquid ratios (secondary) and homogenization temperatures of 210 ± 6°C. If the arsenopyrite crystallized together with the vein quartz at 432 ± 60°C and the pseudosecondary population of inclusions represents the crystallizing fluid, a pressure of 2.3 ± 1.0 kilobars can be estimated.

Hydraulic fracturing could account for the formation of sub-horizontal veins of the observed mineralogy and paragenesis if greenschist grade metamorphic fluid was sufficiently overpressured under conditions of tectonic stress. If the above hypothesis correctly predicts vein formation, the bulk transport of vein constituents including gold and tungsten by means of greenschist grade regional metamorphic dewatering may be an important feature of mineralization in similar terrains.

ACKNOWLEDGEMENTS

I would like to thank Dr. Marcos Zentilli for supervising this project. More importantly, however, I am indebted to him for his stimulating discussions and enthusiasm for geology which have given me the opportunity to address geological problems with a sense of curiosity and a sense of wonder.

I also wish to thank Dr. F. J. (Sam) Sawkins for his help and encouragement in the study of fluid inclusions and for the use of his laboratory facilities at the University of Minnesota in 1973. Mr. Gordon Brown and Professor G. C. Milligan of Dalhousie devised a rapid and effective method of preparing thin polished chips for the fluid inclusion work.

Arsenopyrite analyses were greatly aided by Dr. Ulrich Kretschmar who lent the use of the standards used in his indispensable study of the arsenopyrite geothermometer. Mr. Bob MacKay of Dalhousie University was very patient in helping set up a smooth system of analysis on the electron microprobe.

Discussion with fellow students at Dalhousie has aided in any clarity of ideas that has been attained. I would like especially to thank Dr. Gregor Herb (Sun Oil, Calgary) for discussions about mass dewatering, Dr. Patrick Ryall (University of Penang, Penang, Malaysia), for discussions and technical advise, and Tom Lane and Blaine Hall for geological discussions.

I wish to thank the Izaak Walton Killam Trust for generous financial

support in 1972-73 and 1973-74.

Funds for laboratory and field work have been provided by the Department of Energy, Mines and Resources, Ottawa (Research Agreement 1135-013-4-181/74, 75), the National Research Council of Canada and Dalhousie University, through grants to Dr. M. Zentilli.

CHAPTER I

INTRODUCTION

The gold-bearing quartz vein deposits of southwest Nova Scotia are a distinctly defined metallogenetic unit. Relating the mechanism and time of genesis, and subsequent modification of this unit to the stratigraphic, metamorphic, tectonic and magmatic history of the Meguma platform should be possible by investigating their relationships using techniques of economic geology. Structural style, paragenetic relationships, sulphide assemblages and fluid inclusion characteristics provide time, pressure, and temperature, and chemical constraints modelling the setting and genesis of this metallogenetic unit.

I.1 Geographical setting of the study area

The study area lies between the Atlantic ocean and the Bay of Fundy and is separated from the rest of Nova Scotia by the east-west-trending, tectonostratigraphic discontinuity of the Cobequid-Chedabucto fault zone. The area lies between 43° and 45 $^{1/2°}$ north latitude and between 61° and 66$^{1/2°}$ west longitude (Figure I.1).

This area is circled by all-weather paved provincial highways and is crossed by many all-weather highways. Good gravel roads and numerous woods roads make most of the area readily accessible by automobile and few localities far removed from a road. Connection to international transport

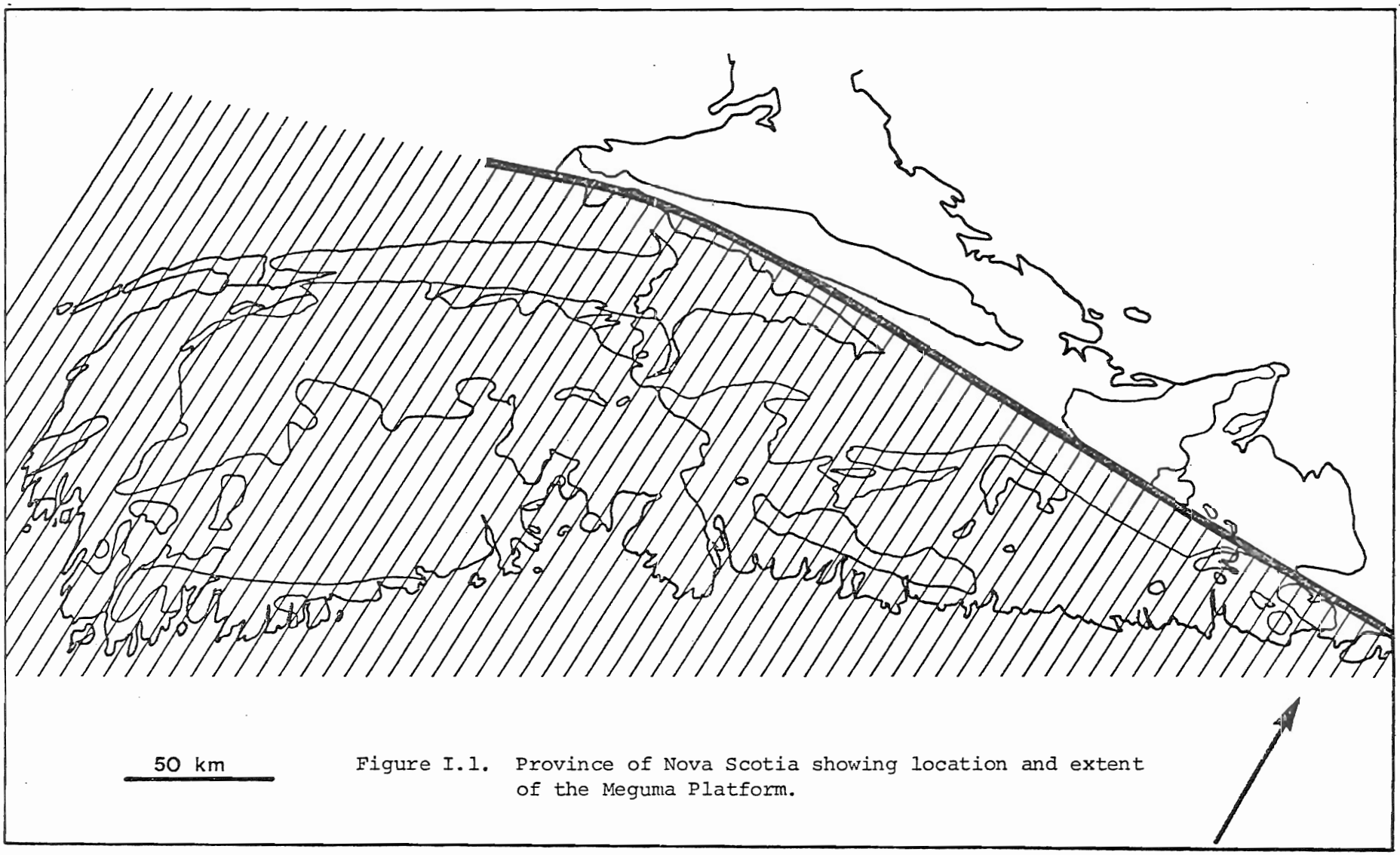

Figure I.1. Province of Nova Scotia showing location and extent of the Meguma Platform.

is through the internation airport and year-round port of Halifax in the centre of the region. Access to the rest of the continent is by air, the Trans-Canada Highway system and rail.

The bulk of the region is a dissected upland underlain by slates, quartzites and granites. The northern edge is a lowland underlain by Carboniferous carbonate and clastic sediments. Along the northwestern border is a 200 km long cuesta of Triassic basalt. Between the cuesta and the upland is the Annapolis Valley, which averages about 8 kilometres in width and is underlain by Triassic clastic rocks.

The climate of the study area is humid and maritime. Average precipitation is 100-140 centimetres with 180-200 centimetres of snow. Humidities are generally above 80 per cent and precipiation is spread evenly throughout the year. Summers are cool, July temperatures averaging 16°C to 19°C, and winters relatively mild with January temperatures averaging -2°C to -8°C. Temperature ranges are not extreme (Putnam, 1940).

Vegetation is dominated by second-growth coniferous forest.

The economy of the study area is dominated by the regional service centre and port of Halifax. The Annapolis Valley and the lowlands underlain by Carboniferous rocks support agriculture based on fruit and vegetable and dairy products. An extensive near-shore fishery is supported on the wide continental shelf. Extensive silviculture is practiced, especially for pulpwood, in the uplands. Gold mining was an important aspect of the

economy in the late nineteenth century and the earliest portion of this century but has been insignificant since 1945. No mines are presently active.

I.2 Regional geological setting of the study area

The gold-bearing quartz veins which were used as sample localities in this study are located within the metasediments of the Meguma Group, which cover about 16,200 square kilometres of southwestern Nova Scotia. The Meguma Group is restricted to a distinct geological province of the Canadian Appalachians hereafter called the Meguma Platform. The Meguma Platform is bounded on the north by the Cobequid-Chedabucto fault zone which separates it from the tectonostratigraphically different terranes of the Cobequid Mountains (Kelly, 1967), the Antigonish Highlands (Benson, 1974) and Southeast Cape Breton (Weeks, 1954). Seaward, on the Scotian Shelf, the Meguma Platform ends under a thick Mesozoic and Cenozoic sedimentary wedge.

The oldest exposed rocks of the Meguma Platform are those of the Meguma Group (Stevenson, 1959 ; Woodman, 1904) which is subdivided into two formations. The Goldenville Formation (Woodman, 1904) is the older and consists dominantly of quartz-rich greywacke and interbedded slate with minor conglomerates, all variously metamorphosed. Slate interbeds generally increase in thickness and number toward the top. Primary structures commonly observed are bedding, graded bedding, cross-bedding, scour and fill, slumps, ripple marks, flaser structures, ball and pillow structure,

clastic dykes, concretions, flute marks and groove casts (Taylor, 1967, 1969; Schenk, 1970).

The Goldenville Formation is overlain by the Halifax Formation (Ami, 1900). The Halifax Formation is composed of thinly laminated slate with small amounts of interbedded siltstone and argillite (Woodman, 1904; Stevenson, 1959; Taylor, 1969; Schenk, 1970, and others). The boundary between the Halifax and Goldenville Formations is conformable and ranges from sharp to gradational: where gradational, a metagreywacke/slate ratio of unity is taken as the boundary (Schenk, 1970). Primary structures are less common than in the Goldenville Formation but ripple marks, scour and fill structures, and worm burrows can be seen.

The primary structures and the bedding sequences suggest that deposition of the bulk of the Meguma Group was by turbidity currents (Phinney, 1961; Schenk, 1970, 1971).

Current directions measured in the Meguma Group indicate a source to the south and east of the present Platform (Schenk, 1970). The framework grains of greywackes of the Meguma Group are, with few exceptions, over sixty-five per cent quartz and usually over eighty per cent quartz. Feldspars and lithic fragments make up the bulk of the remainder. Potassic feldspar/plagioclase ratios are greater than one. Lithic fragments are quartzite, slate, and gneissic granite. No direct evidence of a volcanic or volcanoclastic contribution is seen. The mineralogical compositions of the Meguma rocks indicate a cratonic source (Schenk, 1970; Crook, 1974).

Schenk (1971) has suggested that the northwestern African shield satisfies restrictions imposed by current directions and mineralogy.

A few poorly-preserved graptolites from the upper portions of the Halifax Formation have been identified as Tremadocian (lowermost Ordovician or uppermost Cambrian) (Crosby, 1951 as per Crosby, 1962; Cumming, 1952 as per Smitheringale, 1960). Detrital muscovite from the Goldenville Formation has been dated at 487 ± 29 million years or Lower Ordovician (Poole, 1971). The time relationships with other Lower Paleozoic rock units are obscure and the author can only concur with Schenk (1971): "Until better fossils are found, I suggest that the Meguma is mainly Cambro-Ordovician, with possible extension into the latest Precambrian."

Thickest measurements within the Meguma Group are difficult to assess: the base of the Goldenville Formation is nowhere defined, continuous sections are not available, beds are not distinctive, repetitive bed sequences are commonplace, and beds cannot be traced laterally (Stevenson, 1959; Taylor, 1967; Schenk, 1970). Estimates by various workers allow some idea, however (Faribault as per Malcolm, 1912; Taylor, 1967, 1969; Smitheringale, 1960): estimates of thickness for the Goldenville Formation ranges between five and seven kilometres, apparently with little regional differences. The thickness of the Halifax Formation has been estimated from 500 metres in the west to over four kilometres toward the centre of the Platform. The Halifax Formation is especially difficult to measure because long sections are scarce, cleavage usually obscures bedding, and fault and slump structures

are common. Outcrops are generally poor because the slaty Halifax Formation is more deeply weathered and eroded than the quartzitic Goldenville Formation. In summary, the flyschoid Meguma Group may be five to ten kilometres thick. Definitive analysis awaits detailed structural and stratigraphic work, based on better stratigraphic and age control and a consistent facies model.

The Meguma Group is overlain in the northwest by the White Rock Formation. The contact appears to be conformable toward the centre of the Meguma Platform but at its western extremity, at Cape St. Mary, the contact has been described as locally unconformable (Taylor, 1965). The formation ranges from 100 metres in thickness near Wolfville, comprising two quartzite beds with intervening finer grained metasedimentary rocks and minor volcanics, to 500 metres or more with an increasing amount of volcanics to the southwest (T. Lane, pers. comm., M.Sc. in progress). The fauna suggest an age no greater than Caradocian (Late Ordovician) (Boucot, 1971, pers. comm. to T. Lane and L. Jensen as per Schenk, 1971).

The White Rock Formation is overlain conformably or disconformably by the Kentville Formation which consists of black slates with minor siltstone and ranges from 600 metres in thickness near Fales River in the centre of the Platform to 1000 metres in the southwest near Digby. The graptolite fauna is Ludlovian (Late Silurian) (Cumming, 1957, in Smitheringale, 1960).

The New Canaan Formation, consisting of about 300 metres of waterlain volcanics with minor slate, siltstone and limestone, occurs locally within or above the Kentville Formation (Crosby, 1962). Ludlovian conodonts

have been collected from the limestones (L. Jensen, pers. comm.).

The Kentville and New Canaan Formations are overlain conformably or disconformably by the Torbrook Formation. The Torbrook Formation is composed mostly of shale, siltstone, and quartzite and has minor intercalations of limestone and quartzitic iron-formation. It ranges in thickness from 1.5 to 3 kilometres, thickening to the southwest. The abundant fauna are Early Devonian (to Emsian) (Smitheringale, 1960; L. Jensen, pers. comm.). The Torbrook Formation is overlain with marked angular unconformity by Carboniferous, Triassic, or Pleistocene sedimentary rocks.

The lower Paleozoic sedimentary rocks (Meguma Group to Torbrook Formation) are regionally metamorphosed, mostly to greenschist grade. They are folded into large-scale folds which trend northeast and exhibit an associated penetrative axial-plane cleavage. The regional metamorphism and folds affecting these rocks have been attributed to the Acadian Orogeny (Fyson, 1967; Taylor and Schiller, 1966). A more detailed discussion of the metamorphism and structure is given in Chapter II.

Cutting the strata and the structure of the foregoing formation is a granodiorite/adamellite complex (McKenzie, 1974; McKenzie and Clarke, 1975). Biotite granodiorite predominates. The largest pluton is in the central Meguma Platform and is exposed over more than 6400 square kilometres. Many smaller plutons outcrop throughout the Meguma Platform. These plutons cut the folded and regionally metamorphosed Torbrook Formation (Emsian) and are overlain by little-deformed Lower Carboniferous sedimentary rocks

which contain plutonic clasts. K-Ar and Rb-Sr dates range from 417 ± 38 to 350 ± 7 million years B.P. and average, as well as cluster around, 371 ± 7 million years B.P. (Fairbairn, et al., 1964; Cormier and Smith, 1973; Reynolds, et al., 1973; McKenzie and Clarke, 1975). A number of more basic plutons outcrop in the southwest (Taylor, 1969). Many of these plutons, especially the smaller ones and those in the extreme east and west are little studied.

The intrusive rocks are overlain by clastic sedimentary rocks of the Horton Group (Lower Carboniferous) and clastic, evaporitic, and carbonate rocks of the Windsor Group (Lower Carboniferous). These are conformably overlain by feldspathic sandstones of the Scotch Village Formation (Crosby, 1962; Bell, 1960, 1929). These rocks are variously folded by what has been termed the Maritime disturbance (Fyson, 1964, 1967). These rocks are in turn overlain unconformably by sandstones and shales of the Triassic Annapolis Formation. Triassic North Mountain Basalts conformably overlie the Annapolis Formation and the thin sandstones and limestones of the Triassic Scots Bay Formation conformably overlie the basalt (Crosby, 1962; Klein, 1962). The Triassic formations are gently tilted into very large synclines. A few sands and clays of Cretaceous age survive in some river valleys (i.e., Musquodoboit Valley; Lin, 1971).

Pleistocene till and drift cover most of the Meguma Platform, commonly to depths greater than ten metres. Drumlin fields are common (Wilson, 1938; E. Nielsen, pers. Comm., Ph.D. in progress). This glacially transported cover and resultant poor drainage makes outcrop scarce away from the coast

and major rivers.

I.3. Gold-Bearing quartz vein distribution in the study area.

Over sixty localities have been described where gold occurs in quartz veins within the Meguma Group (Malcolm, 1912, 1929). Virtually all of these localities are in areas of the Meguma in which greenschist regional metamorphic grades are evident. They most commonly consist of groups of veins which are conformable to the bedding (i.e., veins are confined to slate beds between thicker quartzite beds). These groups veins are typically about a kilometre long, several hundred metres wide and are centered near an anticlinal dome.

The groups of veins are usually called districts and are extensively described by Malcolm (1912, 1929) and in the Annual Reports of the Geological Survey of Canada by Faribault, who worked in the gold fields between the 1880's and the 1930's mapping individual districts and one-mile-to-one-inch map areas. These maps and plans are very useful for location and enumeration of gold districts and quartz veins.

Much geological work was done on these quartz veins while they were being exploited between the 1860's and 1930's: this work is summarized and listed in Malcolm (1912, 1929). Mineralogic and petrologic descriptions as well as regional geometry were dealt with and explained in terms of the dogma of the time (Lindgren, 1933; Emmons, 1937; Malcolm, 1929). Newhouse (1936) used opaque mineral petrography and concluded that the gold and quartz veins were zoned with respect to, and genetically related to, the Devonian

Figure I.2. Province of Nova Scotia: numbers indicate location of gold districts where mining and/or prospecting activity has occurred since 1850. Numbers refer to index of gold districts found in Appendix II.

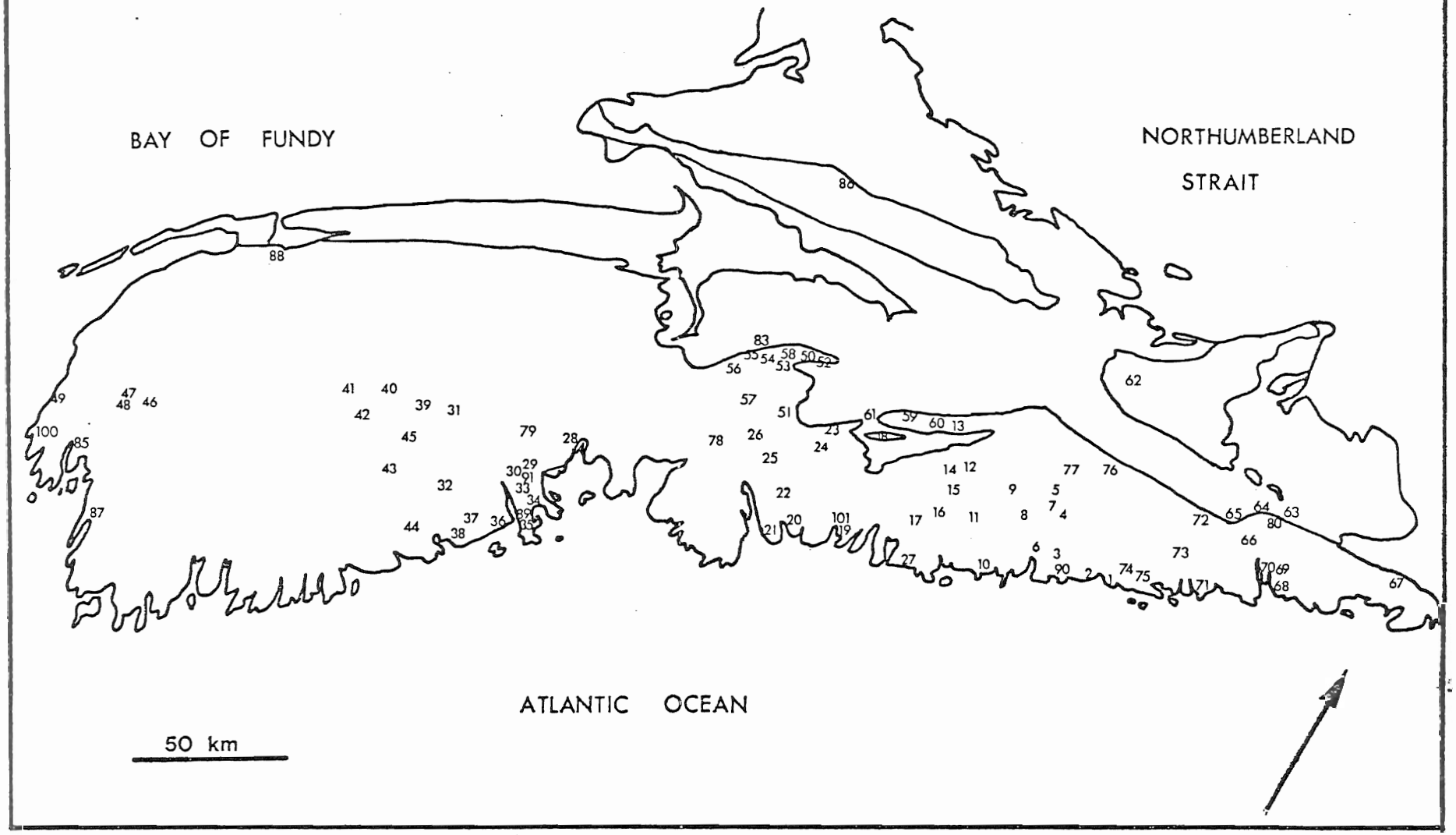

granitic plutons, despite extensive field evidence to the contrary pointed out by Faribault (1899). Newhouse's work has been cited by workers who followed him and his conclusions used as assumptions in their work.

Prior to this study, little work had been done on these vein deposits in terms of experimental results in the synthesis of sulphide, silicate, and carbonate minerals at elevated temperatures and confining pressures. Fluid inclusions had been noted but no descriptive or quantitative investigations had been carried out. If some new data could be gathered to shed some light on the pressure-temperature regime of mineralization, the old descriptive work and recent advances in economic geology could be applied to the problem of the nature of the relationship between the quartz veins and the granites.

I.4 Mining History of the study area.

Over 1,000,000 troy ounces of gold were produced from about fifty districts between 1868 and 1952. The bulk of this production was obtained near the turn of the century, with the last work of any scale ending during World War II. Nearly twenty per cent of this production was from the largest district: Goldenville in Guysborough County. Ten districts produced more than 40,000 troy ounces, 23 districts more than 10,000 troy ounces, and 38 districts more than 1,000 troy ounces.

The development of gold mining in Nova Scotia was controlled by the availability of foreign capital and had a boom-and-bust development character (Drummond, 1918; Malcolm, 1912, 1929). Generally an entire slate bed

between quartzite beds was mined to obtain a workable width: some non-quartz-bearing slate was hand-cobbed and all the rest was crushed using stamp mills. Separation was generally a combination of gravity techniques and almalgamation, although cyanide was occasionally used. A single district was typically mined by several individual mines of varying scale of operation with the names, sizes, and efficiency of all in continuous flux. The result today is an extensive area of ground littered with waste heaps and debris of various sizes; riddled with open clasts, pits, and shafts of various sizes and ages; and criss-crossed by exploration and production trenches of many lengths and depths.

I.5 Present investigation

This study was embarked upon to see if a synthesis of geological studies done on the Meguma Platform; the economic geology done on the gold districts from the first work of Faribault (1886) to the work of Newhouse (1936); vein mineral assemblage data; and fluid inclusion data could shed any new light on the time/space relationships between the country rocks, structures, and gold-bearing quartz veins.

An analysis of the regional geology, especially the structural relations through time and space, was done by synthesizing field observations and the relevant literature.

Fifty of the sixty-two historically productive gold districts were visited, inspected and sampled during 1973. Vein and wall rock petrology including thin and polished section description was done over the following

year. Structures and textures as they relate to vein formation were given special attention.

Fluid inclusions in quartz and carbonates were closely examined and homogenization temperatures were determined from heating stage experiments. Sulphide mineral suites and compositions, especially arsenic/sulphur ratios in arsenopyrites, were determined by ore microscopic techniques and electron microprobe analysis.

The object of the project was to get some idea of the time, temperature, pressure, and chemistry of formation of the gold-bearing quartz veins. As a result of investigating these conditions a model is proposed for the genesis of these veins.

In this report, the writer first summarizes the structural and metamorphic geology of the Meguma Group rocks of the gold districts as a prelude to describing the geometry, mineralogy, and textures of the gold-bearing quartz veins (Chapter II).

Sulphide mineral assemblages are then considered (Chapter III). Background and development of a geothermometer using arsenopyrite compositions is given and data presented in an attempt to fix a temperature of crystallization of the sulphide minerals.

Fluid inclusions are described in Chapter IV and characteristics of inclusions in vein quartz are presented in an attempt to establish some chemical constraints on the crystallizing fluids. Results of homogenization

experiments, together with estimates from an arsenopyrite geothermometer are used to estimate a pressure of crystallization of the vein mineral assemblage.

A summary of observations of Chapters II through IV is presented in Chapter V with a discussion of the developments of ideas about genesis of the veins from the literature. The observations of this report are then discussed and a set of limitations placed on the setting of genesis of the veins.

Pore-pressure phenomena are discussed in Chapter VI in light of the limitations on settings of vein genesis summarized in Chapter V.

A model for genesis of gold-bearing quartz veins of the Meguma Group is presented in Chapter VII which appears consistent with the restrictions presented in Chapters II through VI.

CHAPTER II

DESCRIPTIVE GEOLOGY OF THE GOLD DISTRICTS

1. Introduction

The shape and mineralogy of the gold-bearing quartz veins have been described by many workers, most prominently E. R. Faribault, during operation of the mines. This work is intensively summarized in Malcolm's books (1912, 1929). Faribault's many plans of mining districts at various scales, and geological maps at the scale of one inch to one mile are useful in describing the structure of the Meguma Group. Fyson (1966) has recently studied deformational styles in the Meguma Group and placed these in a framework of an homogeneous strain history. The metamorphic fabrics have been studied and described by Taylor and Schiller (1966).

The present author has attempted to synthesize this work with the guidance of his own field observations. The following sections are the result, and a list of conclusions of this work will give an idea of the observational limitations to any models of vein formation.

2. Structural Geology

The structural history of the Meguma Group has been investigated by Fyson (1966), who examined outcrops throughout the Meguma and interpreted the strain features. The author examined outcrops within and near gold-quartz districts and found no marked disagreement with Fyson's observations.

The following paragraphs draw freely from Fyson (1966).

The strain features of the Meguma Group rocks can be accounted for by response to three different episodes of deformation, each with characteristic strain orientations. Compaction features, bedding plane fissility (S_0), and normal faults are consistent with a vertical orientation of the axis of maximum compression. Regional folding (F_1), and slaty cleavage (S_1) are consistent with maximum compression in a horizontal direction, trending generally southeast-northwest, and a minimum compression in a vertical direction. Kink folds (F_2 and F_3), sinistral faults, and dextral movement along S_1 are consistent with a maximum compression in a horizontal east-west direction and minimum compression in a vertical direction.

Open to tight folds (F_1) with generally sharp hinges typify the pre-granite rocks of the Meguma Platform. Axes are spaced two to eight kilometres apart and are parallel to subparallel. Axial planes are near vertical with slight variation but in no preferred direction. Axial trends vary from northeast-southwest in southern Nova Scotia curving to east-northeast and finally to east toward Chedabucto Bay. Folds plunge gently to the northeast and southwest forming culminations at about ten kilometre spacings. Culminations are not aligned between axial trends as they might be if the result of cross-folding.

Penetrative slaty cleavage (S_1) subparallel to F_1 axial planes is pervasive in the pre-granite rocks of the Meguma Platform. It is defined by small oriented mica and chlorite crystals.

Slickensides on siltier bedding planes perpendicular to F_1 axes have been interpreted as evidence for flexural slip. Similar planes with slickensides can be seen to cut and displace bedding (S_0) and slaty cleavage (S_1) in the manner of normal faults. A radial fault set of small displacements is comonly associated with F_1 crestal culminations. These generally displace S_0 bedding and S_1 cleavage.

Meguma Group, White Rock, New Canaan, Kentville, and Torbrook rocks are similarly effected by F_1 and S_1. Regional metamorphic minerals of greenschist grade define S_1. Regional metamorphic minerals representing assemblages of higher than greenschist grade generally show no preferred orientation in relation to S_1. Granites of the Meguma Platform cut F_1 and S_1 and their contact metamorphic aureoles obliterate S_1. The contact metamorphic minerals show no preferred orientation in relation to S_1.

S_0 and S_1 are deformed by Z-shaped kink folds (F_2). Short limbs are up to two metres in length and have been rotated in a clockwise sense seen in profile (Fyson, 1966, Figure 4). F_3-kinks occur in zones across the foliation in contrast to F_2-kinks. Axial planes are steep and strike northwest. Fractures and faults commonly follow the axial planes of F_3 kink zones (S_3). Some F_3-kinks can be found which deform andalusite and cordierite crystals formed by contact and regional metamorphism.

Long, northwest striking, sinistral faults which cut F_1 appear related in space and sense of movement to the F_3 S-kink zones. Minor magnitude dextral faults parallel S_1 are common. Some have been observed within the granites. These would be a conjugate set to the sinistral faults if maximum

compression was in a horizontal east-west direction. F_2 and F_3 kinks are also consistent with maximum compression in a horizontal east-west direction.

All features are cut by small displacement, variable strike, normal faults and vertical joints. Fyson (1966, pg. 938) describes some recumbent kinks from Halifax Formation rocks near Wolfville. These features would indicate maximum compression in a near vertical direction.

Though Fyson based his conclusions on a limited number of isolated outcrops, they are spread throughout the Meguma Platform and show homogeneous deformation pattern for the Lower Paleozoic rocks of the Platform.

From the above, a sequence of structural episodes can be visualized as having occurred in four stages: a) burial, b) collision, c) post-tectonic, and d) residual.

(a) Deposition, compaction, diagenesis, and initial deep burial took place under conditions of increasing maximum stress in a vertical direction and may be referred to as the burial stage. Stress in this direction continued to increase with increasing depth of burial but this increase was overtaken in magnitude by both horizontal axes some time after the deposition of the Torbrook Formation (Lower Devonian).

(b) The maximum effective stress then became mainly northwest-southeast and the stress in the burial or vertical direction became subordinant. Greenschist grade regional metamorphism, F_1 regional folding, and S_1 penetrative cleavage took place in pre-granite rocks of the Meguma Platform

during these stress conditions. These conditions have been attributed to continental collision between North America and Africa (Bird and Dewey, 1970; Schenk, 1971) and strain results may be described as the collision stage.

(c) F_2 and F_3 kink folds and sinistral and dextral faults are consistent with a change in orientation of the stress field to maximum effective stress trending east-west. Regional metamorphism of grades higher than greenschist grade, completion of regional metamorphism, granite intrusion and contact metamorphism occurred during this stress field orientation which can be described as the post-tectonic stage.

(d) Horizontal stress was relieved and vertical stress again became the maximum effective stress. Normal faulting, recumbent kinks, and exhumation to present levels took place under these conditions. This can be viewed as a residual stage.

3. Metamorphic Petrography

The metamorphic assemblages of the pre-batholithic rocks of the Meguma Platform have been studied and described by Taylor and Schiller (1966). The following is a brief summary of their descriptive work.

Regional metamorphic assemblages correspond to either greenschist or almandine-amphibolite metamorphic facies (Turner and Verhoogen, 1960; Taylor and Schiller, 1966). Greenschist facies rocks of the Meguma group

are typified by biotite + muscovite + quartz ± epidote ± albite ± chlorite assemblages while the almandine-amphibolite facies rocks contain quartz + plagioclase + biotite + almandine + muscovite with lesser amounts of andalusite, staurolite, cordierite, and sillimanite. Contact metamorphic rocks of the Meguma group are typically hornblende-hornfels facies of quartz + muscovite + biotite ± cordierite ± andalusite ± plagioclase with some garnet. Greenschist facies muscovite and chlorite have crystallized in the matrix portion of the rock and are oriented to define the penetrative cleavage; biotite, quartz and feldspar tend to be unoriented indicating that this facies was synkinematic. Almandine-amphibolitic facies minerals tend to be unoriented. Contact effects metamorphose greenschist facies minerals or superimpose their assemblages on greenschist assemblages, indicating post-greenschist facies intrusions. Contact effects are typically seen 0.8 to 4.5 kilometres from granite contacts in greenschist facies rocks. No contact effect is seen in almandine-amphibolite rocks.

The ranges of conditions for each of the facies are: greenschist - 300°-500°C and P_{H_2O} of 3 to 8 kilobars; almandine-amphibolite - 550°-750°C and P_{H_2O} of 4 to 8 kilobars (Turner and Verhoogen, 1960). Taylor and Schiller (1966) suggested the lower pressure ranges as the most likely.

4. Morphology of the Quartz Veins

Quartz veins in the Meguma Group are of two basic morphological types. These have been called "interbedded veins" and "cross veins" (Faribault, 1899; Malcolm, 1912).

Interbedded veins most commonly occur in slate beds which are intercalated between quartzite beds. These slate beds range greatly in thickness but are generally less than ten times the width of any quartz veins within them and less wide than the underlying and overlying quartzite beds. The individual interbedded veins vary in thickness from a few millimetres to a few metres.

Within the slate bed, veins are most common at the two quartzite-slate contacts. Veins in this position appear folded, as are the quartzite beds, into large F_1 folds.

Quartz veins within a slate bed but not so close to the quartzite contacts are commonly folded on a smaller wavelength than regional F_1 folds but have axial planes with a similar strike to the regional F_1 folds. Amplitudes of this fold style range from just slightly more than the width of the vein to several times the width of the vein. Folds with higher amplitude occur in thicker slate units. Wavelengths increase as the vein width increases.

These two scales of folding are often present in the same slate bed (Figure II.1.) and an individual vein can change from one to the other if it diverges from the wall of the slate bed.

These characteristics are similar to those described in the literature, where a more competent layer (in this case the vein) has been plastically folded within a less competent layer (here the enclosing slate). Such style of folds can be seen at crests as well as on steep limbs of F_1 anticlines

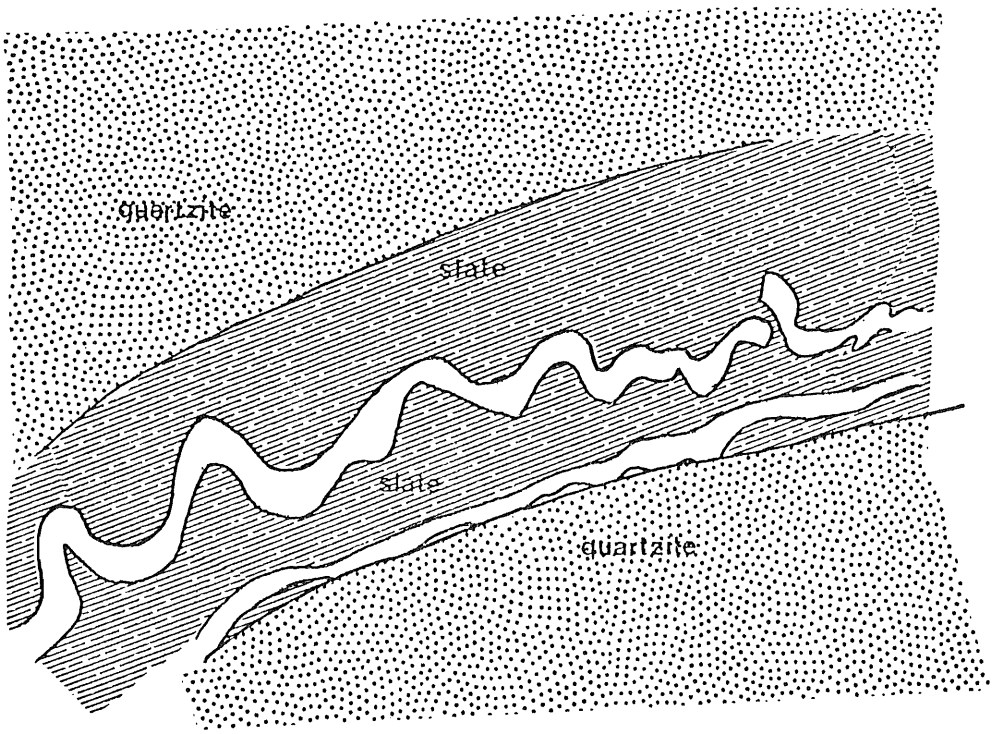

Figure II.1. A folded and an unfolded quartz vein in alternating slates and quartzites of the Meguma Group. This sketch is after a photograph of a working face at Mount Uniacke - plate XVI of Malcolm (1912).

(Goldenville and Salmon River for example: Malcolm, 1912, Figures 9, 10 and 11). This suggests that the layer may have been essentially horizontal when buckled and later folded into the larger wavelength of F_1 folds (e.g. Ramsay, 1967, p. 396-397). Furthermore, the axial plane slaty cleavage is deflected around these smaller folds of the quartz veins (e.g. Malcolm, 1912, Plate VIII) indicating (Ramsay, 1967 p. 181) that either the folded shapes which deflect the cleavage were present before deformation or that the folded shapes grew during deformation. Deformation textures observed in and between mineral grains within the veins (see chapter II.5) imply that the veins were first crystallized and subsequently deformed by folding. (Arsenopyrite grains within the slates and in the quartzites near interbedded quartz veins also deflect the slaty cleavage. Their long axes are commonly perpendicular or at a large angle to the slaty cleavage, they commonly show cataclastic textures and they are accompanied by pressure "shadows" with quartz, thus suggesting that they had crystallized previous to the deformation and development of the slaty cleavage). Veins formed after the main period of deformation would cut slaty cleavage and if the veins had been folded after the deformation resulting in F_1 and S_1 structures, they would fan the slaty cleavage: the latter mechanisms do not appear to have been responsible for the observed deflection.

Interbedded veins invariably occur in groups (Figure II.2). These groups are made up of a parallel sequence of veins parallel to the folded bedding. The top and bottom of these groups are usually eroded or not exposed. In some districts, especially Mooseland, the vein group can be seen to die

Figure II.2. Generalized corss section of a portion of the Meguma Platform illustrating the location of groups of veins vis-a-vis the structural features. Cross cutting relationships of the batholiths (+'s) and the thermal aureole (stipled) of the batholiths is also illustrated. Diagram is not to scale.

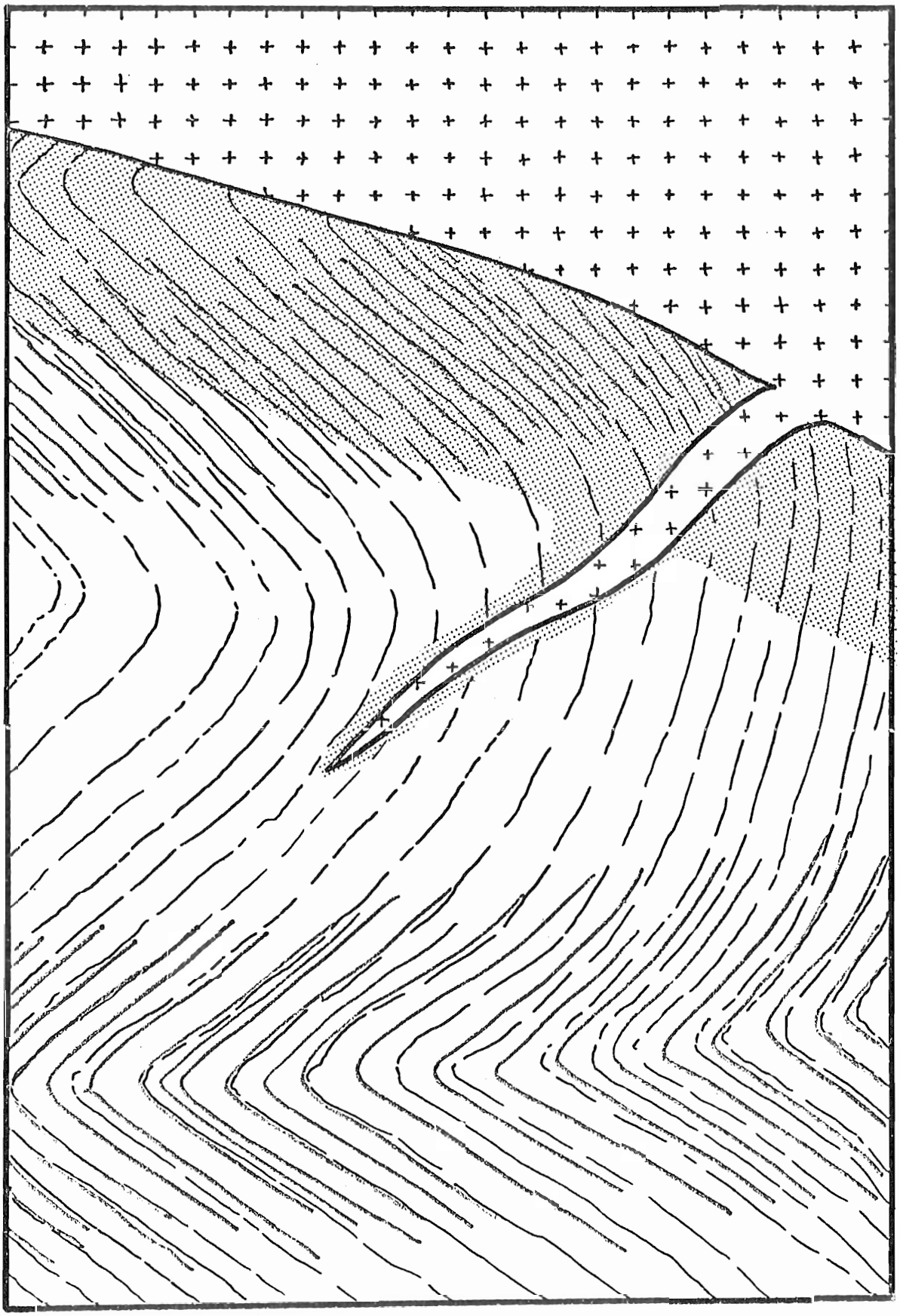

out upward as the slate/quartzite ratio becomes very large. In most districts, however, the slate/quartzite ratio is fairly constant throughout the exposed group of quartz veins.

The largest exposures of groups of interbedded quartz veins occur at anticlinal culminations. The veins commonly persist with relatively constant thickness along the axis of the culminated fold for distances of up to four kilometres (e.g. Goldenville, Oldham). They pinch out, however, down the flanks of the anticline within a few hundred metres. Groups of interbedded veins are also found a few hundred metres from the anticlinal axis. Faribault (1899) has stated that this type of interbedded vein group is found where more open folds occur.

At angles to the interbedded quartz veins small irregular veins occasionally merge with the interbedded veins. These short veins have been called angulars and are much smaller in size that the interbedded veins with which they are associated. They sometimes link adjacent interbedded veins and are more common where the walls of the interbedded veins are irregular.

Another morphological feature of groups of interbedded veins has been described as "rolls". These are irregular-shaped folds which occur in the flanks of large anticlines. They repeat in each underlying interbedded vein. A plane through these rolls varies from vertical as does the axial plane of the F_1 folds. Where roll sets are found on all sides of a culmination these planes radiate from the culmination axis at low angles to the axial plane: however, most districts are not well enough known to define more than one such plane. Rolls are associated with zones of angulars.

All known groups of interbedded quartz veins have recorded gold production.

The second group of quartz veins have been called cross veins. These are near vertical, unfolded, veins which cut F_1 and S_1 at various angles. These veins occur throughout the pre-granite Meguma Platform rocks. These veins are not related to gold production unless they occur within interbedded vein groups or intersect pyrite-pyrrhotite-arsenopyrite rich beds associated spatially with such vein groups.

Chapter VII of this report presents a model whereby the geometric characteristics of both interbedded and cross veins are placed within the deformational framework of the Meguma Group rocks.

5. Mineralogy and Textures of the Quartz Veins

The mineralogy of the quartz veins under consideration is remarkably consistent. Quartz, carbonate, and arsenopyrite-pyrite-pyrrhotite typify them.

Quartz is the dominant mineral: it often makes up all of the vein and rarely is relegated to less than fifty percent by volume. It is variously coloured from milky to grey in response to the density of fluid inclusions. Clear, free-growing crystals are rare. In thin section most quartz grains exhibit little undulose extinction but within most sections grains of varying

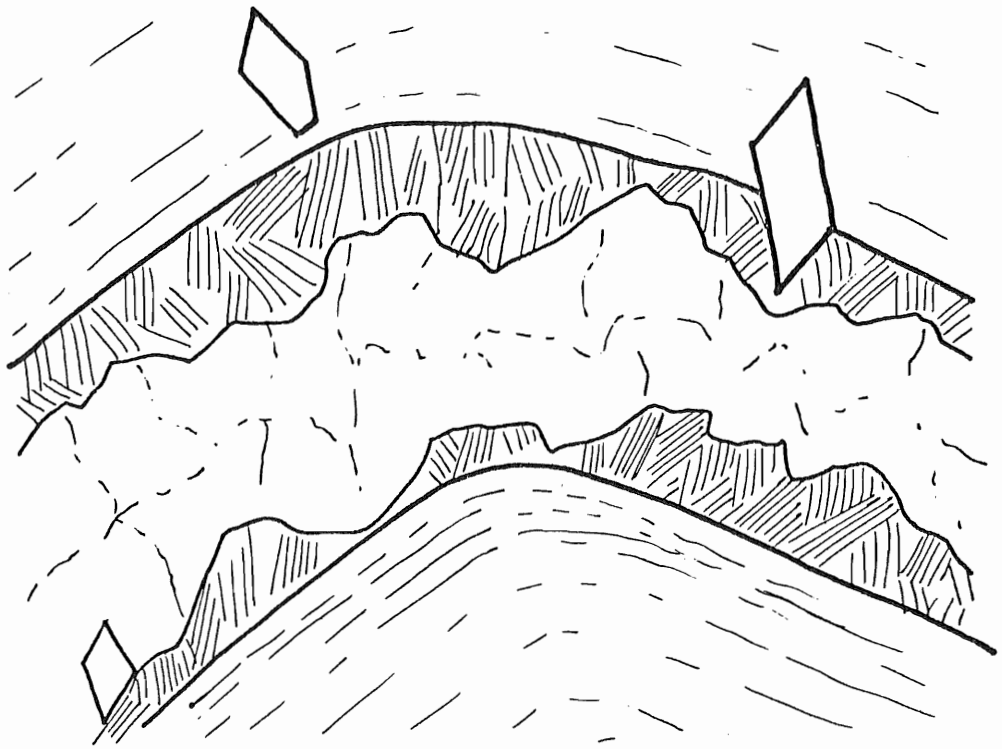

Figure II.3. A generalized cross-section of a quartz-carbonate-arsenopyrite vein in slate of the Meguma Group. Carbonate occurs at the vein walls, quartz in the central portion of the vein, and arsenopyrite crystals in the slate and the carbonate. Quartz and carbonate also occur in the cement of the country rock.

degrees of undulose extinction can be seen giving some measure of post-crystallization strain. If minerals other than quartz are present, quartz dominates the centre portion of the vein cross-section. Quartz quite often veins and coats carbonate crystals and occasionally veins sulphide minerals. Most cross-veins are composed only of quartz.

Carbonate is the next most abundant vein mineral. It occasionally makes up over 50 percent by volume of a local area of vein but more typically accounts for 5 to 10 percent by volume of interbedded veins. It is usually more abundant at wider and more irregularly shaped parts of a vein. The carbonate exhibits various colours: usually it is white or pink on a fresh surface and a tarnished bronze colour on a weathered surface. Regardless of colour, electron microprobe analyses show that most are calcite having low iron or magnesium content. Thus it is believed that many reported instances of ankerite (e.g. Malcolm, 1912) are in fact calcite. Carbonate most commonly occupies the portion of the vein nearest the wall rock exhibiting sharp boundaries with the wall rock and crystal-like terminations into the massive quartz which occupies the centre of the vein. This can often be seen repeated in parallel to subparallel veins which in many places occur at carbonate wall rock boundaries of larger veins. Some carbonate crystal faces are coated by, and cut by thin quartz layers so that a vein in which the carbonate has weathered will often appear as a central quartz band surrounded on each side by quartz boxwork.

Iron-arsenic sulphide minerals are generally present in all veins but rarely make up more than a few per cent of a vein's volume. These minerals

Figure II.4. Arsenopyrite grain (black) which has failed brittlely and deflects slaty cleavage around it illustrating a common texture near quartz-carbonate-arsenopyrite veins indicating arsenopyrite crystallization before the deformation responsible for slaty cleavage formation.

are arsenopyrite, pyrite and pyrrhotite. Arsenopyrite is the most abundant and has a similar distribution in a typical vein cross-section to the carbonate: indeed, arsenopyrite aggregates are generally found surrounded by carbonate or at carbonate wall rock and carbonate-quartz contacts. Arsenopyrite is often veined by quartz and can be found cutting carbonate wall rock boundaries. Pyrite is less abundant than arsenopyrite. It is occasionally found alone, disseminated in a vein but usually is found intimately in contact with arsenopyrite. Pyrrhotite is occasionally found as the dominant sulphide mineral but more commonly is found with arsenopyrite and pyrite aggregates as very small grains or as blebs within arsenopyrite crystals. These three sulphides exhibit sharp boundaries with each other and are common in wall rock as well as the veins. More detailed discussion of this sulphide assemblage is presented in Chapter III.

Other sulphide minerals present in small amounts are chalcopyrite, galena, and sphalerite. Chalcopyrite is found as small isolated grains in cracks in quartz. Galena occupies a similar habit and is only rarely seen. Sphalerite has been reported from several districts and said to occupy a position similar to galena.

Country rock inclusions commonly make up a small volume of the vein. These are typically slate inclusions made up of chlorite and sericite. Biotite, apatite, and sulphides are rare associated minerals. The inclusions are angular. They commonly can be fitted back into the wall rock with minimal rotation.

Trace minerals which are seen in the veins are feldspars (potassium feldspar more commonly than albite), rutile, and scheelite.

Rutile occurs in long slender black crystals and has consistently been misidentified in the literature as tourmaline: for example Newhouse (1963) at Moose River. Rutile is most abundant in localities where scheelite is found and most commonly occurs as radiating crystal groups within the quartz-rich portion of the vein and as planar groups at the contacts of the veins with the wall rock.

Scheelite is an important mineral in some districts and has been mined from Moose River. It typically occurs in pods down-plunge in gold-bearing groups of interbedded quartz veins (Miller, 1974). Scheelite occurs in quartz veins where it occurs with carbonate at the vein wall and in fist shaped pods. When scheelite is present rutile tends to be more abundant, carbonate tends to be more iron rich, and gold content is very low. Scheelite crystals are usually veined by quartz. Electron microprobe analyses show high purity $CaWO_4$ with no detectable molybdenum content (Miller, 1974).

Feldspar. Much has been said about the albite with Nova Scotia gold-bearing quartz veins (Emmons, 1937; Newhouse, 1936) but feldspar is a rare vein mineral and potassium feldspar is the dominant feldspar. It usually is seen as small bands in the smaller districts (Mill Village, Voglers Cove) and as isolated small pods (Mount Uniacke) at the contacts of the vein with the wall rock.

Gold is the most important trace mineral. It occurs as visible grains within grains of all the vein minerals and as small grains and coatings associated with arsenopyrite crystals. It is generally associated with carbonate and arsenopyrite-rich parts of a vein.

Carbonate and arsenopyrite-pyrite-pyrrhotite tend to be more abundant at rolls and thickenings. Gold is most commonly associated with areas of the vein enriched in carbonate and arsenopyrite-pyrite-pyrrhotite and is enriched with them at vein irregularities. Gold grades have been reported as higher in folded veins than in unfolded veins of the same mineralogy: folded veins represent a relative thickening of the quartz in any mine working, and might have been interpreted as enrichment, but this possibility is difficult to assess. Gold also occurs in the slate in the vicinity of interbedded quartz veins.

Cross veins are much more quartz-dominated than interbedded veins. Carbonate-sulphide-gold mineralization tends to be restricted to intersections of cross veins and interbedded beins as at Central Rawdon or Brookfield or where cross veins intersect sulphide rich beds as at Cow Bay. Angulars have identical mineralogies as the interbedded veins they merge with.

Gold-bearing quartz veins are restricted to areas of the folded Meguma metasediments with greenschist grade regional metamorphism. Wall rock metamorphic mineral assemblages indicate mainly the quartz-albite-muscovite-chlorite subfacies as described by Taylor and Schiller (1966). Epidote and

biotite are present in lesser amounts. Near the veins, wall rocks are commonly no different than at great distances from the veins. They often differ, however, in containing small augen-shaped blebs or pods of vein-assemblage minerals. The blebs are oriented parallel to the interbedded veins and often deflect the cleavage. The vein mineral assemblages does not vary greatly from the mineral assemblage of the cement of the Meguma Group rocks within the greenschist facies regional metamorphic area. In short, there does not appear to be an alteration aureole surrounding the veins or vein groups: the regional metamorphic assemblages and the vein assemblages are strikingly similar.

Several districts are within the contact metamorphic aureoles of nearby granitic bodies. Forest Hill, Cochrane Hill, Country Harbour, and Beaver Dam are within contact metamorphic zones and garnet, biotite, and cordierite are commonly observed in the wall rock at these districts. The vein assemblages are similar to other districts except for some loss of carbonate at the vein walls: its place taken by almandine and micas. Contact metamorphic minerals can be seen to be superimposed upon the greenschist assemblage fabric in the wall rocks (Taylor and Schiller, 1966).

6. Summary

Any explanation of the formation of the gold-bearing quartz veins must be consistent with the geological observations summarized below.

1. For any volume of Meguma, strain features indicate a relatively homogeneous history: burial conditions followed by pronounced compression in a SE-NW direction followed by a less pronounced horizontal compression in an E-W direction during which Devonian batholithic bodies were emplaced followed by only small scale and scattered residual strain.

2. Large regional folds and penetrative axial plane cleavage are the dominant strain feature and occurred in response to SE-NW compression.

3. Interbedded veins more commonly occur in slate beds between thicker quartzite beds. Interbedded veins always occur in groups of parallel veins. All such groups have associated gold production. Cross veins occur throughout the Meguma Group rocks but are productive only where they intersect groups of interbedded veins.

4. The interbedded veins are deformed in response to the same SE-NW compression as are the country rocks.

5. Groups of interbedded quartz veins are most commonly located near anticlinal axes of major regional folds.

6. Groups of interbedded quartz veins are located within the area of greenschist grade regional metamorphism. Greenschist metamorphic minerals define the axial plane cleavage. This cleavage is deflected by folded quartz veins as would be expected if the veins behaved as competent layer, during buckling and cleavage formation. On the basis of the mineral assemblages, temperatures and pressures of this regional

metamorphism may be estimated at the lower end of greenschist grade conditions: 300° to 500°C and 3 to 8 kilobars.

7. The regional metamorphic assemblage and the vein assemblage are similar. There is no "hydrothermal alteration" aureole around the veins.

8. The quartz veins under study exhibit a constant mineralogy, which is always present where gold production is reported: dominantly quartz, secondly carbonate, minor amounts of arsenopyrite-pyrite-pyrrhotite, and country rock fragments. Chalcopyrite, galena, sphalerite, feldspar, rutile, scheelite, and gold are trace minerals.

9. In cross section, the minerals exhibit consistent relationships. Carbonate occurs in sharp contact with both vein walls and in crystal face terminations in contact with quartz which occupies the median part of the vein. Sulphide minerals tend to be most abundant at the carbonate-wall rock contact and within the carbonate.

10. Gold is associated with areas of the veins with the most carbonate and sulphide minerals. These minerals are most abundant in vein rolls, irregularities, and thickenings. Small angular veins of similar mineralogy are more common at these same localities.

11. Contact metamorphic effects are a later overprint on the regional metamorphic greenschist assemblage and the vein mineral assemblage.

In the next two chapters hypotheses for vein formation will be evaluated after consideration of the details of quartz and iron-arsenic sulphides.

CHAPTER III

ARSENOPYRITE

III.1 Background

The Fe-As-S system, Figure III.1, was investigated by L. A. Clark (1960a, b) using a dry synthesis method. This method allowed definition of phase boundaries between 400 and 800°C at the vapour pressure of the system (about one bar: Clark, 1960a, 1367-1368). At lower temperatures, most reactions would not go to completion in experimentally reasonable times.

Clark delimited the phases in the Fe-As-S system at about one bar pressure as in Figure III.1 and defined geologically important invariant points. The invariant point governed by the reaction pyrite+arsenopyrite$\leq$pyrrhotite+liquid or vapour, above which pyrite and arsenopyrite cannot exist together in equilibrium, was fixed at 491 ± 12°C. The invariant point, above which arsenopyrite cannot crystallize, and which is governed by the reaction arsenopyrite pyrrhotite+loellingite+liquid or vapour was found to be 702 ± 3°C.

By weighing the reactants and products of arsenopyrite synthesis, he was able to establish that iron had a relatively small variation from unity in product equations. Arsenic and sulphur were seen to have a similar behaviour but the ratios of the two could not be determined by this method

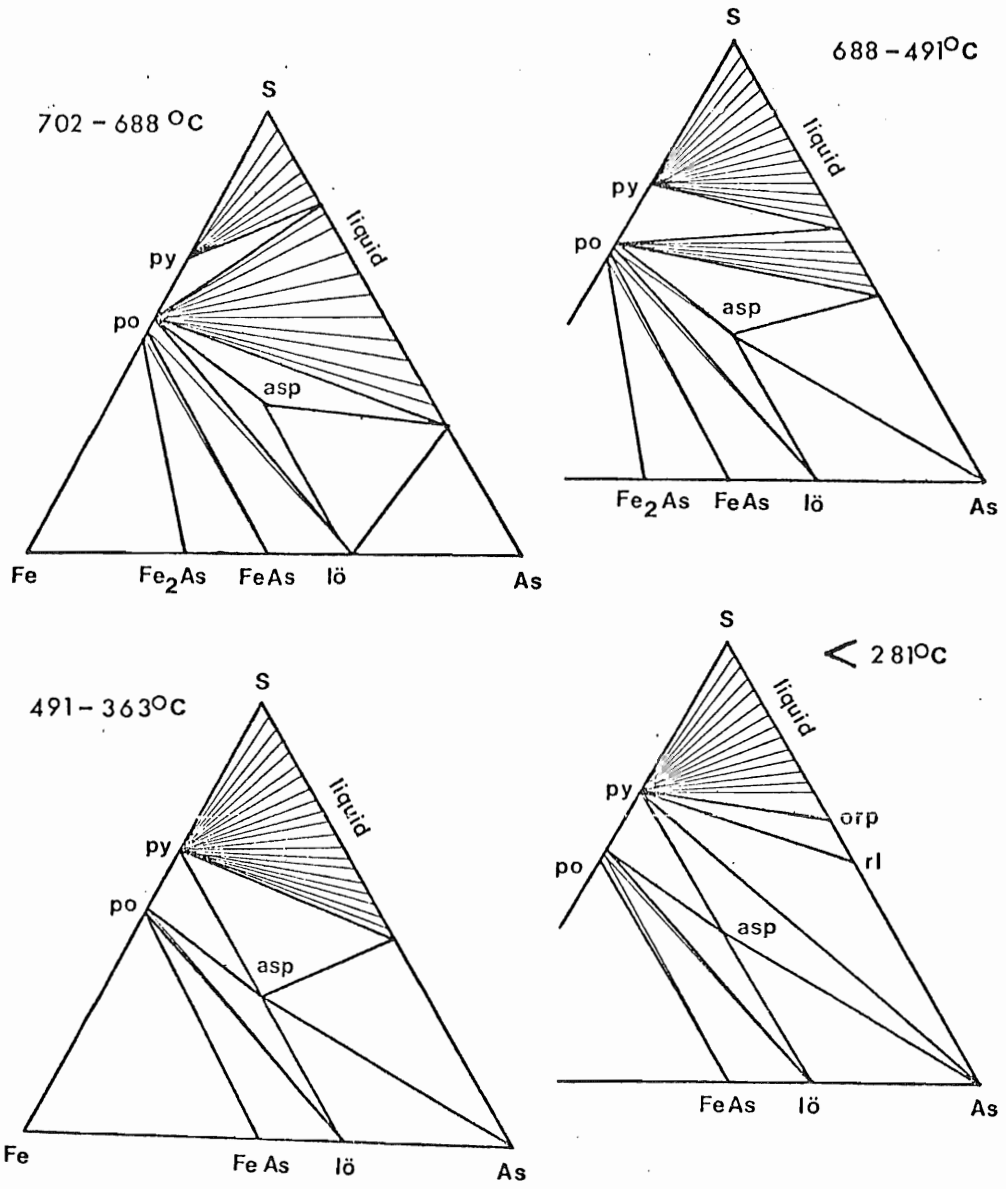

Figure III.1. Isothermal, polybaric sections in the system Fe-As-S. Sections are drawn midway between indicated limits. (After Barton, 1969 and Kretchmar, 1973, Figure 2-1).

(Clark, 1960a, p. 1633; Morimoto and Clark, 1961).

Clark observed that the (131) reflections of arsenopyrite, as measured from x-ray diffractograms, varied systematically with the assemblage and different temperatures of crystallization of each experimental run. It was then shown that arsenopyrite (131) reflections vary linearly with respect to the arsenic-sulphur ratio. Chemical analysis of arsenopyrites confirmed these relations and allowed a calibration of a (131) versus atomic per cent arsenic curve (Morimoto and Clark, 1961). This relationship presented a rapid and reproducable method to measure the arsenic/sulphur rations of the synthetic arsenopyrite crystals.

Arsenic/sulphur rations of arsenopyrite crystals grown at different temperatures were found to vary linearly with temperature for each different Fe-As-S assemblage. This observation formed the basis for a geothermometer in which atomic per cent arsenic (to represent As/S ratio as determined by arsenopyrite (131) reflections), was related to temperature of crystallization (Morimoto and Clark, 1961).

One of the necessary conditions for arsenopyrite composition to be an effective geothermometer is that its composition must not have changed after crystallization. Clark (1960b) and, more recently, Kretschmar (1973) conducted many tests to evaluate this possibility. They were unable to change the composition of arsenopyrite without recrystallizing it even at time periods of 304 days at temperatures of 550°C. Kretschmar also tried to change arsenopyrite compositions under five kilobars pressure but was

unsuccessful. Thus, arsenopyrite should reflect the conditions at the time of crystallization if, since then, the temperature conditions have been below melting levels (702°C ± 3°C) and pressures have been at levels below five kilobars.

Pressure was also seen to affect (131) reflections of arsenopyrite systematically. A geobarometer was formulated using a limited set of pressure syntheses at less than two kilobars. This related arsenopyrite (131) reflections to pressure of crystallization (Clark, 1960b). Thus, if the temperature or the pressure could be estimated independently, the other could be estimated using arsenopyrite diffractograms.

Kretschmar (1973) sought to refine Clark's geobarometer and geothermometer. He conducted syntheses in the Fe-As-S system using fluxes, which permitted him to extend knowledge of the system down to about 300°C. Kretschmar more clearly defined the arsenic/sulphur ratio versus temperature of crystallization relations for each assemblage at atmospheric pressure. This is shown in Figure III.2 . His meausrement technique was primarily electron-microprobe analysis (as described below) which he compared with (131) reflections requiring a slight revision of Clark's atomic per cent arsenic versus (131) calibration.

Kretschmar systhesized arsenopyrite at five kilobars pressure to test Clark's geobarometer. The results of these experiments were hard to interpret: arsenopyrites were obtained, which were both more sulphur-rich or more arsenic-rich than arsenopyrite synthesized at the same temperatures

at atmospheric pressure. None of the variation in composition, however, was significantly greater than the error surrounding the value at atmospheric pressure. Kretschmar recalculated Clark's results using the revised (131) versus atomic per cent arsenic calibration and found the pressure effect observed by Clark was less. Kretschmar also noted that the (131) measurement converges on a prominent loellingite (221) reflection as arsenopyrite becomes more sulphur-rich. Clark's two kilobar results in loellingite assemblages are in the range of this interferring reflection: thus the inferred sulphur enrichment could actually be a misidentification. Kretschmar concluded that at constant temperature the trend to sulphur enrichment as a function of pressure increase is probable, but that the amount can be considered not significant as compared to measurement error, at pressures lower than five kilobars. Extensive analyses of natural arsenopyrites (Kretschmar, 1973, Chapter 5) also failed to show any systematic or significant variation in sulphur content due to pressure. Clark's pressure effect should result in some natural arsenopyrites being more sulphur rich than permissible in a low pressure synthesis, but none were found. Kretschmar evoked the theoretical generalization of Barton (1970, page 190) that sulphide systems should not respond markedly to pressure change. Kullerud (1970) assessed pressure affects in sulphide systems which had been studied. None are significant at pressures less than five kilobars vis-a-vis the measurement error of Kretschmar.

In summary, after the work of Clark (1960a, b); Morimoto and Clark (1961); and Kretschmar (1973), an arsenopyrite geothermometer has been well

defined at atmospheric pressure between the crystallization temperatures of about 300 and 610°C if the coexisting mineral assemblage in the Fe-As-S system is known. An arsenopyrite geobarometer, however, appears to be less reliable. It is likely, though not effectively proven, that the pressure effect on arsenopyrite composition at any given temperature causes sulphur enrichment at higher pressures, though by only a relatively small amount at pressures of a few kilobars.

It is, therefore possible to use minerals of the Fe-As-S system to determine the temperature of crystallization of the arsenopyrites in the quartz veins of the present study.

A possible role for arsenopyrite in the deposition of gold was indicated by the pressure experiments. Clark (1960b) notes that during the experiments in which an attempt was made to synthesize arsenopyrite under various confining pressures, arsenic was observed to have diffused through the walls of the gold pressure vessel (0.2 mm thick) at temperatures below about 600°C. At temperatures above about 600°C gold diffused into the arsenopyrite so that upon quenching 5 to 15 areal per cent of the synthesized arsenopyrite product was gold grains. Kretschmar (1973) found a similar effect in his pressure syntheses of arsenopyrite.

Coleman (1957) noted that at Yellowknife, N.W.T. gold was related spatially to arsenopyrite: as coatings, in cracks in arsenopyrite, or in discrete grains very near arsenopyrite grains. He attributed this relationship to a possible solid solution effect between gold and arsenopyrite

Figure III.2. Pseudobinary T-X section showing arsenopyrite compositions as atomic percent arsenic as a function of temperature. (After Kretschmar, 1973, Figure 3-2).

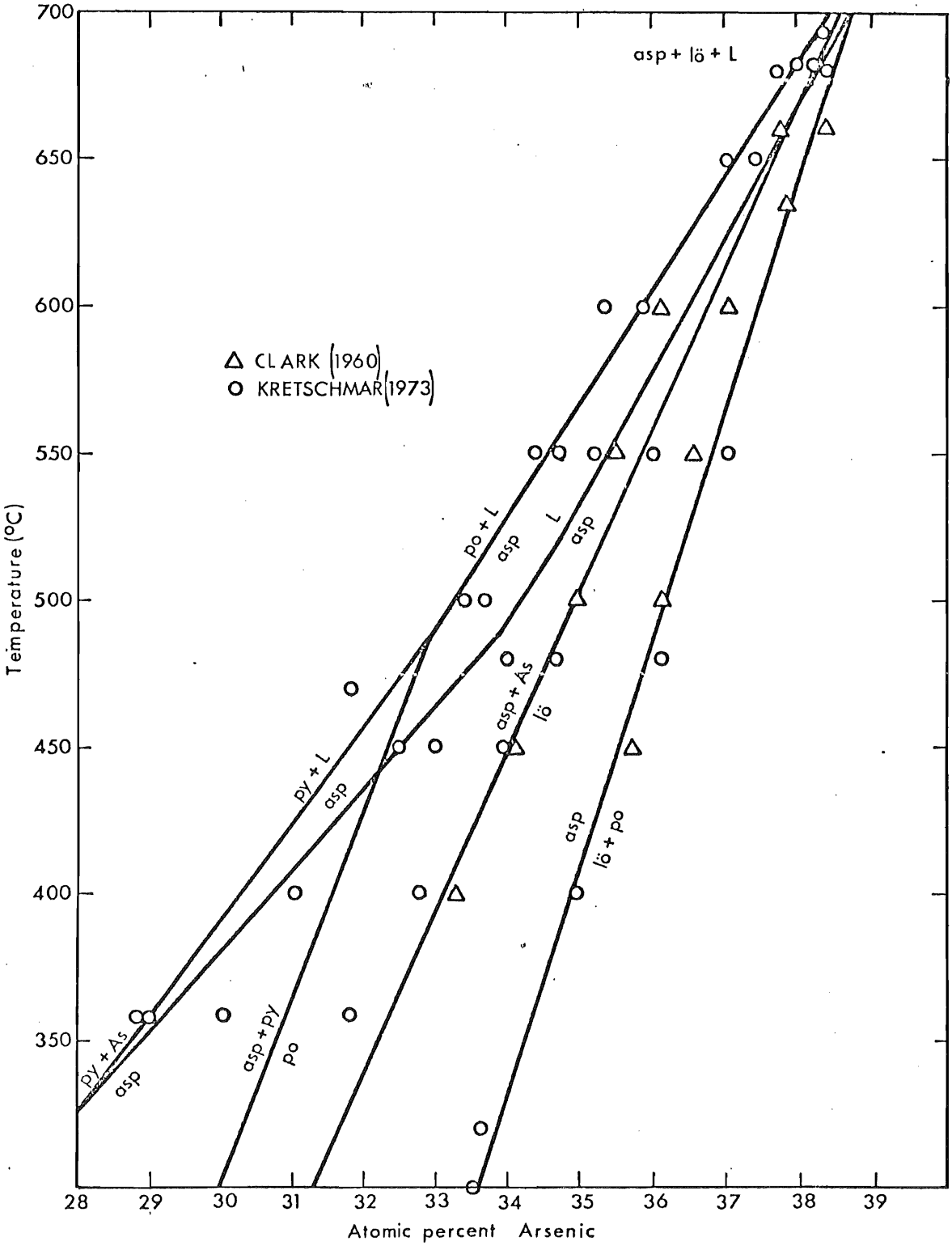
700
650
600
550
500
450
400
350
Temperature (°C)
28
29
30
31
32
33
34
35
36
37
38
39
Atomic percent Arsenic
asp + lö + L
CLARK (1960)
KRETSCHMAR (1973)
po + L
asp
L
asp
asp + As
lö
py + L
asp
asp + py
po
asp
lö + po
py + As
asp

(and perhaps also pyrite) at temperatures of formation of the arsenopyrite. The gold, trapped by the arsenopyrite, would later diffuse out upon cooling and/or be available for later remobilization. Schwartz (1944) has cited many examples of the spatial relationship between gold and arsenopyrite such as that seen at Yellowknife, especially in "mesothermal" quartz vein deposits. Arsenopyrite seems to exhibit this relationship with gold in the Nova Scotia deposits (Malcolm, 1912; Harrison, 1938). If arsenopyrite does play a role in concentration of gold in mesothermal quartz vein systems, the vein systems studied in this report could show the effects of such concentration.

III.2 Instrumentation

Arsenopyrite compositions were determined using a Cambridge Instrument Company Microscan V electron microprobe operated at Dalhousie University. An accelerating voltage of 15 Kilovolts was used along with a beam current of 0.05 milliamps. Each analysis consisted of four twenty second counts (as compared to two to eight ten second counts of Kretschmar). These were averaged using the EMPADR 7 correction program written by J. Rucklidge and E. L. Gasparini of the University of Toronto, Department of Geology. This program uses a complete AZF correction scheme.

A standard, asp 57, and an unknown, asp 200, were provided by Dr. Ulrich Kretschmar (COMINCO). These were numbered and used after Kretschmar, 1973. Verification of homogeneity of asp 57 and asp 200 was done and

results agree with those of Kretschmar (1973). All samples were analyzed against asp 57.

Several spot analyses were made on each sample. These were preceded and followed by analysis of asp 57. Before the final standard was run for each sample a spot analysis was made of asp 200. Chemical analyses of asp 57 from Kretschmar (1973) after Kirkham (1969) were used.

After averaging using EMPARDR 7, any individual spot analyses whose total weight per cent exceeded 101 per cent or was less than 98 per cent was rejected. If an asp 200 standard unknown was outside these limits, the sample with which it was analyzed was also rejected. Several samples were analyzed by electron microprobe for any heavy minerals which might substitute into arsenopyrite. Special attention was given to cobalt and nickel. The only other metal detected in these analyses was a trace amount of copper.

III.3 Results

Ninety-five arsenopyrite compositions from seventeen districts were accepted from electron microprobe analyses. These are presented in Table III.1.

The same standard was used in this study as in that of Kretschmar: asp 57. The same standard unknown was also used: asp 200. Table III.2 compares Kretschmar's first 24 analyses (Table 3-5) of asp 200 versus asp 57 with this study's first 21 such analyses.

TABLE III.1

Mean Arsenopyrite Compositions

DISTRICT	n	ATOMIC % As	ONE s.d.	ATOMIC % S	ONE s.d.	ATOMIC % Fe	ONE s.d.
Upper Seal Harbour	23	32.7	0.9	34.1	0.8	33.2	0.3
The Ovens	12	31.9	0.5	34.6	0.4	33.4	0.2
Cochrane Hill	10	32.5	0.2	34.4	0.2	33.2	0.1
Salmon River	9	32.1	1.3	35.2	1.1	33.1	0.2
Lawrencetown	9	32.1	0.7	34.6	0.7	33.2	0.2
Lake Catcha	7	31.4	0.8	35.4	0.8	33.2	0.2
Cranberry Head	5	32.3	0.7	34.4	0.8	33.3	0.1
Goldenville	4	31.2	0.6	35.6	0.4	33.1	0.2
Whiteburne	4	32.6	1.6	34.5	1.5	33.0	0.2
Caribou	3	32.4	0.4	34.5	0.4	33.1	0.1
Killag	3	31.2	0.4	35.4	0.4	33.3	0.1
Molega	3	31.7	0.2	35.3	0.1	33.0	0.1
Isaac's Harbour	2	32.0	0.1	34.5	0.1	33.5	-
15 Mile Stream	2	31.2	1.7	35.5	1.5	33.3	0.3
Gold River	1	31.1	-	35.6	-	33.3	-
OVERALL	95	32.1	0.9	34.7	0.9	33.2	0.2

TABLE III.2

	MEAN WEIGHT %		MEAN ATOMIC %		ONE s.d. (wt%)		RANGE (wt.%)	
Element	uk	mg	uk	mg	uk	mg	uk	mg
As	44.44	44.61	31.77	31.8	0.45	0.41	43.7-46.1	43.9-45.3
s	21.03	20.95	35.13	35.0	0.31	0.25	19.8-21.6	20.3-21.4
Fe	34.51	34.69	33.10	33.2	0.20	0.32	33.8-35.3	34.2-35.2

Mean asp 200 compositions from electron microprobe data as modified by EMPADR 7. This study (mg) analyzed asp 200 twenty-one times. Ulrich Kretschmar (1973) (uk) analyzed asp 200 twenty-four times.

Figure III.3. Pseusobinary T-X section showing arsenopyrite compositions as atomic percent arsenic as a function of temperature (after Kretschmar, 1973, Figure 3-2). Shaded area indicates error envelope surrounding relevant assemblages for this study (see Chapter III).

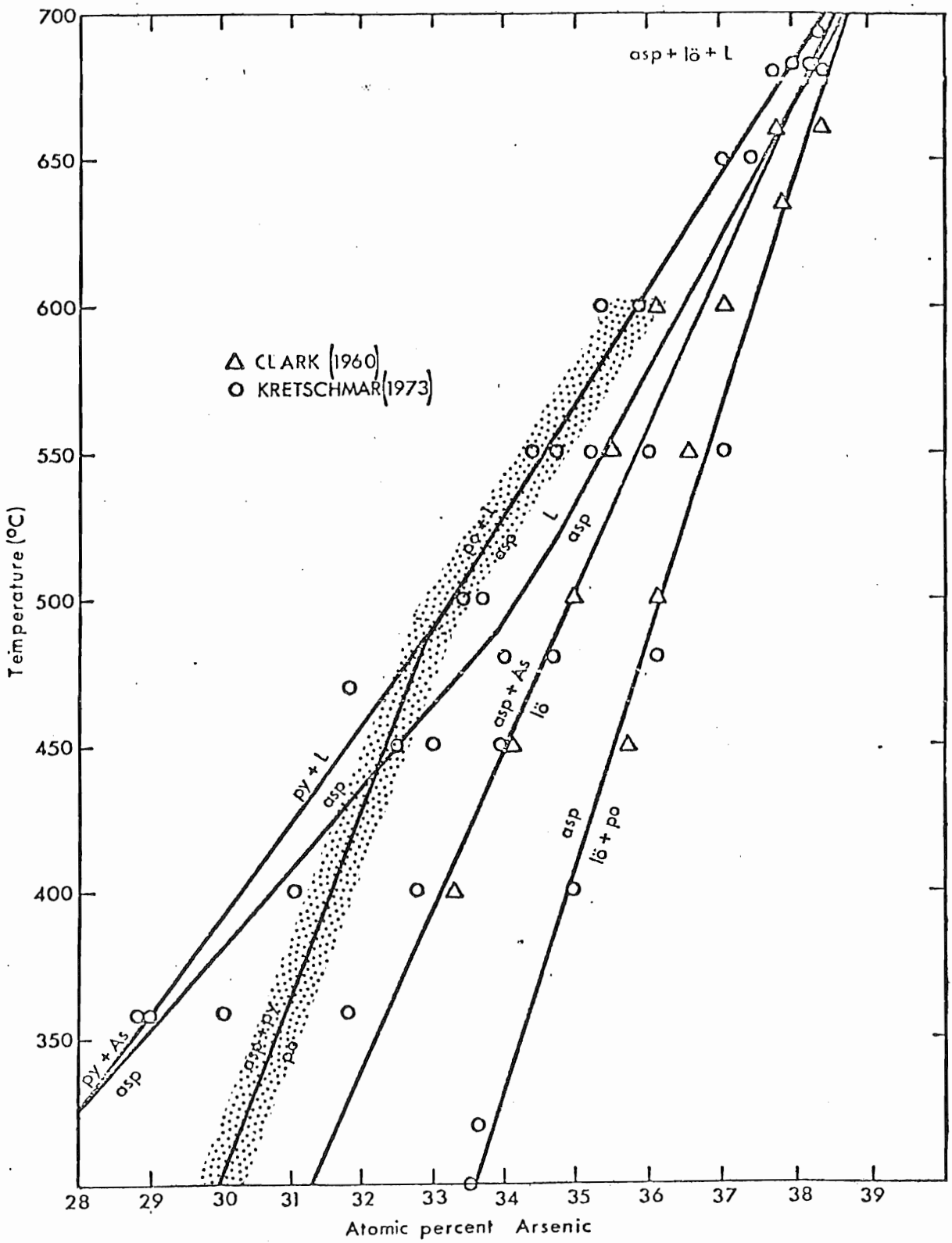
700
650
600
550
500
450
400
350
Temperature (°C)
28
29
30
31
32
33
34
35
36
37
38
39
Atomic percent Arsenic
asp + lö + L
△ CLARK (1960)
○ KRETSCHMAR (1973)
py + L
asp
py + As
asp
asp + py
po
po + L
asp + L
asp + As
lö
asp
L
asp
asp
lö + po

Pyrrhotite and pyrite have been identified in all samples save one from Cochrane Hill in which no pyrite was found. Sharp non-alteration boundaries between sulphide grains are generally present. Arsenopyrite and pyrite are seen to be imprinted on each other in most samples indicating discrete crystallization of each but no preference as to which crystallized first. Pyrrhotite grains are generally non-crystalline, small, inclusion-like grains in both arsenopyrite and pyrite with sharp grain boundaries. Thus it appears that most of the arsenopyrite sulphide suites crystallized in the arsenopyrite-pyrite-pyrrhotite assemblage with some perhaps in the arsenopyrite-pyrrhotite-liquid assemblage. Other suites not analyzed by electron microprobe show a similar assemblage although pyrrhotite is sometimes in such small grains that hand specimen assignment must be done with caution.

III.4 Discussion

All samples analyzed fall within the arsenopyrite-pyrite-pyrrhotite or arsenopyrite-pyrrhotite-liquid assemblages of the Fe-As-S system. This assemblage may be represented at the shaded zone (phase boundary line ± error) in Figure III.3 after Kretschmar (1973, Figure 3-2 and Table 3-8).

Kretschmar estimates the error of his assemblage lines to be between ± 0.4 and ± 0.5 atomic per cent arsenic. This would correspond to an average temperature variation of ± 25°C.

Temperature error was determined graphically by intersections of mean

atomic per cent arsenic error envelope (the error envelope containing one standard deviation on either side of the mean) with assemblage composition x temperature curve envelope.

Table III.3 gives the temperature corresponding to microprobe analyses of atomic per cent arsenic by gold district.

Repeated analyses of asp 200 throughout the study should give a reasonable estimation of maximum maching error (Table III.2). All analyses were within the extremes found by Kretschmar and means and standard deviations were quite closely comparable. This should allow comparision of results found herein to those of Kretschmar.

Arsenopyrite crystals were generally analyzed in at least three spots: near the centre of the crystal, near the edge of the crystal, and once in between these spots. In a three dimensional sense this would be one near the crystal face and two at varying distances from crystal faces.

Crystal Zone	Number of Spot Analyses	Mean Atomic % As	One Standard Deviation
central	9	31.54	0.81
intermediate	41	32.29	0.86
face	36	32.18	0.97
overall	95	32.11	0.91

No significant difference in arsenic content can be seen between the zones of the crystals that were analyzed. Individual crystals show no

TABLE III.3

DISTRICT	n	ATOMIC % As	ONE s.d.	CRYSTALLIZATION T
Upper Seal Harbour	23	32.7	0.9	450 ± 70°C
The Ovens	12	31.9	0.5	419 ± 64°C
Cochrane Hill	10	32.5	0.2	457 ± 30°C
Salmon River	9	32.1	1.3	431 ± 100°C
Lawrencetown	9	32.1	0.7	431 ± 77°C
Lake Catcha	7	31.4	0.8	389 ± 63°C
Cranberry Head	5	32.3	0.7	444 ± 77°C
Goldenville	4	31.2	0.5	379 ± 47°C
Whiteburne	4	32.6	1.6	464 ± 100°C
Caribou	3	32.4	0.4	450 ± 40°C
Killag	3	31.2	0.4	379 ± 42°C
Molega	3	31.7	0.2	406 ± 46°C
Isaac's Harbour	2	32.0	0.1	431 ± 25°C
15 Mile Stream	2	31.2	1.7	379 ± 100°C
Gold River	1	31.1	-	374 ± -°C
OVERALL	95	32.1	0.9	432 ± 60°C

consistant trends in composition across their cross-sections. This indicates either constant conditions during arsenopyrite crystallization or coincidental inverse action of P-T and chemical factors. Most probably arsenopyrite crystallization occurred in all the gold districts within a similar set of physical-chemical conditions although local (within system) conditions varied over time.

To check the effect of Fe-As-S minerals as buffers to arsenopyrite composition, analyses of arsenopyrites taken near the surface of contact between pyrite and pyrrhotite grains were separated:

Arsenopyrite in Contact With	Number of Analyses	Mean Atomic % As	One Standard Deviation
pyrite	20	32.54	0.78
pyrrhotite	10	32.26	0.57
pyrite + pyrrhotite	4	32.52	0.44
overall	95	32.11	0.91

Analyses near pyrite grains averaged slightly higher in arsenic content and analyses adjacent to other Fe-As-S mineral grains exhibited marginally less scatter. Not enough variation from other analyses is present, however, to serve as evidence for any significant chemical variation during crystallization.

Eleven analyses were of arsenopyrites in the country rock: 32.60 mean atomic per cent, one standard deviation 1.05. This mean is slightly

higher (1/2 of one standard deviation) than analyses of vein arsenopyrite but not significantly so.

Variation of arsenic content between districts is generally not significantly different from variation in arsenic content within a single district. Differences in arsenic content of several times the machine error can be found within the same crystal as well as between crystals in the same specimen, specimens in the same district, and specimens from different districts (Appendix I).

The mean and standard deviation of all 95 acceptable analyses give a reasonable summary of arsenic content of arsenopyrite for the districts analyzed. No grouping of districts or trends within districts or within individual crystals separate themselves from these values. Thus, at this stage of testing the technique, it seems to broadly estimate the temperature at which arsenopyrite crystals in the gold-quartz districts under consideration crystallized: 432 ± 60°C.

CHAPTER IV

FLUID INCLUSIONS

1. Background

Fluid inclusions have been described and thought about geologically since the early nineteenth century (Sorby, 1858; Smith, 1953). Recent work with fluid inclusions is reviewed by Roedder (1967, 1972). Unless otherwise noted, the following discussion is summarized from Roedder (1967, 1972).

During the crystallization of a mineral and during fracturing after crystallization, any fluid in contact with it at that time may become entrapped in the crystal. If this fluid is trapped during crystallization, the result is a primary fluid inclusion. If fluid is trapped later, during recrystallization or fracturing, a secondary fluid inclusions results. A secondary fluid inclusion which forms when the fluid is essentially the same (pressure, temperature, and composition) as the fluid which was trapped during crystal growth is a pseudosecondary fluid inclusion.

Thus, fluid inclusions represent samples of fluids at some time in the geological history of the crystal. Just what that time is, is important in any interpretation of the crystallizing fluid made with the aid of fluid inclusions.

It is important to have criteria to differentiate the three types of

fluid inclusions. The only reliable criteria for recognition of primary fluid inclusions is to relate them to recognizable crystal faces. The inclusions are probably not primary however, if these crystal faces coincide with later fractures. Randomly placed inclusions far from others and unrelated to fractures are, more than likely, primary fluid inclusions. Pseudosecondary inclusions will more likely be associated with fracture planes than primary ones but their other properties will be the same. If fluid conditions were constant for long periods of time most fluid inclusions would be pseudosecondary. Secondary inclusions most commonly occur along planes marking fractures or dislocation surfaces. They can be identified by their divergent characteristics from nearby primary inclusions and may provide information about the later fluid history of the mineral.

This story is complicated if necking or leakage occurs. Necking is the process by which large inclusions reform into a set of smaller ones. If different phases are present in the original inclusions, the smaller ones may form with different fractions of the original fluid. Necking is generally easy to identify and its effects when analyzing fluid inclusions can be minimized by considering relatively isolated inclusions. Leakage is the addition or subtraction of material between entrapment and observation. Much has been written on this subject and is summarized by Roedder (1967, 1972) and Sawkins (1964). Leakage has been induced in the laboratory in large inclusions near polished sections at elevated temperatures. The pressure gradients from inclusion wall to atmospheric conditions in these investigations was, however, much in excess of any gradients likely in nature or in normal laboratory conditions. Smaller inclusions, even under severe

conditions, would be much less likely to have experienced leakage. The consistent results of fluid inclusions studies in zoned mineral deposits and zoned crystals within these deposits is the strongest evidence against significant leakage (Roedder, 1960; Schmidt, 1962; Hall and Freidman, 1962; Sawkins, 1964; etc.). If leakage were a major factor any original heterogeneities would tend to equilibrate to a low T-P condition. These studies have shown distinct, geologically reasonable fluid inclusion characteristics supported by independent observations such as stable isotope characteristics (Rye and O'Neil, 1968; Rye and Sawkins, 1974; Heyl, Landis and Zartman, 1974; Landis and Rye, 1974) and sulphide petrology.

The homogeneity of the original fluid and the physical and chemical conditions at the time of entrapment influence the fluid inclusion as it is seen in the laboratory. The fluid entrapped can be homogeneous, made up of two or more immiscible components, or have a gas phase. Water, with rare exceptions, is the dominant constituent of fluid inclusions. At subcritical conditions boiling can produce separate sets of liquid and gas inclusions. Carbon dioxide can produce two types of heterogeneous fluids: one resulting in liquid CO_2 where amount of CO_2 exceeds the amount soluble in the water solution; and the other resulting in CO_2 gas inclusions when crystallization is due to pressure release causing CO_2 effervescence.

A homogeneous fluid, entrapped at an elevated temperature and pressure will commonly evolve into a multiphase inclusion upon exhumation to near-surface conditions. As temperatures decrease, solubilities decrease

causing precipitation of salts, resulting in daughter minerals, and separation of gases such as CO_2.

The characteristic "bubble" is generally the result of surface tension holding the liquid portion into a smaller volume than the thermally expanded liquid entrapped at higher temperatures and pressures. This leaves a few sublimated water vapour molecules in the near vacuum of the bubble. If CO_2 were present in the fluid, CO_2 would be in the bubble also. As CO_2 solubility decreases it will separate into a gas phase. If CO_2 content were great liquid CO_2 could separate. Since CO_2 is markedly less dense than water at room temperatures and pressures, and water is virtually incompressible, the CO_2 will be a very compressed gas. This difference in gas phase characteristics allows easy empirical discrimination between CO_2 and H_2O vapour by observing an inclusion as the crystal is being crushed. A water vapour bubble will collapse while a CO_2 bubble will expand several orders of magnitude in size.

The temperature of entrapment can be estimated by heating the fluid inclusion until it homogenizes. This temperature is a minimum entrapment temperature for it must be corrected for pressure differences between the experiment and actual entrapment and for the salinity of the entrapped fluid. Salinity can be estimated by freezing the inclusion and comparing the temperature observed with the freezing temperature of pure water. These two values, homogenization temperature and salinity, can then be compared to experimental results of temperature-pressure behaviour of water of various

salinities (Burnham, et al., 1969; Kennedy, 1950a, 1954, 1957; Sourijan and Kennedy, 1962; Holser and Kennedy, 1959; Takenouchi and Kennedy, 1964, 1965; Maier and Frank, 1966; especially Klevstov and Lemmlein, 1959; all summarized in Figure IV.6. after Roedder, 1972). Unless an independent estimate of pressure or temperature can be made the homogenization temperature and the salinity only define a minimum entrapment temperature. However, pressure can often be ascertained on the basis of stratigraphic or petrological parameters, permitting introduction of the necessary pressure correction. Fluid inclusions therefore can be effective and reliable geothermometric tools. Conversely if the homogenization temperature and an independent temperature are known, fluid inclusion data can be used to estimate entrapment pressure. In this study an independent estimate of temperature is available from arsenopyrite analysis; thus, if fluid inclusions could be found in minerals which crystallized under the same conditions as the arsenopyrites, homogenization experiments might furnish an estimate of confining pressure during crystallization.

2. Procedures and instrumentation

Samples of vein quartz and carbonate from forty gold districts in Nova Scotia were collected and studied. Suitable specimens for fluid inclusion investigation were selected by examining small shards of carbonate and quartz under the transmitted-light microscope using oils of the same refraction index as the mineral. The oils present light dispersion which precludes resolution of objects inside the specimen.

Shards with fluid inclusions of sufficient size to allow distinction of phases were crushed while observing under the transmitted light microscope. A fairly low power ($\leq$ 192x) was necessary because specimens tended to move while being crushed making it difficult to observe individual inclusions throughout decrepitation. The crushing stage consisted of two rectangular brass plates. A hinge connected the plates at one narrow edge and a large screw at the other. A quartz disc was placed in a hole in the middle of each to allow light to pass through. A shard was placed on one quartz disc in a drop of water or oil of the proper refractive index. The two plates were then placed on top of one another and the screw set. The stage was placed under a transmitted light microscope and an inclusion was located. This inclusion was observed and the screw slowly tightened until the inclusion decrepitated. If the inclusion bubble contains only water vapour, the bubble will collapse. If the fluid inclusion contains CO_2 liquid or vapour, it will generate a bubble much larger than the original fluid inclusion which will then slowly dissipate.

Selected samples were then sectioned to approximately 0.5 mm (500μ) thickness, ground with 600 mesh grit on one side, and polished on the other. These chips were then thoroughly cleaned.

Polished chips were described and fluid inclusion characteristics noted and sketched.

Portions of the polished chip were then used in heating stage experiments and others used in cooling stage experiments. Inclusions were small

and their numbers great, so that relocation of individual inclusions after an experiment was usually impossible.

Heating stage and cooling stage experiments were conducted initially in the laboratory of F. J. Sawkins of the Department of Geology and Geophysics, University of Minnesota in Minneapolis, in December of 1973.

Further experiments were conducted at Dalhousie University on heating and cooling stages built by the author and modelled after apparatus at the University of Minnesota.

The heating stage consists of an aluminium cylinder 5.6 cm tall and 5.1 cm in inside diameter. This cylinder sits on a quartz disc. Upon a ledge on the inside of the cylinder rests another quartz disc upon which the sample is placed. An aluminum spacer is placed upon this and another quartz disc placed on top of this spacer, creating a wafer-shaped specimen chamber 1.0 cm high and 4.2 cm in diameter. Another aluminum spacer is placed over this and another quartz plate at the top of it and flush with the top of the aluminum cylinder. A resistance wire was coiled around the cylinder to provide a heat source and the whole oven enclosed in a box of asbestos board and the spaced packed with alumina insulation. The resistance coil is attached to a variable transformer to provide a heating control. Temperature is meausred by a chromelalumel thermocouple placed in the specimen chamber. The exact position of the thermocouple can be adjusted for each sample. The thermocouple is standardized in an ice-water bath and its output measured on a millivolt meter. The thermocouple was standardized at

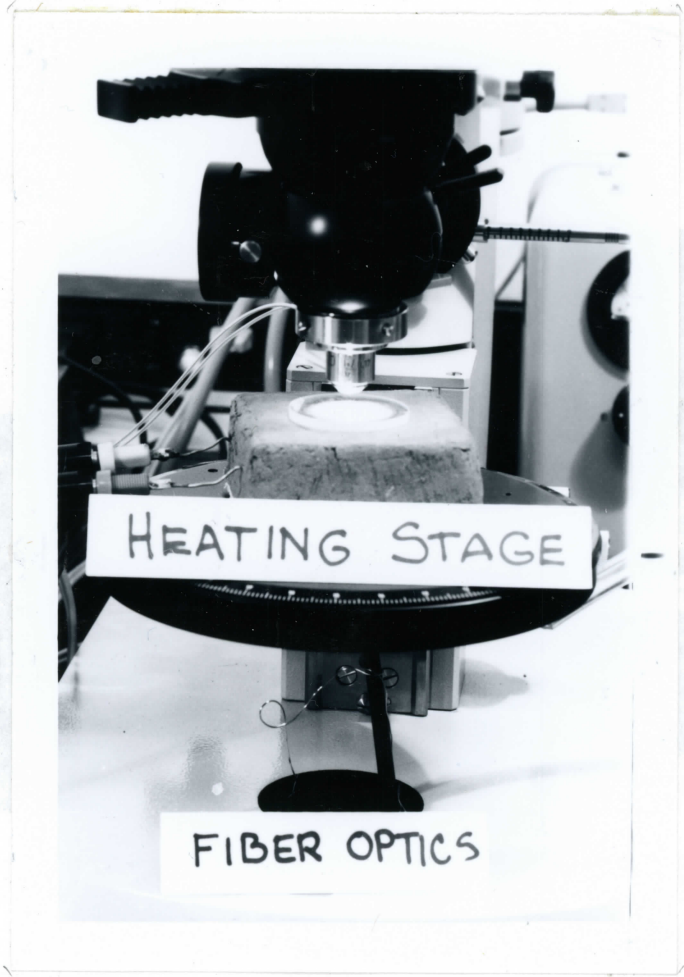

Figure IV.1. Heating stage.

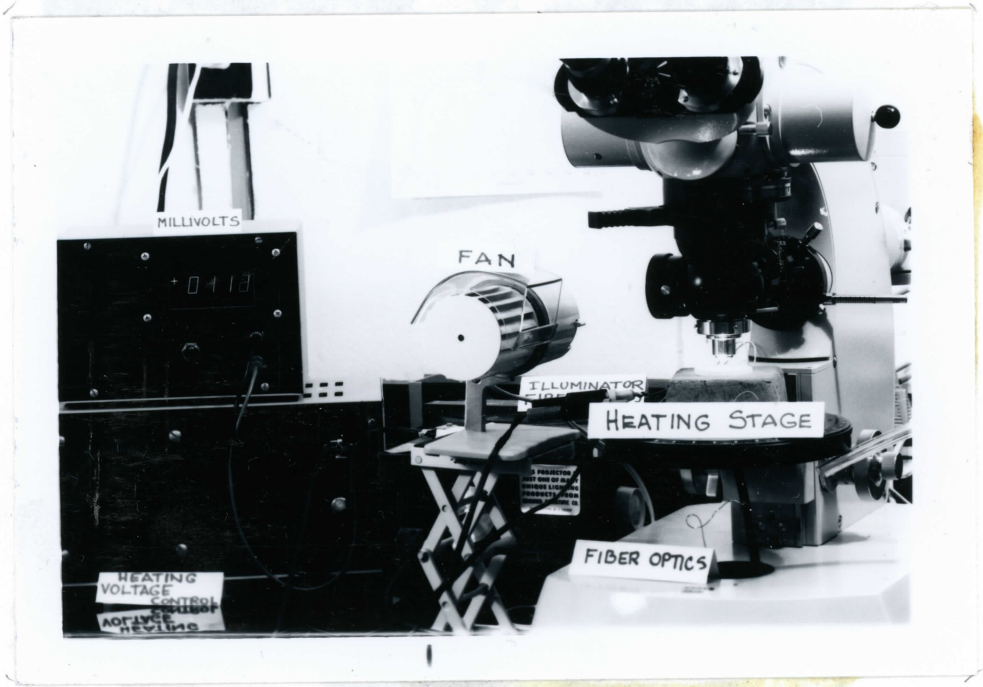

Figure IV.2. Heating stage.

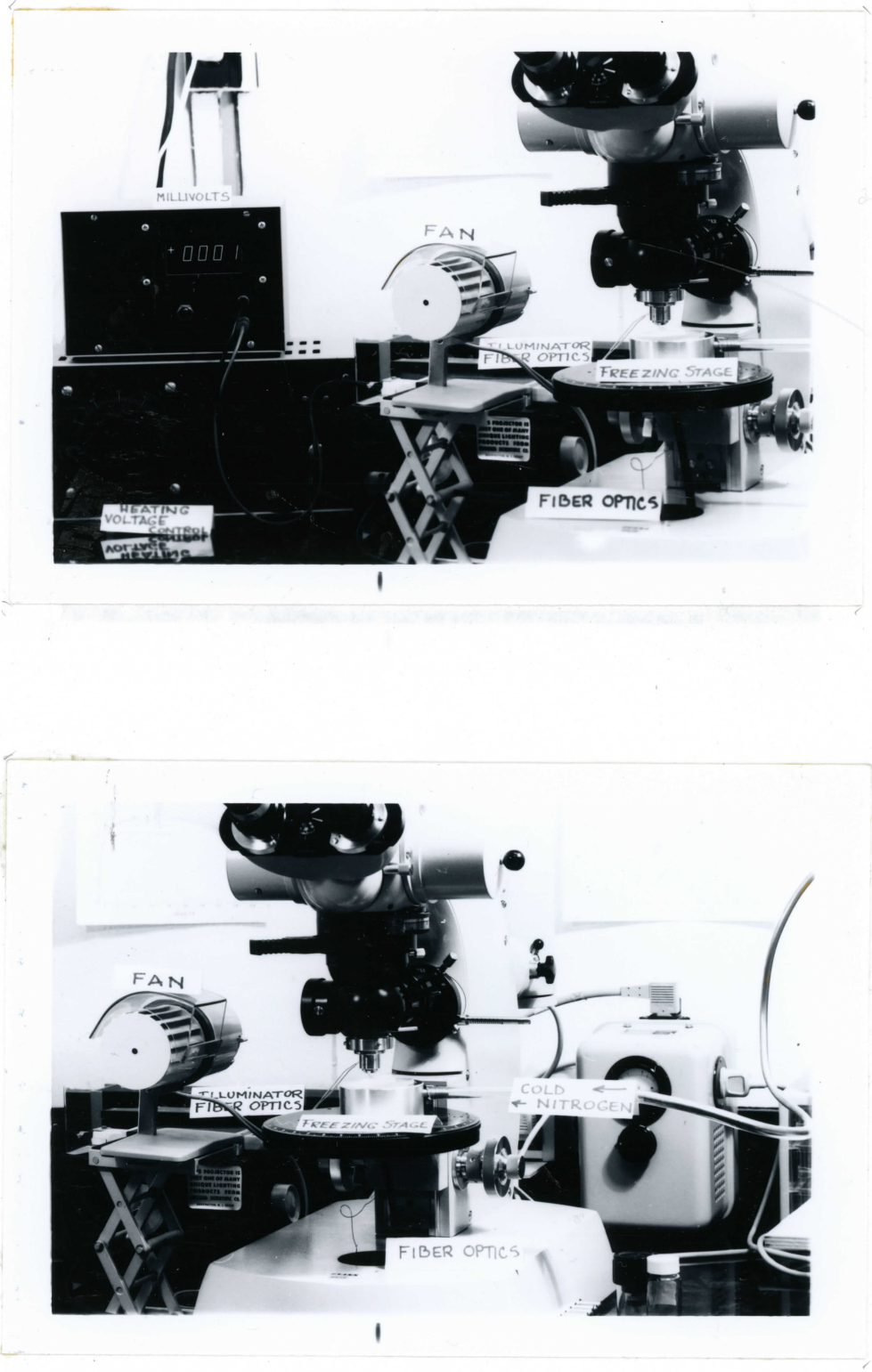

Figure IV.3. Freezing stage.

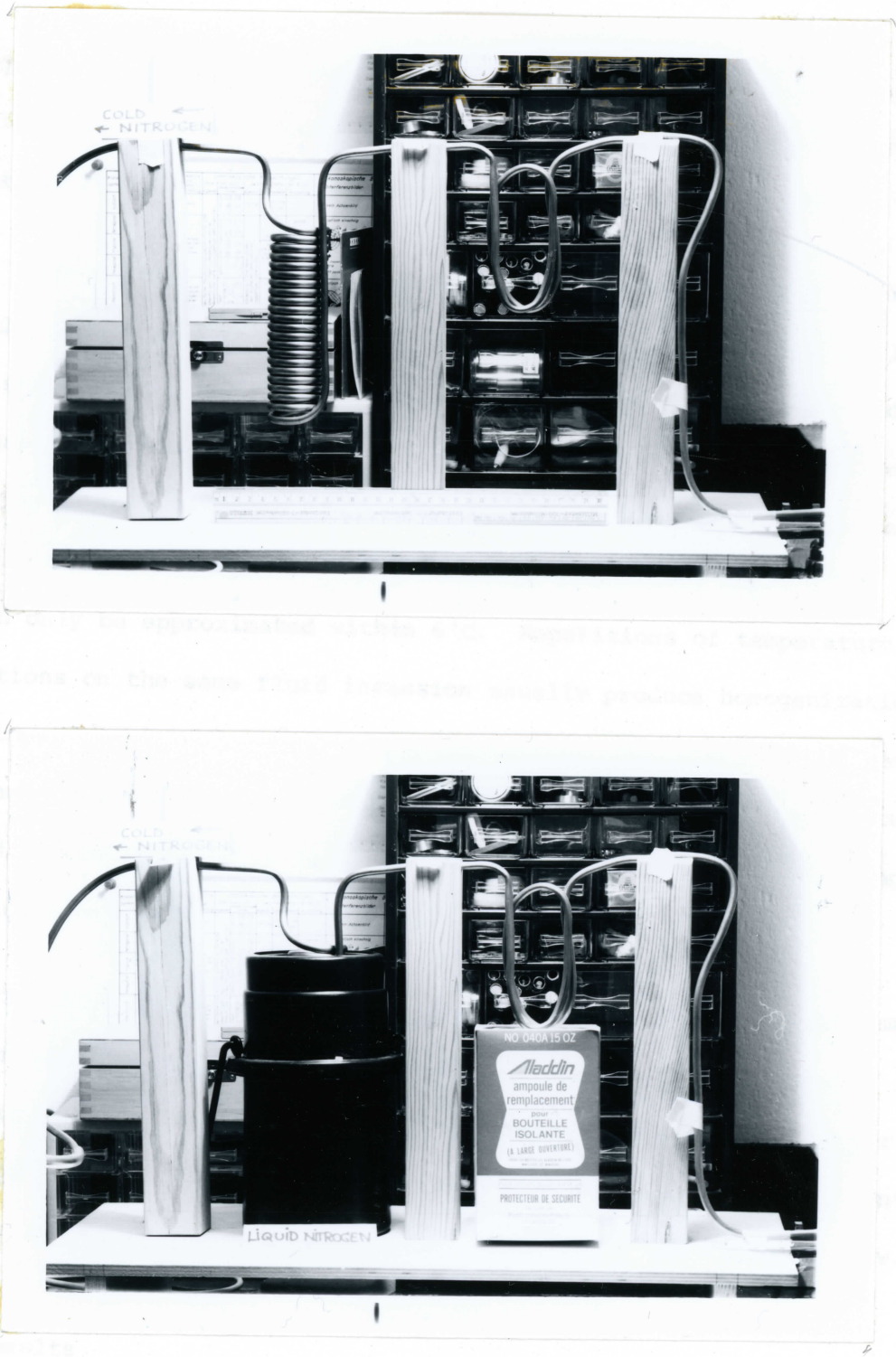

Figure IV.4. Cooling coils for gaseous nitrogen coolent of cooling stage.

frequent intervals with TEMPILSTIKS which melt at a given temperature. At least six different melting temperatures were used and calibrations were always linear. Calibrations could always be repeated to within 1°C.

Homogenization temperatures were difficult to determine accurately. As the bubble is heated it grows smaller until at a critical, small diameter the surface tension is enough to collapse it and it disappears suddenly. Before disappearance the bubble usually begins rapid motion inside the inclusion and the stopping of this motion is the last that can be seen of the bubble and is taken as the homogenization temperature (T_H). This point can often only be approximated within 6°C. Repetitions of temperature determinations on the same fluid inclusion usually produce homogenization temperatures within this error of approximation. The precision of the stage is therefore more than adequate vis-à-vis the accuracy of temperatures determined. Final approaches to T_H are done slowly to minimize any temperature gradients within the stage (Roedder, 1962; Sawkins, 1966).

The freezing stage follows a similar plan in dimension and temperature measurement but the temperature control is supplied by a stream of dry gaseous nitrogen cooled by passing the stream, enclosed in a copper tube, through vacuum jars of liquid nitrogen. The temperature can be controlled easily to within 0.2°C by varying the velocity of the nitrogen flow.

3. Results

Fluid inclusions found in specimens of vein quartz from various gold-

quartz districts of the Meguma platform of Nova Scotia showed little variation in type, or ratios of types, between specimens. Most samples showed thousands of fluid inclusions per 1-2 square centimeter chip. Exceptions exhibited severe undulose extinction. A few fluid inclusions could be found even in these strained crystals, but difficulties in seeing into these crystals could have allowed many inclusions to escape observation.

Most of the fluid inclusions are extremely small, being less than 5μ in diameter. These inclusions tend to be grouped together on planes and approach shapes of negative crystals. It is impossible to differentiate original growth planes from later glide or fracture planes in these quartz grains so inclusions occurring along planes are classed as secondary. The larger inclusions along these planes differ greatly in shape and size. These inclusions have vapour bubbles which vary in size but generally fall between about 20 and 5 per cent of the volume of the inclusion. Inclusions with large vapour bubbles are also present but in much smaller numbers. Many other inclusions are not related to any plane: these are most likely to be unaffected by necking and should be largely pseudosecondary. The range of inclusion size is not as great as those along planes and inclusions of 5 to 40μ are common. The vapour bubble has a narrower range of size in relation to fluid inclusion averaging about 10 to 20 per cent of the inclusion volume.

Solid phases were not observed in any fluid inclusions.

Crushing stage experiments resulted in vapour bubble expansion by several orders of magnitude when fluid inclusions were decrepitated in

refractive index oil (D5893A at 25°C; R.I. = 1.54). It was very difficult to observe an individual inclusion decrepitate because of the magnification necessary and the violent movements of the specimens; but all inclusions observed showed vapour bubble expansion. A double rimmed bubble could sometimes be seen before decrepitation indicating that the liquid CO_2 phase was present at room temperature.

Wetting characteristics and fluidity to vapour phase movements are consistent with the liquid phase of H_2O.

Freezing of the liquid phase was not observed. This could be due to the small size of the inclusions, prohibiting the nucleation of ice crystals (Roedder, 1963; Roedder, 1971), or the ice being invisible because of crystallization into only one transparent crystal (Roedder, 1962; Roedder, 1971; Roedder, personal communication 1974; Sawkins, personal communication, 1973). Salinities of these fluid inclusions is not great, however, for no solid phases exist. Cooling did increase the separation of liquid from gaseous CO_2 confirming observations of crushing experiments.

Heating stage experiments were limited by the optics required. Long focus objectives are necessary for focusing into the furnace limiting effective magnification to 320x. Inclusions of 20-40μ were used for most measurements.

Representative inclusions were sought which were isolated by at least several times their diameter from other fluid inclusions to avoid inclusions which had necked down during their history. Inclusions located in

planes tend to be flatter, larger, and closer together than isolated inclusions. Inclusions of both types were homogenized to see how they contrasted.

Figure IV.5. shows measurements of homogenization temperature recorded in this study. All inclusions measured were in quartz grains which were in intimate contact with carbonate and arsenopyrite grains. Fluid inclusions in carbonate grains occur along glide planes and are clearly secondary. Isolated fluid inclusions in carbonate grains are rare.

The isolated inclusions fall clearly within two groups: one larger group, mean T_H = 262°C ± 9.9°C (one standard deviation, n = 15); and one smaller group, mean T_H 210°C ± 6. °C (one standard deviation, n = 3). The grouped inclusions exhibit wide scatter (mean T_H 225°C ± 37.6°C, n = 8) but tend to have values dispersed about the smaller group of isolated inclusions.

These results are consistent with the assumption that isolated inclusions have not necked or leaked and define a large group of pseudosecondary inclusions and a smaller group of secondary inclusions. Measurements of inclusions in close proximity along planes which presumably define fractures or glide planes represent secondary inclusions which have necked and leaked to varying degrees.

If the pseudosecondary inclusions represent homogeneous fluids entrapped as the quartz crystal grew that entrapment could not have taken place below about 262°C ± 10°C. Any confining pressure at the time of

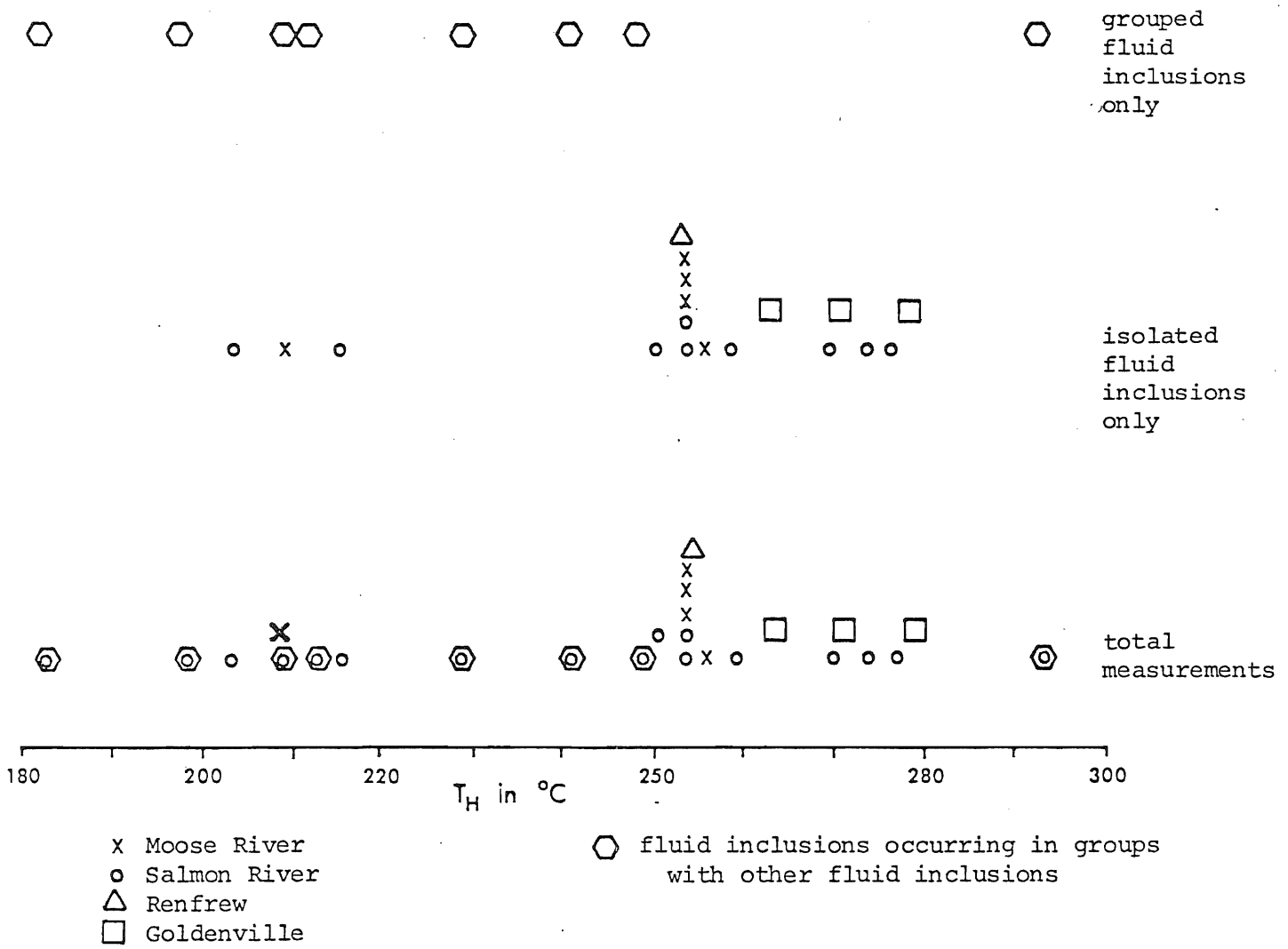

Figure IV.5. Fluid inclusion homogenization temperatures illustrating the two distinct groups of isolated fluid inclusions discussed in Chapter IV.

entrapment would raise this temperature.

By comparing P-T effects upon these fluid inclusions with experimental data on P-T effects of H_2O-CO_2-NaCl solutions as summarized in Figure IV.6. (after Roedder, 1965; after Kennedy, 1950a, Maier and Frank, 1966; and Lemmlein, 1956), an estimation of pressure can be obtained if an independent estimate of temperature is available. Figure IV.6 also plots temperature of entrapment against density (volume of liquid phase/volume of vapour phase) at room temperature and pressure. The density of a two phase fluid inclusion, in which the liquid is H_2O, is a function of the entrapment temperature alone if the fluid was entrapped below the critical conditions; or a function of both entrapment temperature and confining pressure if the fluid was entrapped above the critical conditions. If it is assumed that the fluid inclusions were entrapped at or near the time of crystallization of nearby arsenopyrite, a pressure may be estimated by using the independent arsenopyrite temperature from the previous chapter: 432 ± 60°C. This pressure estimate ranges from 1300 bars to 3200 bars at 0.0% salinity. As previously discussed, salinity is low: considerably less than five weight % NaCl equivalent (Roedder, 1972; Sawkins, pers. comm.). This salinity would raise the pressure limits slightly but not by more than a few hundred bars and most likely much less (Klevstov and Lemmlein, 1959). Therefore, if the previous assumptions estimate the history of the isolated fluid inclusions, a reasonable estimate of the confining pressure at entrapment, quartz crystallization, and arsenopyrite crystallization might be 2.3 ± 1.0 kilobars.

Figure IV.6. Pressure estimation for pseudosecondary fluid inclusions filling at 262 ± 10°C if initial filling was at the temperature estimated for arsenopyrite crystallization of 432 ± 60°C.

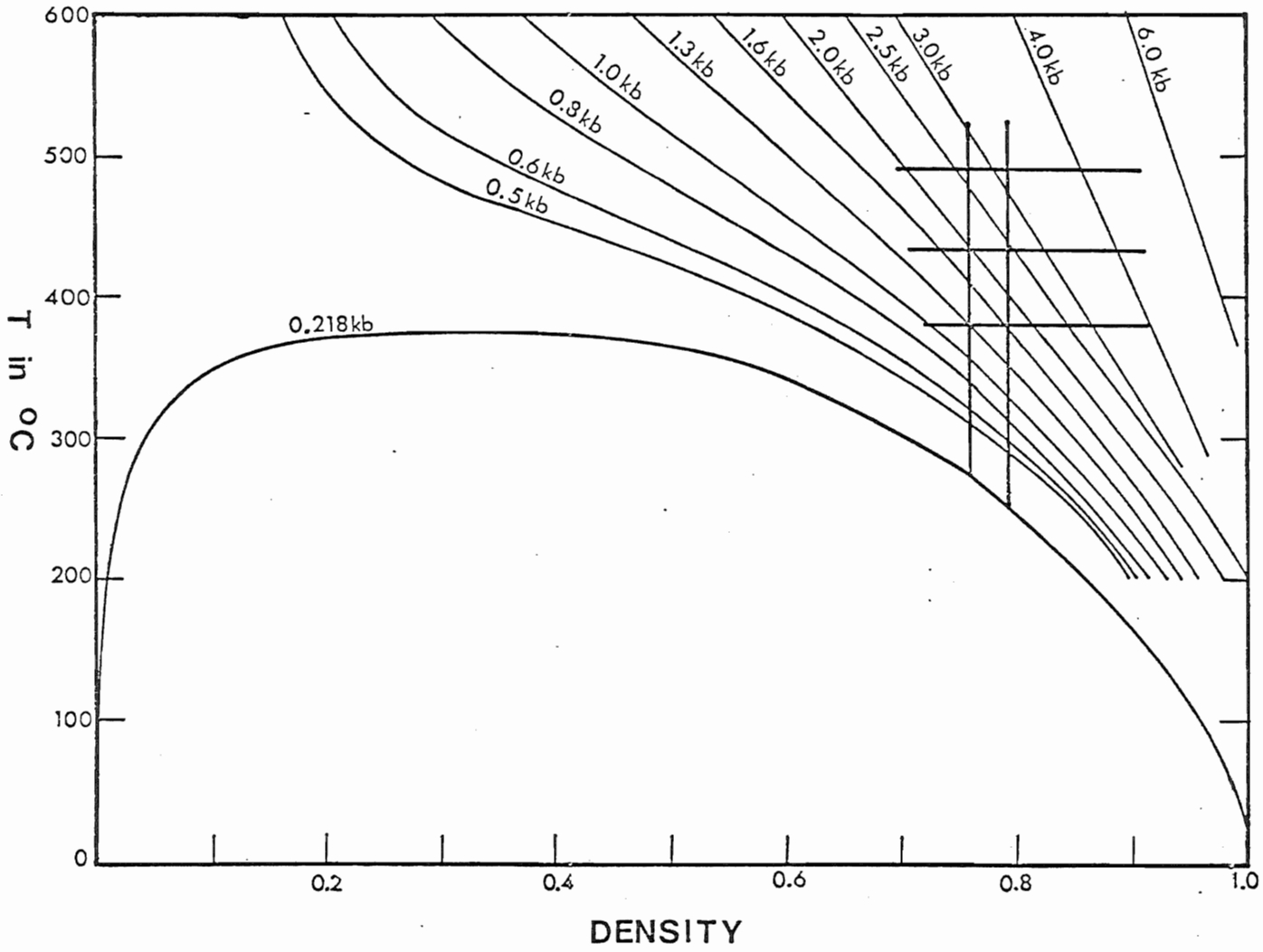
600
500
400
300
200
100
0
T in °C
0.218kb
0.5kb
0.6kb
0.8kb
1.0kb
1.3kb
1.6kb
2.0kb
2.5kb
3.0kb
4.0kb
6.0 kb
0.2
0.4
0.6
0.8
1.0
DENSITY

Figure IV.7 suggests interesting entrapment conditions for the secondary fluid inclusions. The lack of grades of regional metamorphism in the gold districts significantly higher than greenschist grade suggests that the temperature of the country rock probably at no time exceeded by more than 50-100°C the temperature of arsenopyrite crystallization. The lack of any wall rock alteration around the veins indicates that the crystallization temperature of the vein assemblages was not strikingly different from the surrounding country rock during the time of crystallization. Thus the arsenopyrite crystallization temperature of 432° ± 60°C closely approximates the maximum temperature of the vein and country rock assemblages. If the secondary fluid inclusions represent residual fluids remobilized along glide planes of quartz grains during deformation, their characteristics may give a clue to the P-T conditions during that deformation. If the deformation is related to post-crystallization folding of the quartz veins (see Chapters II and VII), the temperatures should not be appreciably lower since axial plane slaty cleavage is defined by greenschist grade metamorphic minerals. Under constant temperature conditions the secondary fluid inclusions estimate a pressure of about 3.3 ± 0.8 kilobars or about one kilobar higher than the primary entrapment pressure estimated by the pseudosecondary fluid inclusions and arsenopyrites. If real, this pressure difference could represent

1. less pressure in the original vein, perhaps aiding crystallization; or
2. an increase in tectonic stress from the time of initial entrapment to the time of folding.

Figure IV.7. Pressure estimation for secondary fluid inclusions filling at 210°C (T_H) if at temperature of arsenopyrite crystallization of 432 ± 60°C. (Pseudosecondary filling temperature 262 ± 10°C represented in smaller vertical lines.)

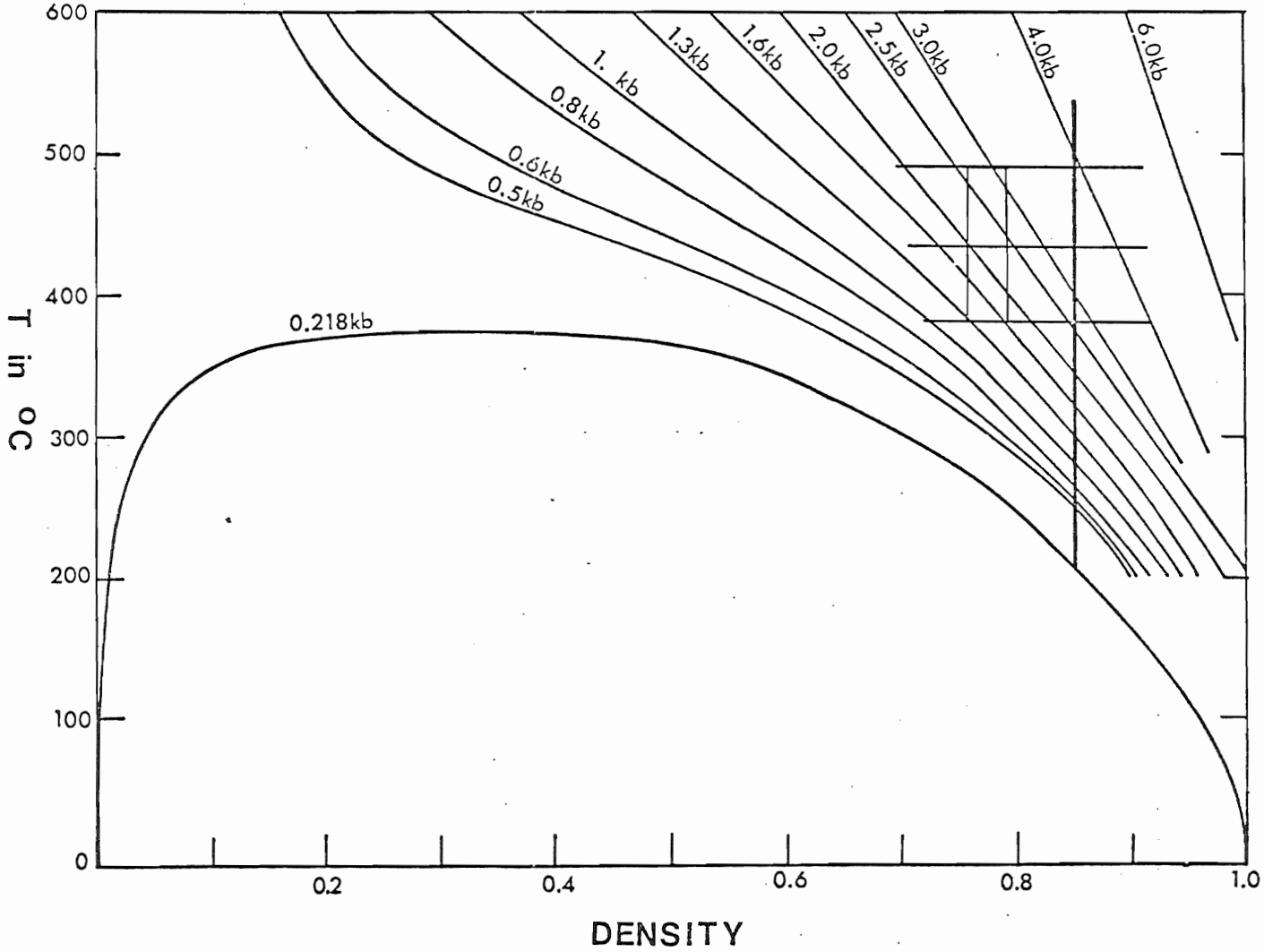
600
500
400
300
200
100
0
T in °C
0.218kb
0.5kb
0.6kb
0.8kb
1. kb
1.3kb
1.6kb
2.0kb
2.5kb
3.0kb
4.0kb
6.0kb
0.2
0.4
0.6
0.8
1.0
DENSITY

4. Summary

The observations and measurements of fluid inclusions considered in this study are discussed and listed below.

1. Visible fluid inclusions were separated into two categories. Fluid inclusions with wide size range which occur in planar groups of nearby inclusions are most likely secondary and necking probably affected a a large number of them. Fluid inclusions not related to planar groups and isolated from other fluid inclusions have smaller ranges of size and the proportion of that size occupied by the gase phase; these do not show necking features but could be pseudosecondary or secondary. Criteria for identifying primary fluid inclusions were lacking.

2. The fluid inclusion compositions are H_2O in a liquid phase and CO_2 comprising the bulk of the vapour phase. Salinities are low.

3. Isolated fluid inclusions from quartz grains intimately related spatially to carbonate and arsenopyrite grains exhibit homogenization temperatures which fall into two distinct groups. One large group averages 262°C (one standard deviation: 9.9°C) and most probably represent minimum entrapment temperatures of pseudosecondary fluid inclusions. Another group have lower temperatures of homogenization averaging 210°C (one standard deviation: 6.0°C): these are most likely secondary inclusions. Homogenization temperatures of fluid inclusions along planes and in groups show a wider scatter of values but tend to have values dispersed about the smaller, lower temperature group of isolated

inclusions.

4. An estimate of the confining pressure of entrapment can be made using homogenization temperatures of pseudosecondary fluid inclusions, estimates of arsenopyrite crystallization temperatures, and experimental data from other workers in the system H_2O-NaCl-CO_2. This pressure is 2.3 ± 1.0 kilobars.

CHAPTER V

DISCUSSION OF VEIN GENESIS

V.1. Introduction

The previous chapters have discussed observations on the gold-bearing quartz veins of the Meguma Group. Measurements of mineralogical parameters to estimate pressure and temperature conditions have also been made. This chapter will attempt to assemble those observations and measurements into a framework of constraints to models of vein genesis, setting the stage for discussing a consistent model of vein formation and its implications.

A brief summary of conclusions from the previous chapters which bear upon vein genesis follows: for more detailed discussion of these points consult the appropriate chapter.

1. For any volume of Meguma, strain features indicate relatively homogeneous history: burial conditions followed by pronounced compression in a SE-NW direction followed by a less pronounced horizontal compression in a E-W direction during which Devonian batholithic bodies were emplaced followed by a return to burial conditions.

2. Large regional folds and penetrative axial plane cleavage are the dominant strain feature and occurred in response to SE-NW compression.

3. Interbedded veins occur in slate beds between thicker quartzite beds.

Interbedded veins always occur in groups of parallel veins. All such groups have associated gold production. Cross veins occur throughout the Meguma Group rocks but are productive only where they intersect interbedded vein groups.

4. The interbedded veins are deformed in response to the same SE-NW compression as are the country rocks.

5. Interbedded quartz vein groups are preferentially located near anticlinal axes of major regional folds.

6. Interbedded quartz vein groups are located within the area of greenschist grade regional metamorphism. These metamorphic minerals define the axial plane cleavage. This cleavage is deflected by folded quartz veins as would be expected if the veins were a competent folded layer during cleavage formation. On the basis of the mineral assemblages, temperatures and pressures of this regional metamorphism may be estimated at the lower end of greenschist grade conditions: 300° to 500°C and 3 to 8 kilobars.

7. The regional metamorphic assemblage and the vein assemblage are similar. There is no "hydrothermal alteration" aureole around the veins.

8. The quartz veins under study exhibit a constant mineralogy which is always present where gold production is reported: dominantly quartz, secondly carbonate, minor amounts of arsenopyrite-pyrite-pyrrhotite, and country rock fragments. Chalcopyrite, galena, sphalerite, feldspar, rutile, scheelite, and gold are trace minerals.

9. In cross section, the minerals exhibit consistent relationships. Carbonate occurs in sharp contact with both vein walls and in crystal face terminations (open-space filling) in contact with quartz which occupies the median part of the vein. Sulphide minerals tend to be most abundant at the carbonate-wall rock contact and within the carbonate.

10. Gold is associated with areas of the veins with the most carbonate and sulphide minerals. These minerals are most abundant at vein rolls, irregularities, and thickenings. Small angular veins of similar mineralogy are more common at these same localities.

11. Contact metamorphic effects are a later overprint on the regional metamorphic greenschist assemblage and the vein mineral assemblage.

12. The arsenopyrite geothermometer estimates a temperature of vein crystallization of 432°C ± 60°C. Confining pressure of vein crystallization should not greatly affect this estimate.

13. The fluid inclusion compositions are H_2O in a liquid phase and CO_2 comprising the bulk of the vapour phase. Salinities are low: probably less than 5% NaCl by weight equivalent.

14. Using arsenopyrite geothermometry and fluid inclusion geobarometry a confining pressure estimate of 2.3 ± 1.0 kilobars for vein crystallization is obtained.

These observations allow limitations of relative time, physical conditions, chemical conditions, and stress conditions to be constructed for vein formation in relation to folding, cleavage formation, and regional metamorphism.

V.2. Discussion of observations and measurements relating to vein genesis

The temperature of vein crystallization is estimated by the arsenopyrite geothermometer discussed in Chapter III at 432°C ± 60°C. The arsenopyrite grains are intimately associated with the other major minerals of the veins. They have sharp contacts with pyrite, pyrrhotite and carbonate and are veined by quartz. Arsenopyrite grains in the country rock show no different associations or compositions from arsenopyrite grains in the veins. There are no significant differences between arsenopyrite associations or compositions among the districts: variations between districts being no greater than variations within hand specimen-scale samples. None of these observations is inconsistent with using the arsenopyrite compositions as an estimator of crystallization temperature of the veins.

Fluid inclusions near arsenopyrite-carbonate aggregates have characteristics identical to those in more central portions of a vein. Pseudosecondary fluid inclusions have consistent homogenization temperatures in all samples and districts where measurement was attempted. Since homogenization temperature is dependent up temperature and pressure of entrapment, these conditions appear to have been similar throughout any one interbedded quartz vein and among all interbedded quartz veins examined.

Pressures of entrapment estimated from homogenization temperatures and arsenopyrite compositions range between 1.5 and 3.5 kb.

Due to uncertainities resulting from the measurement techniques, only a rather broad estimation of pressure-temperature range of vein crystallization was possible but even this puts many restrictions on conditions of vein formation. Both temperatures and pressures are beyond primary or diagenetic conditions and are within the lower low grade regional metamorphic grade of Winkler (1974). No regional or local gradients are recognized.

Components of the veins do not display evidence of disequilibrium conditions with each other or with the regional metamorphic assemblages around them. Sulphide assemblages within the wall rocks are the same as within the veins and several arsenopyrite compositions measured in these wall rock assemblages were not significantly different in arsenic content and range of composition from arsenopyrite compositions in vein assemblages.

Interbedded veins have been folded by F_1 folds and deformed veins deflect an axial plane cleavage defined by greenschist regional metamorphic minerals. Thus vein crystallization had to occur after the onset of greenschist regional metamorphic conditions (as indicated by P-T estimates) but before F_1 folding and S_1 cleavage which were completed before greenschist conditions were completed as unoriented biotites and feldspar grains indicate. Vein crystallization could have been as late as incipient folding but their orientation at formation must have been essentially planar and

and horizontal. The stress conditions must have been essentially the same as those that resulted in F_1 and S_1 strain features: NW-SE horizontal maximum effective stress and vertical minimum effective stress.

The vein components are of constant ratios and textures throughout the interbedded vein districts. The textures indicate initial precipitation of carbonate from the vein walls, accompanied by sulphides and, followed by filling of the remainder of the vein by massive quartz. The temperature conditions during the formation of the veins cannot have exhibited prolonged periods of decrease, or the minerals defining cleavage would have stabilized in orientation before folding and not have continued to define axial planes. Thus precipitation by pressure decrease seems the most likely mechanism since chemical homogeneity exists between vein minerals and cement minerals throughout the region affected by greenschist regional metamorphism.

Sharp (1965) studied precipitation in H_2O solutions saturated with carbonate and silica. At temperatures greater than 300°C, quartz should precipitate in preference to carbonate by at least a ratio of 1000:1 because calcite solubilities are highest at lowest temperatures while quartz solubilities are highest at highest temperatures. Salinity differences will affect the temperature of onset of these conditions but not the amounts.

CO_2 in the system, however, greatly affects carbonate solubility (Sharp and Kennedy, 1965). At any constant CO_2 pressure calcite solubility increases exponentially with increasing temperature. A fluid rich in CO_2 will tend to precipitate carbonates if subjected to a substantial pressure

drop but any accompanying drop in temperature would redissolve the carbonate very rapidly (Sharp and Kennedy, 1965).

Thus it would appear that the only way to get the observed sequence of deposition under the P-T conditions estimated for vein formation would be a sudden substantial pressure drop followed by rapidly precipitated carbonate followed by rapidly precipitated quartz (Anderson and Burnham, 1965). The quartz must protect the carbonate from being rapidly redissolved by the solution and the carbonate must be deposited rapidly enough to keep from being overwhelmed in amount by the quartz. That CO_2 is present in the solutions is evident from the CO_2 content of the quartz fluid inclusions and the presence of carbonate itself in the wall rocks and the veins.

In summary, any mechanism of vein formation must satisfy the conclusions of this discussion.

(1) P-T conditions within 432°C ± 60°C and 2.3 ± 1.0 kilobars.
(2) Interbedded vein mineral assemblages appear to have crystallized in equilibrium with the surrounding country rock within greenschist regional metamorphic conditions.
(3) At formation, interbedded veins appear to have been essentially planar and horizontal in orientation.
(4) Vein formation took place under the same stress conditions that resulted in later F_1 folds and S_1 cleavage: NE-SW horizontal maximum effective stress and vertical minimum effective stress.
(5) The precipitation mechanism was most likely a sudden substantial drop in pressure and caused rapid precipitation of the vein minerals.

V.3. Evolution of hypothesis of gold district quartz vein genesis in the literature

At the initiation of this study, the prevailing view concerning the origin of the gold-bearing quartz veins appeared to be that the veins were genetically related to the post-tectonic granitic bodies: i.e. Rose (1970): "The deposits show a spatial relationship to the intrusive Devonian granites and appear to have been deposited from solutions generated by them."

The evolution of this particular genetic interpretation deserves careful consideration.

Since the first work on the gold districts in Nova Scotia the genesis of the veins has been controversial. W. Malcolm in his review of 1912 summarized the main point of contention:

> "Three different opinions have been held as to the origin of the solutions by which the fissures were filled:
>
> (1) that the minerals were deposited from descending solutions;
>
> (2) that they were dissolved out of the country rock;
>
> (3) that they were deposited from ascending fluids.
>
> Little evidence has been adduced in favour of the first, and the two most generally held are the second and third." (page 107).

J. W. Dawson, after inspection of the gold districts, concluded that " ... while certain field relations indicate that the veins were formed prior to the granite intrusion, the question of the source of the solutions is still open." (Dawson, 1878).

E. R. Faribault, who spent almost fifty years describing the gold districts, was more adamant about the relationship between the veins and the granites: " ... granite dykes and veins have been observed to always cut the interstratified quartz veins wherever they come in contact with them. The granite has thus no relation to the auriferous character of the veins, and need not again be referred to." (Faribault, 1899, page 1). This together with the observation that gold often occurred in the country rock led Faribault to contend that the minerals of the quartz veins were from the adjacent country rock. Faribault also envisioned a mechanism to form the quartz veins:

> "It was during the progress of the slow folding of the measures, that the rich quartz veins and large saddle-lodes of quartz were formed ..." (page 4).
>
> "In a certain thickness of sheets of paper or cloth, bent into an anticlinal fold, a slipping of the several layers on each other will take place, the sides of the fold will be tightly compressed, while, on top, openings will be formed. In the same manner in the folding of this great thickness of strata,

> the beds separated along the planes of stratification, and moved along these planes, the upper bed sliding upward on the lower inclined bed." (page 6).

No new mechanisms of vein emplacement have been mentioned in the literature, but his views on the origin of solutions and timing of events were rarely mentioned, much less agreed to.

Malcolm, who summarized Faribault's work disagreed with him in favour of ascending solutions:

> " ... the observed facts seem to be best explained on the theory that the veins were formed by the deposition of quartz, sulphides, and gold in cross fractures and interbedded openings occurring chiefly in the black or pyritous slate beds of the Goldenville formation, that the conditions necessary for the formation of the veins was a great deal of fracturing across the bedding planes, permitting the passage of ascending thermal solutions, and that these fractures were produced where the two horizontal orogenic forces manifested themselves in the formation of domes or plunging anticlines". (Malcolm, 1912, page 110).

Malcolm did not state, however, where the "ascending thermal solutions" had come from.

Waldemar Lindgren, in his fourth edition of Mineral Deposits, (4th edition, 1933), overlooking the field evidence presented by Faribault, hardens the stance of Malcolm: "The gold-bearing veins were probably formed soon after the granitic intrusion", (page 563). W. H. Emmons (1937) in his survey, Gold Deposits of the World seconds the motion: "The veins probably were formed in Devonian times in connection with the intrusion of the granite." (page 85). W. H. Newhouse (1936) turned "probably" into dogma with a study of polished sections of gold ores where he concluded that the quantity of gold varied with distance from the granite: "The solutions that formed the gold veins are believed to have come from the granite at depth, and the deposits are zoned to the large intrusive masses of granite, which acted as local heat centers." (page 830). Subsequent work and observations (e.g. Douglas, 1944) are based on the conclusions of Newhouse.

The present study confirms and generalizes the field relations as seen by Faribault. Granite emplacement occurred under very different conditions than vein formation. NW-SE maximum strain and regional metamorphism were completed when the granites were emplaced under E-W maximum compression.

The usual evidence for "ascending thermal solutions" of Malcolm, Lindgren, Emmons, and Newhouse; wall rock alteration in the sense of Lindgren; is lacking. Pressure and temperature estimates for wall rock regional metamorphism and vein crystallization are not different, which confirms field evidence for vein formation during and in equilibrium with greenschist regional metamorphism.

Newhouse divided the gold districts into three zones. The furthest zone contained one distrcit: West Gore. West Gore is an antimony producer with byproduction of gold. Mineralization consists of stibnite, native antimony, arsenopyrite, pyrite, and gold with quartz, calcite, and crushed slate making up the gangue. Mineralization is associated with near-vertical cross-cutting faults in Halifax slates very near the contact with carboniferous clastics (Stevenson, 1959). In mineralogy, location, geometry, and structural control West Gore is distinctly different from the rest of the gold districts of the Meguma and placing it in a zonal classification with them is misleading. The middle zone of Newhouse contains most of the gold districts. Within this zone he contends that production is related to distance from the granite: however, using the maps he uses, a linear correlation coefficient of -0.187 (r^2 = 0.051, n = 15) is obtained between miles from granite and production (NSDM Ann. Rept., 1967) which is not a significant trend. The inner group of Newhouse contains those districts within the contact metamorphic aureole of the granite: as discussed previously this post-dates vein formation.

In short, Faribault's observations are confirmed and his conclusions concerning timing and fluid origin are seen as much closer approximations to the truth than those of subsequent workers.

Faribault's mechanism of vein formation, however, does not satisfy the restraints placed upon it by the relative timing of events. If vein formation preceded folding, a mechanism dependent on folding cannot be invoked, and if vein formation accompanied incipient folding of a plastic deformation style, flexural slip would not be consistent with rock plasticity.

CHAPTER VI

PORE PRESSURE PHENOMENA

The formation of the interbedded veins considered in this study seems to take place in a differential stress field in a relatively short time. For a mineralizing solution to be available to enter a protovein in a short time it must be near at hand. The formation pore fluid of the surrounding rocks satisfies this criterion. This chapter will investigate the behaviour of formation pore fluids at elevated temperatures and pressures and under differential stress.

The Meguma Group rocks of the gold districts exhibit plastic deformation in the form of F_1 folds. They also exhibit brittle deformation preserved as interbedded quartz veins with open-space filling textures. The discussion of the previous chapter offers evidence for this brittle deformation occurring before the plastic deformation but under roughly similar P-T, chemical, and stress conditions.

If a differential stress is applied to a body of rock, its strain response can be indicated graphically by Figure VI.1. (after Ramsay, 1967, Figure 6-3).

Up to some level of stress (σ_1), the rock will deform elastically. Beyond a certain yield stress, σ_1 on the diagram, the rock will begin deforming plastically; that is, if the stress is released the rock will maintain its deformed state. The yield point is affected by temperature,

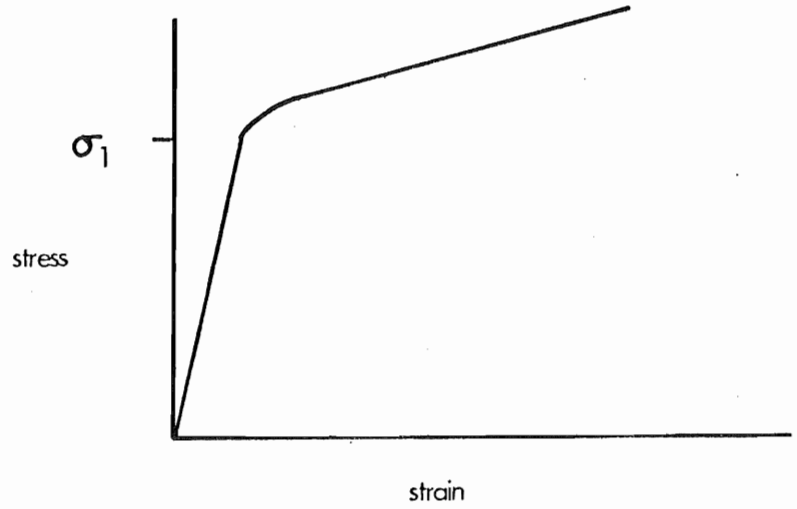

Figure VI.1. Generalized stress-strain relationships in elastic-plastic material. σ_1 = yield point dividing elastic behaviour at lower stress from plastic behaviour at higher stress.

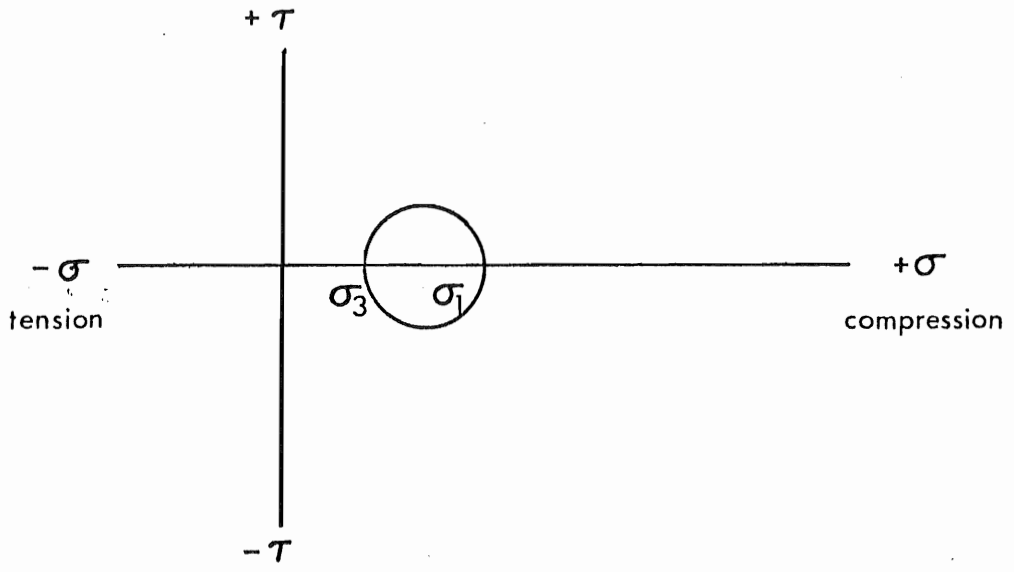

Figure VI.2. Differential stress represented on a Mohr diagram for stress. σ_3 = minimum compressive stress, σ_1 = maximum compressive stress.

pressure and strain rate; increasing with increasing confining pressure, decreasing with increasing temperature, and increasing with increasing strain rate.

Below the yield stress the rock may deform by sudden fracture: brittle failure.

The conditions of brittle failure may be seen clearly by using a Mohr diagram for stress. Normal stress is plotted on the abscissa and shear stress as the ordinate. Any differential stress may be shown as a circle centre $(\sigma, + \sigma) / 2$ and diameter $\sigma_1 - \sigma_3$. If σ_3 is held constant and σ_1 is gradually increased failure will occur at some critical differential stress.

If σ_3 is changed several times and σ_1 increased each time until failure, a curve connecting the tangents of the critical differential stress circles can be constructed. This is called a Mohr failure envelope and an example is shown in Figure VI.3.

These experiments are commonly carried out using triaxial testing apparatus in which the confining pressure is controlled with a confining jacket and a pressurizing fluid: thus σ_3 always equals σ_2. The deviatoric stress is imparted by a piston and can be varied continuously. Such empirical experiments tend to define parabolic failure envelopes (Ode, 1960; Ramsay, 1967). This behaviour is that predicted by Griffith (1921, 1925, cited in Secor, 1965; Brace, 1960) on the basis of the behaviour of

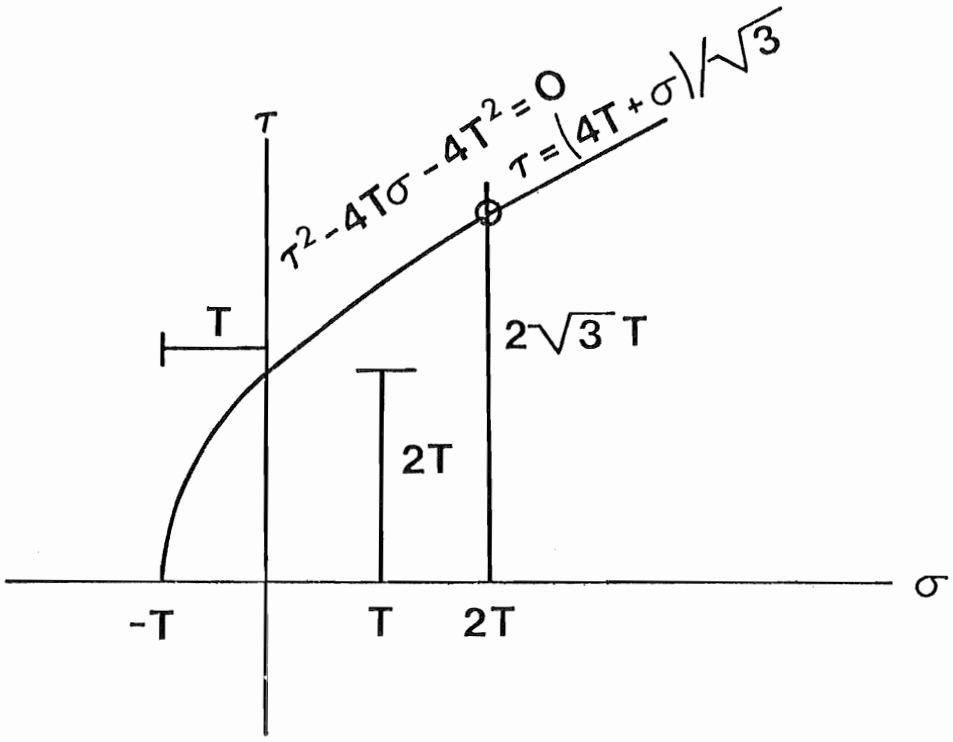

Figure VI.3. Mohr diagram for stress with failure envelope. τ = shear stress, σ= normal stress, T = tensile strength.

microscopic and submicroscopic cracks. In the compressive region the Griffith model predicts failure at levels which are too low: in this region failure is best predicted by a straight line closer to Coulomb criterion (McClintock and Walsh, 1962; Secor, 1965; Phillips, 1972). These two curves can be joined so that the Coulomb criterion corresponds to average experimental slopes found in experiments (Hubbert and Rubey, 1959, p. 124). Such a combined Mohr envelope is shown in Figure VI.3. (after Secor, 1965, Figure 1).

The point where the failure envelope intersects the τ axis marks the cohesive strength of the rock. It is twice as much as the tensile strength which is represented by the intersection of the failure envelope with the σ axis at -T.

The failure point is represented on Figure VI.4 by point P. The angle 2θ between tangent point P, the stress circle centre $(\sigma_1 ; - \sigma_3) / 2$, and the origin estimates twice the angle the resulting fractures will make with the maximum compressive stress (σ_1) axis.

Hubbert and Rubey (1959; Rubey and Hubbert, 1959) developed the theoretical considerations of the effect of pore fluid pressure on rock behavior under differential stress conditions in order to understand the mechanisms of overthrust faulting. (P. C. Gretener, 1969, offers a summary of Hubbert and Rubey's work, a practical review of subsequent work and examples of the theory's usefulness in predicting phenomena.) Hubbert and Rubey (1959) showed that the concept developed by Terzaghi (1936) in explaining soil stability by effective stress can be applied to rocks.

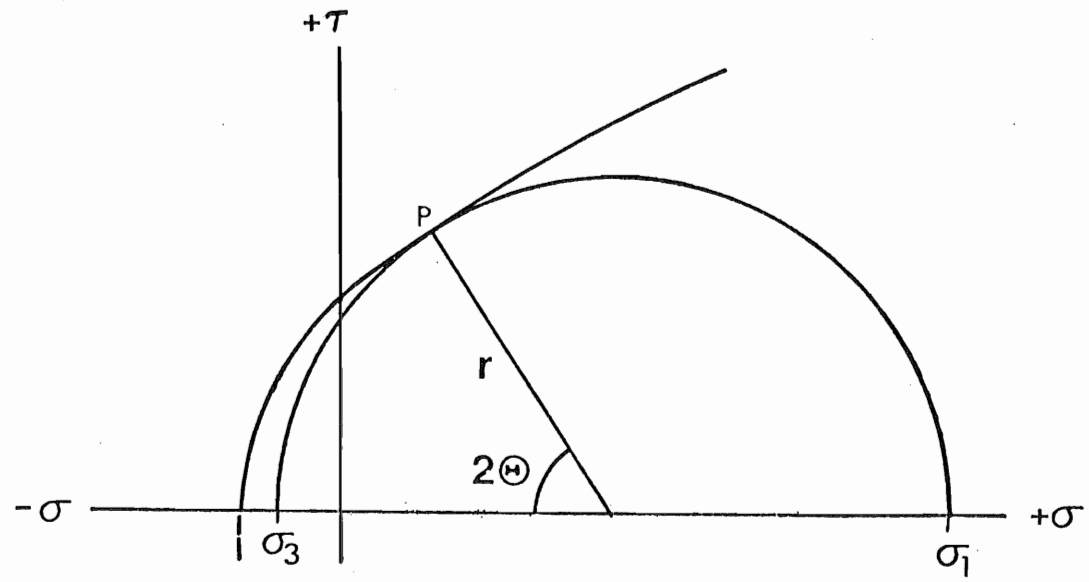

Figure VI.4. Mohr diagram for stress with failure envelope illustrating failure criterion. (After Secor, 1965, Figure 2). Further explanation in text of Chapter VI.

The concept can be summarized by $S = \sigma + p$ where total stress (S) is made up of an effective stress component (σ), which can be viewed as matrix stress or grain-to-grain pressure, and a fluid pressure component (p). Thus any change in the fluid pressure component under constant conditions will result in an opposite change in the effective stress component. The importance of this equation to the prediction of brittle behaviour lies in the apparent control of such failure only by the effective stress (σ) (Hubbert and Rubey, 1959). This prediction has been confirmed experimentally (Handin et al., 1963; Jaeger, 1963). Normal fluid pressure is equivalent to the weight of the water column at a given depth or the hydrostatic pressure. Fluid pressure levels below normal are rare in nature. High fluid pressures (overpressures, of petroleum technology) are common, however. If the total vertical stress is taken as the weight of the overburden ($S_d = \rho_B gd$ where S_d = overburden pressure or lithostatic pressure, ρ_B = bulk density of overburden, g = acceleration of gravity, and d = depth) or lithostatic pressure, a useful measure of fluid pressure is the ratio of the fluid pressure to the lithostatic pressure ($\lambda = P/S_d$). Normally (λ_n) the ratio is about 0.45, but the ratio cannot exceed 1.0. If λ equals or exceeds 1.0, the overburden, or lid, will lift to create more porosity thus lowering λ below 1.0. Values of λ in excess of 0.9 have been found in oil wells in Iran (Mostofi and Gansser, 1957).

Under differential stress conditions, the role of fluid pressure in porous rock is also important.

An increase in pore pressure in the rock represented would affect all

the stress directions equally, so that σ_z^1 becomes $\sigma_z-\Delta p$, σ_y^1 becomes $\sigma_y-\Delta p$, and σ_x^1 becomes $\sigma_x-\Delta p$. On a Mohr diagram, Figure VI.8., the implication is clear: the differential stress remains constant ($\sigma_z-\sigma_y = (\sigma_z-\Delta p)-(\sigma_y-\Delta p)$) but the ratio will increase ($\frac{\sigma z - \Delta p}{\sigma y \quad \Delta p} > \frac{\sigma z}{\sigma y}$); or, in other words, the differential stress is unchanged but the effectiveness is increased as the failure envelope is neared.

An instance of the practical application of this analysis is presented by Gretener (1969). Hydrocarbon wells are fractured to improve permeability of the producing horizon. The procedure is to close off the producing section of the well and then to raise the fluid pressure of that section. At a certain pressure (Pc) the interval fractures and fluid pressure drops (Pi) as fluid is injected into the interval. No difference in stress state has occurred, only an addition of fluid pressure until the differential stress was moved to the left on the appropriate Mohr construction to intersect the failure envelope (Figure VI.5.).

A similar effect can be invoked to explain the correlation of earthquake activity with injection of liquid wastes at the Denver arsenal in the mid-1960;s (Healy, et al., 1968; Gretener, 1969).

A more directly relevant application is the work of Secor (1965) in applying the concept of effective stress to joint formation. Joints are a widespread feature and geological evidence points to their formation as soon as a rock begins to deform brittlely. Lack of displacement and commonplace plumose markings indicate that they are tensional features. Traditional rock deformation theory, however, holds that tensional

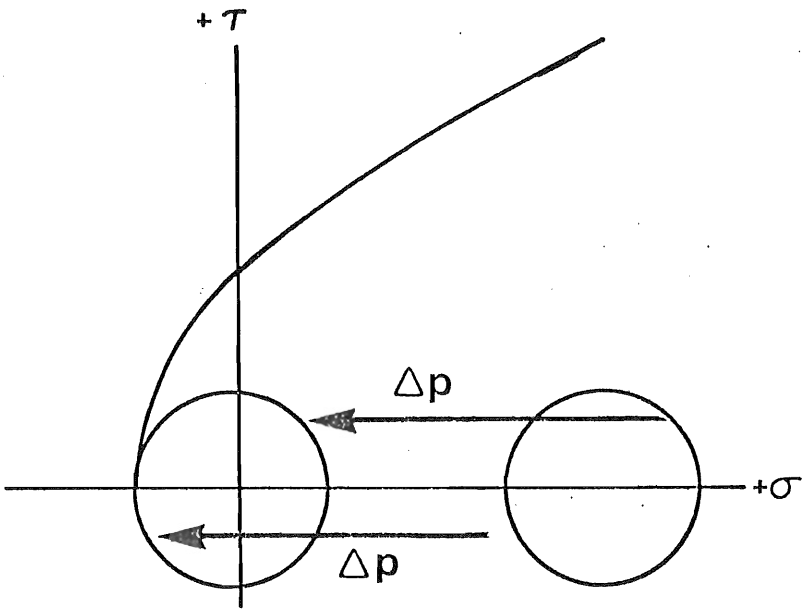

Figure VI.5. Mohr diagram for stress illustrating failure in tensile region as a result of an increase in pore fluid pressure ($\Delta\rho$).

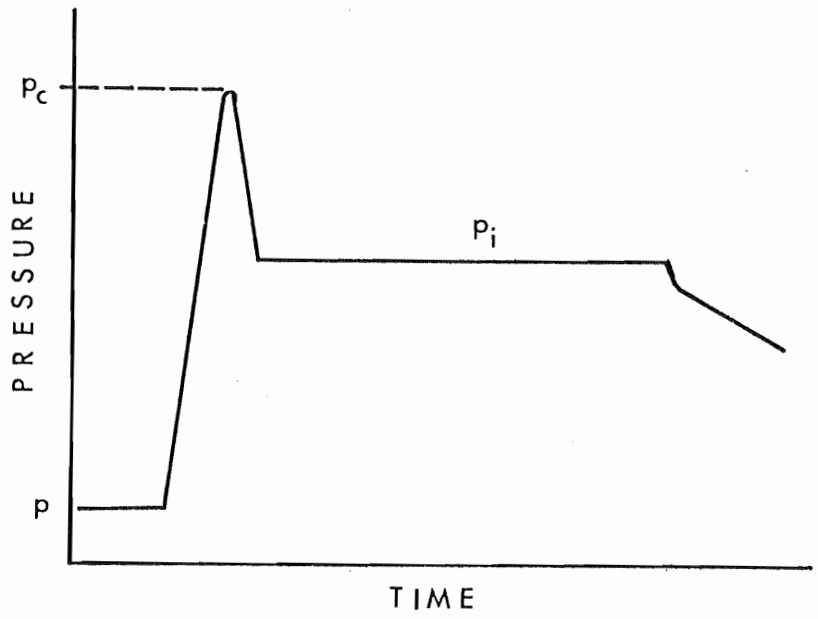

Figure VI.6. Generalized fluid pressure curve for a hydraulic fracturing operation in a petroleum well. (After Gretener, 1969, Figure 17).

conditions can only occur at very shallow depth and the observed relationships should be impossible.

One of the total principal stresses must be vertical if the Earth's surface is taken as a horizontal surface. This restricts the possible total stress field orientations to the three depicted in Figure VI.7 (after Secor, 1965, Figure 4).

The conditions for tension failure, as shown on a Mohr diagram, are $\sigma_3 = -T$ (Figure VI.8 , after Secor, 1965, Figure 3). If the differential stress becomes too large, the envelope can not be met in the zone of tension; thus, σ_1 cannot exceed + 3 T (Figure VI.8).

As discussed above, $S = \sigma + p$, $\lambda = \frac{P}{S_{vert}}$, and $S_{vert} = \rho_B gd$. Thus, $\sigma_{vert} = \rho_B gd\ (1-\lambda)$. Substituting for the maximum differential stress, the maximum depth of tension conditions can be seen to be $d_{max} = \frac{+3T}{\rho_B g(1-\lambda)}$ where the maximum stress is vertical and $d_{max} = \frac{3T}{n\rho_B g(1-\lambda)}$ where the intermediate stress is vertical, σ_1 being n times greater than σ_2 (Secor, 1965, 640-641). Substituting reasonable values for bulk density (ρ_B) and tensile strength (T), Secor found that jointing under extension could occur at great depths with only slightly abnormal fluid pressures even in weak rocks. The flow characteristics of Iranian oil wells under evaporite caps and very high λ's seem to confirm that open fractures can be maintained at considerable depths by pore fluid pressures (Mostofi and Gansser, 1957).

Using a similar analysis, it can be shown that under stress conditions where the minimum stress axis is vertical, that horizontal extension features

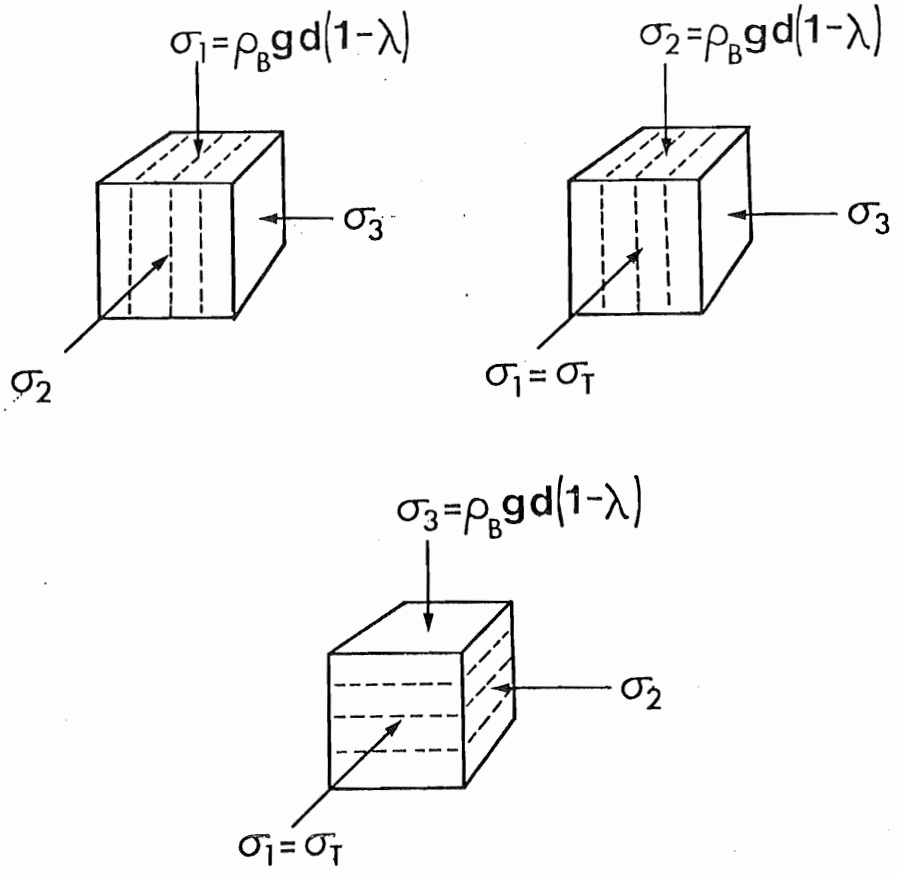

Figure VI.7. Three possible configurations of effective stress in the earth's crust and orientation of initial tensile failure. σ_1 = greatest effective stress, σ_2 = intermediate effective stress, σ_3 = least effective stress, $\rho_B gd\ (1-\lambda)$ = stress normal to earth's surface as a result of the bulk density of the fluid saturated rock (ρ_B), the acceleration due to gravity (g), the depth of overburden (d), and the ratio of pore fluid pressure to overburden.

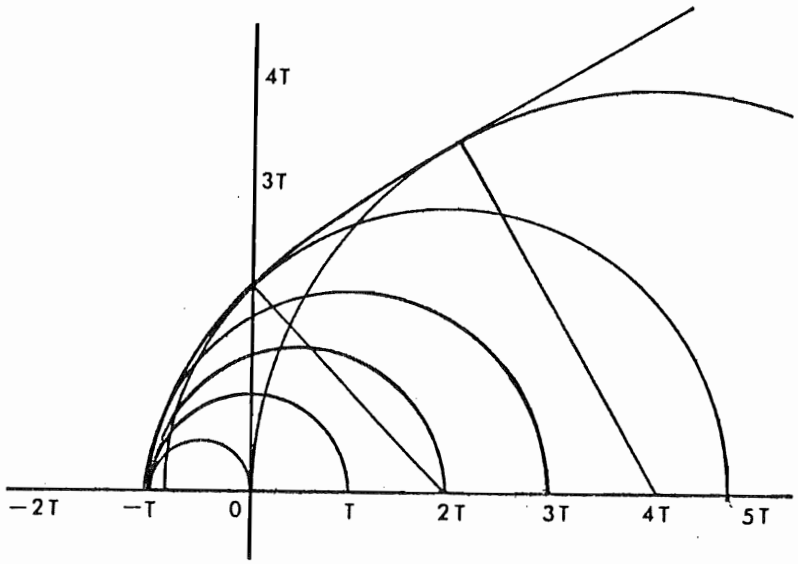

Figure VI.8. Mohr diagram for stress with failure envelope and a family of stress circles indicating failure criteria. (After Secor, 1965, Figure 3).

can be expected to form under moderate differential stress and elevated fluid pressure (see next chapter).

It has been shown above that an effective stress and a differential stress can induce brittle fractures under different conditions and at different orientations under elevated pore fluid pressures. A consideration of causes of above normal pore fluid pressure is therefore important.

The tendency in any abnormally pressured zone will be for the pore fluid to migrate or leak toward zones of more normal pressure. Due to this leakage, overpressuring must be a dynamic process. Furthermore, to maintain an overpressure for a geologically significant amount of time, leakage must be slower than active overpressuring. A process causing abnormal fluid pressure will thus be more effective if the permeability of the rock is low.

Three general methods of producing abnormal fluid pressures can be envisioned. First, the lithostatic pressure can be decreased. This could occur upon rapid removal of overburden outstripping the fluid's ability to re-equilibrate to the decreasing hydrostatic pressure (Watts, 1948).

Secondly, the pore space available for the fluid could be decreased. Compaction disequilibria are the most common example of this effect. As low permeability clays are compacted in subsiding basins, porosity decrease by compaction occurs. If the rate of compaction, as caused by sedimentation rate or tectonic loading is rapid, overpressuring commonly occurs (Hubbert and Rubey, 1959; Magara, 1973; Burst, 1969). Tectonic stresses

(σ_1 horizontal) could also cause compaction disequilibria (Hubbert and Rubey, 1959). Mineral precipitation into the pore spaces, if sufficiently rapid, would not only decrease pore space, but affect permeability and thus the leakage rate (Levorsen, 1954).

Finally, abnormal fluid pressure could be caused by an increase in the fluid volume. Artesian flow is an example of this mechanism (Hubbert and Rubey, 1959). The expansion of the pore fluid in response to increasing temperature is another example (Levorsen, 1954). Pore fluid can be added from outside by magmatic water influx or infiltration of gases (Platt, 1962; Tkhostov, 1963). Phase changes in the rock could potentially be the most effective causes of fluid input, especially where accompanied by volume changes (Bredehoeft and Hunshaw, 1968). Diagenetic reactions such as gypsum to anhydrite (Heard and Rubey, 1966) or montmorillonite to illite (Powers, 1967; Burst, 1969; Perry, 1972; Magara, 1975) produce large quantities of water and result in volume changes. Hydrous-anhydrous low grade regional metamorphic reactions also produce large volumes of water (Heard and Rubey, 1966).

In summary, it has been shown how extension features can be produced at depth in weak rocks if the pore fluid pressure is sufficiently but not prohibitively abnormal. The Mohr diagram for stress and the Mohr failure envelope allow visualization of the behaviour of rocks subject to varying stresses and fluid pressures and allow estimations of the orientations of

the predicted fractures. Lastly, methods of inducing abnormal fluid pressure were investigated and several must be considered in the history of the Meguma Group.

CHAPTER VII

CONCLUSIONS

In Chapter V it was shown that the interbedded quartz veins of the Meguma Group most likely crystallized at a temperature and pressure consistent with the regional metamorphic grade of the country rock, and that the vein minerals exhibited no evidence of P-T disequilibrium with the metamorphic minerals of the country rock. It was also shown that the attitude of the veins was essentially planar and horizontal when they crystallized; therefore, they were crystallized before F_1 folding.

The only way the observed vein mineral textures (carbonate before quartz) can be precipitated, at the P-T conditions which have been indicated, appears to be rapidly into open fractures.

The discussion of Chapter VI explained a way of analyzing the response of a rock to different stress conditions with special attention being paid to extension failure in a brittle manner under considerable depths, temperatures, and pore fluid pressure. In this chapter the history of the Meguma Group will be considered in terms of temperature, stress, pore fluid pressure and failure in light of the limitations to formation mechanisms discussed in Chapters V and VI.

For any gold district-sized block of Meguma Group rock, within the greenschist grade regional metamorphic zone, the geological sequence was similar.

Deposition of muds and silts was followed by compaction and diagenesis into shales and greywackes. Burial conditions continued but were soon overtaken in importance by tectonic conditions and the onset of regional

metamorphism. Horizontal groups of veins were formed and then the block was folded into F_1 regional-scale folds ending with the formation of S_1 penetrative axial plane cleavage. Regional metamorphism conditions peaked and ended soon after S_1 cleavage formation. Tectonic stresses than eased and shifted from NW-SE to E-W and brittle failure F_2 and F_3 kinks began to form. During these conditions granitic batholiths were emplaced into the Meguma and accompanying contact metamorphism overprinted or destroyed regional metamorphic fabrics. Kink formation and similarly oriented faulting continued after batholith intrusion. Return to burial conditions and exhumation mark the remainder of the history of the block of Meguma. Veining, F_1 folding, S_1 cleavage, and regional metamorphic features are pervasive throughout the block of Meguma under consideration, but kinks, batholiths, and contact metamorphic features may be more difficult to find in any individual block.

The relevant portion of this history to vein formation is that portion from deposition to the end of regional metamorphic conditions. This can be seen as a period of constantly increasing temperature although at varying rates. The stresses affecting the block of Meguma during this period of time was initially that of maximum stress vertical and increasing with burial. At some point before folding took place, this stress condition changed to that of a tectonic maximum stress oriented NW-SE with vertical stress becoming the least stress axis orientation.

The pore fluid conditions in the block of Meguma under consideration should be dependent on character and changes of permeability, porosity, and

fluid supply. From deposition the muds and silts which would become the Meguma would have had poor permeability. Initial porosity of pelitic sediments can be as great at 50%. As compaction proceeded this porosity would become considerably reduced causing hydrodynamic conditions as the water in the initial porosity moved toward more hydrostatic areas. Flyschoid sediments have poor lateral continuity along with poorly permeable shale components making any block as well as any shale bed poorly permeable. Rock types such as this are commonly overpressured in subsiding basins (Hubbert and Rubey, 1959; Gretener, 1969; Perry, 1972; Burst, 1969; Powers, 1967): the American Gulf coast being an example. Diagenetic reactions would tend to dewater mixed layer clays and remove water from less mature clays toward illite which is stable at higher temperatures (Burst, 1969; Magara, 1975). Both compaction and clay diagenesis will tend to decrease porosity, decrease permeability, and increase pore fluid; all of which tend alone to produce overpressured conditions. As temperature increase and burial pressure continue into the realm of metamorphism and each increases in rate as tectonic stress conditions supersede burial conditions, all three causes of overpressure intensify as clays dewater to chlorites and muscovites; and porosity and permeability further decrease with increasing confining pressure. Upon completion of regional metamorphism, water production from within the block should cease. Cementation will be essentially complete, stabilizing porosity and permeability changes. Reorientation of the fabric by establishing a penetrative cleavage should temporarily, at least, improve permeability

(Alterman, 1973; Powell, 1972; Leith, 1905; Siddans, 1972; Maxwell, 1962; Powell, 1974; Wood, 1974). Evidence of failure during this time period is not inconsistent with the temperature, stress, and pore fluid history of the block of Meguma under consideration. Plastic failure in the form of F_1 folding deforms and thus follows brittle extension failure preserved as interbedded quartz veins.

To get a clearer view of the nature of this failure, let an individual greywacke/quartzite-shale/slate-greywacke/quartzite sequence be considered.

At the temperature of vein formation greenschist grade metamorphic reactions should be active: completing the transformation of clay minerals to muscovite-group mica minerals, chlorites, and water; and transforming the muscovites and chlorites to aluminum-richer chlorites, quartz and water (Winkler, 1974 for discussion of reactions). All reactions produce water and completely transform the shales into less water-rich mineral constituents. Reactions in the shales must make up the bulk of the water production in to shale-silt/sand sequence. This pore fluid increase in the shales would tend to flow towards areas of less pore fluid pressure: towards and into the coarser grained units. Pore pressure in a shale unit would thus tend to be less near coarser grained units and greater at the centre of the shale unit. This trend would be aggravated by decreasing porosity at the margins of the dewatering shale unit. The centres of these shale units are often locations of interbedded quartz veins. The representation of such extension features on Mohr stress diagrams are dependent upon elevated pore pressure (Secor, 1965). Figure VII.1 represents the

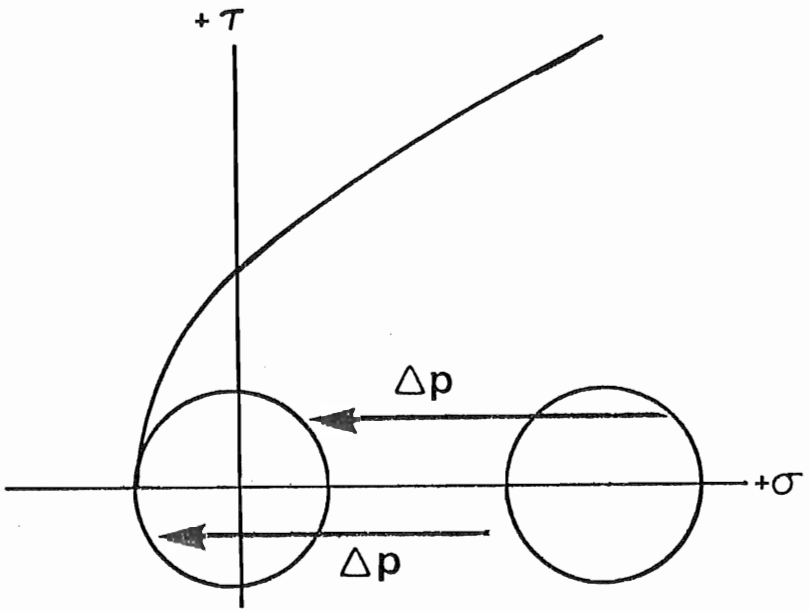

Figure VII.1. Mohr diagram for stress illustrating failure in tensile region as a result of an increase in pore fluid pressure ($\Delta\rho$).

conditions at failure: σ_1 = maximum stress, σ_3 = minimum stress, σ_1' = maximum effective stress at failure, and σ_3' = minimum effective stress at failure.

For such extension features to be horizontal, σ_1 must be horizontal and σ_3 vertical. These conditions could have been met, in the block of Meguma under consideration, during tectonic conditions before plastic failure.

If the interbedded quartz veins represent pre-plastic extension failure due to hydraulic fracturing, the history of rock failure or deformation in the block of Meguma containing a group of such veins may now be summarized.

Elastic deformation takes place after deposition during compaction and diagenesis while temperature and overburden pressure increase as porosity and permeability decrease. Pore pressure will tend to be elevated throughout but present analogs of subsiding basins indicate overpressuring would probably be insufficient for brittle failure although diapiric effects on various scales could be initiated.

As the temperature and burial pressure continue to increase a tectonic pressure begins to act on the block. The combined temperature-pressure conditions instigate fluid-producing reactions of greenschist regional metamorphism. The production of water is at a rate faster than escape from the rock, as permeability is low, causing increasing pore fluid pressures. This overpressuring reaches critical values in some slate units and hydraulic extension fractures are generated parallel to the maximum effective

stress as predicted by the Mohr diagram for stress. The porosity is thus increased and the pore pressure reduced below critical levels.

The continued increase in temperature soon results in plastic failure of the rock as a whole and regional plastic folds are generated. Axial plane slaty cleavage forms, rotating preferential permeability to the vertical and further decreasing pore fluid pressure. Plastic failure ceases, probably in response to combined P-T decrease, for regional metamorphism soon ends and post-plastic brittle deformation defines another stress orientation.

Implications of hydraulic fracturing as a process of vein formation

Certain limits are placed upon the constituents of the fluid and the way in which they will precipitate if hydraulic fracturing caused the formation of the veins.

The mechanism depends on excess pore fluid pressure, and its release by flowing into the new pores it has helped create. At the temperatures and pressures in this case, the pore fluid must be largely a metamorphic fluid made primarily of products and reactants in the greenschist reactions: H_2O, CO_2, and quartz-feldspar-chlorite-muscovite constituents. Salinity should be low as should heavy metal content. Heavy metals could be contributed from molecules which were adhered to illite grain surfaces as the illite dewatered to form muscovite and chlorite but the contribution would not be great. These limitations on fluid content do not seem to be

exceeded by the fluid inclusion compositions or mineralogy of the veins, although more CO_2 in the fluid inclusions and carbonate in the veins is found that might be expected. Although both are known to be components of greenschist reactions, their absolute importance is little understood (Winkler, 1974).

Carbonate solubility in aqueous solutions increases with increasing pressure, but this effect is masked by an exponential decrease in solubility with any temperature increase (Ellis, 1963; Sharp and Kennedy, 1965; Sharp, 1965). Aqueous NaCl solutions saturated with respect to silica at temperatures above 300°C should not contain significant carbonate in solution (Sharp, 1965). The other major constituent of the fluid in question, however, significantly affects the solubility of carbonate. "... at constant temperature the solubility increases steadily as the partial pressure of CO_2 increases exponentially." (Sharp and Kennedy, 1965, p. 391). Thus, the presence of carbonate in the vein mineral assemblage is most likely directly dependent on the partial pressure of CO_2 at the time of crystallization.

If the veins are produced by hydraulic fracture, the pore fluids will move into the initial fracture over a pressure drop. The initial pore fluid pressure is $P_{H_2O} + P_{CO_2}$. Both components will respond similarly to the total pressure drop unless H_2O becomes subcritical at the decreased pressure. This would occur at such low pressures that the effect could only be instantaneous: supercritical conditions resuming with any repressuring. When the partial pressure of CO_2 drops as the

pore fluid enters a fracture, the temperature effect would make carbonate virtually insoluble in the solution and very rapid precipitation would be expected at the fracture walls. A small amount of silica would be expected to precipitate also, in response to the drop in P_{H_2O}. As the fluid pressure built back up to previous levels either as the fluid filled the fracture or the fracture closed ($S_v = \rho_B gd$) the carbonate would tend to redissolve unless the precipitated silica, which would redissolve more slowly, protected it.

As gravity closed the fracture, the pore fluid which flowed into the fracture would begin to hold the fracture walls apart ($\lambda > .465$) and cease further closure at a pore fluid pressure less than that of the pore fluid pressure responsible for the fracture ($\lambda >> .465$). Thus the fracture would continue for some time to have a lower pore pressure than the surrounding rock and pore fluids from them would tend to circulate into the fractures provided the permeability was sufficient. This could explain why veins are more commonly found where a significant amount of the wall rock is quartzite rather than slate. If the fracture were in slate only, flow would not be of great enough volume to supply the silica to preserve the fracture: a small carbonate band or an unfilled parting may be all that remains to mark the fracture. If circulation was established with a coarser grained and thus more permeable unit, however, enough circulation might be expected to allow precipitation of significant quantities of quartz.

Summary

A mechanism for the formation of horizontal veins under tectonic

stress conditions and greenschist regional metamorphism has been proposed which depends upon excess pore fluid pressure produced by metamorphic reactions and low permeability of pelitic rocks of the Meguma Group. Enough slate must have been present to allow critical build-up of pore-fluid but not so much as to inhibit the establishment of pore fluid circulation with more permeable quartzite units which was necessary to provide fluid volume needed to precipitate the observed quantity of silica.

The constituents of the veins and fluid inclusions would be expected to produce the observed paragenesis under the pressure, temperature, metamorphic and time conditions of this rapid, brittle-failure mechanism.

REFERENCES

Alterman, I. B., 1973. Rotation and dewatering during slaty cleavage formation: some new evidence and interpretations. Geology, 1, pp. 33-36.

Ami, H. M., 1900. Synopsis of the geology of Canada. Trans. Roy. Soc. Can., new series, VI, pp. 187-226.

Anderson, G. M. and Burnham, C. W., 1965. The solubility of quartz in supercritical water. Am. J. Sci., 263, pp. 494-511.

Arnold, R. G., 1962. Equilibrium relations between pyrrhotite and pyrite from 325° to 743°C. Econ. Geol., 57, pp. 72-90.

Barton, P. B., Jr., 1969. Thermochemical study of the system Fe-As-S. Geochim. et Cosmochim. Acta, 33, pp. 841-857.

Barton, P. B., Jr., 1970. Sulfide petrology. Mineral Soc. Am. Spec. Paper 3, pp. 187-198.

Barton, P. B. and Toulmin, P., 1961. Some mechanisms for cooling hydrothermal solutions. U. S. Geol. Surv. Profess. Paper 424D, pp. 348-352.

Bell, W. A., 1929. Horton-Windsor district, Nova Scotia. Geol. Surv. Can. Mem. 155.

Bell, W. A., 1960. Mississippian Horton Group of type Windsor-Horton district, Nova Scotia. Geol. Surv. Can. Mem. 314, pp. 2-17.

Benson, D. G., 1974. Geology of the Antigonish Highlands, Nova Scotia. Geol. Surv. Can. Mem. 376.

Bird, J. M. and Dewey, J. F., 1970. Lithosphere plate-continental margin tectonics and the evolution of the Appalachian Orogen. Bull. Geol. Soc. Am., 81, pp. 1031-1060.

Black, P. M., 1974. Oxygen isotope study of metamorphic rocks from the Ouegoa District, New Caledonia. Contrib. Mineral. Petrol., 47, pp. 197-206.

Boyle, R. W., 1955. The geochemistry and origin of the gold-bearing quartz veins and lenses of the Yellowknife greenstone belt. Econ. Geol., 50, pp. 51-66.

Boyle, R. W., 1966. Origin of the gold and silver in the gold deposits of the Meguma Series, Nova Scotia. Can. Mineralogist, 8, pp. 662.

Boyle, R. W., 1974. The geochemistry of gold and its deposits. Bull. Can. Inst. Mining Met., 67, number 743, pp. 61.

Brace, W.F., 1960. An extension of Griffith theory of fracture to rocks. J. Geophys. Res., 65, pp. 3477-3480.

Brace, W.F., 1961. Mohr construction in the analysis of large geologic strain. Bull. Geol. Soc. Am., 72, pp. 1059-1080.

Bredehoeft, J. D. and Hanshaw, B. B., 1968. On the maintenance of anomalous fluid pressures I. Thick sedimentary sequences. Bull. Geol. Soc. Am., 79, pp. 1097-1106.

Bredehoeft, J. D., Raleigh, C. B., and Healy, J. H., 1974. Control of earthquakes at Rangely, Colorado. Bull. Am. Assoc. Petrol. Geol., 58, pp. 1432.

Burnham, C. W., Holloway, J. R., and Davis, N. F., 1969. The specific volume of water in the range 1000 to 8900 bars, 20° to 900°C. Am. J. Sci., 267-A, pp. 70-95.

Burst, J. F., 1969. Diagenesis of Gulf Coast clayey sediments and its possible relation to petroleum migration. Bull. Am. Assoc. Petrol. Geol., 53, pp. 73-93.

Cameron, H. L., 1938. Preliminary geological report on the Johnson Brook area Country Harbour Mines, Guysboro County, Nova Scotia. N. S. Dept. Mines, Ann. Rept., part 2, pp. 29-35.

Campbell, J. D., 1958. En Echelon folding. Econ. Geol., 53, pp. 448-472.

Carstens, H., 1966. Deformation in vein genesis. Norsk. Geol. Tidsskr., 46, pp. 299-307.

Chapman, R. E., 1974. Clay diapirism and overthrust faulting. Bull. Geol. Soc. Am., 85, pp. 1579-1602.

Clark, A. H., 1964. Preliminary study of the temperatures and confining pressures of granite emplacement and mineralization, Panasqueira, Portugal. Trans. Inst. Mining Met., 73, pp. 813-824.

Clark, A. H., 1965. The composition and conditions of formation of arsenopyrite and leollingite in the Ylojarvi copper-tungsten deposit, southwest Finland. Bull. Comm. Geol. Finlande, number 217, 56 pp.

Clark, L. A., 1960a. The Fe-As-S system. Variations of arsenopyrite composition as a function of Tand. P. Ann. Rept. Director Geophys. Lab., Year Book 59, pp. 127-130.

Clark, L. A., 1960b. The Fe-As-S system: phase relations and applications. Econ. Geol., 55, pp. 1345-1381, 1631-1652.

Clark, L. A., 1960c. Arsenopyrite As:S ratio as a possible geobarometer. Bull. Geol. Soc. Am., 71, pp. 1844.

Coleman, L. C., 1957. Mineralogy of the Giant Yellowknife gold mine, Yellowknife, N.W.T. Econ. Geol., 52, pp. 400-425.

Cooke, H. C., 1946. Canadian lode gole areas. Can. Dept. Mines Res. Econ. Geol. series, number 15, Ottawa, pp. 1-4, 8-9, 79-81.

Cormier, R. F. and Smith, T. E., 1973. Radiometric ages of granitic rocks, southwestern Nova Scotia. Can. J. Earth Sci., 10, pp. 1201-1210.

Crook, K. A. W., 1974. Lithogenesis and geotectonics: the significance of compositional variation in flysch arenites (graywackes). Soc. Econ. Paleontol. Mineral., Spec. Publ. 19, pp. 304-310.

Crosby, D. G., 1962. Wolfville map-area, Nova Scotia. Geol. Soc. Can., Mem. 325, 67 p.

Dandurand, J. L., Fortuné, J. P., Pérami, R., Schott, J., and Tollon, F., 1972. On the importance of mechanical action and thermal gradient in the formation of metal-bearing deposits. Mineral. Deposita, 7, pp. 339-350.

Dawson, J. W., 1878. Acadian Geology, (third edition). London.

DeGrazia, A. R. and Haskin, L., 1964. On the gold content of rocks. Geochim. et Cosmochim. Acta, 28, pp. 559-564.

Desborough, G. A. and Carpenter, R. H., 1965. Phase relations of pyrrhotite. Econ. Geol., 60, pp. 1431-1450.

Douglas, G. V., 1948. Structure of the gold veins of Nova Scotia. Structural Geology of Canadian Ore Deposits, Can. Inst. Min. Met., pp. 919-926.

Drummond, R., 1918. Minerals and Mining, Nova Scotia. Mining Record Office, Stellarton, Nova Scotia, 368 p.

Ellis, A. J., 1959a. The solubility of carbon dioxide in water at high temperatures. Am. J. Sci., 257, pp. 217-234.

Ellis, A. J., 1959b. The solubility of calcite in carbon dioxide solutions. Am. J. Sci., 257, pp. 354-365.

Ellis, A. J., 1963. The solubility of calcite in sodium chloride solutions at high temperatures. Am. J. Sci., 261, pp. 259-267.

Emmons, W. H., 1937. Gold Deposits of the World. McGraw-Hill, New York, 562 p.

Fairbairn, H. W., Hurley, P. M., Pinson, W. H., and Cormier, R. F., 1960. Age of the granitic rocks of Nova Scotia. Bull. Geol. Soc. Am., 71, pp. 399-414.

Fairbairn, H. W., Hurley, P. M. and Pinson, W. H., 1964. Preliminary age study and initial Sr^{87}/Sr^{86} of the Nova Scotia granitic rocks by the Rb-Sr whole rock method. Bull. Geol. Soc. Am., 75, pp. 253-256.

Faribault, E. R., 1886-1939. Annual Reports of the Geol. Surv. Can. and numerous maps and plans of gold districts published by the Geol. Surv. Can.

Faribault, E. R., 1899. The gold measures of Nova Scotia and deep mining. J. Can. Mining Inst., II, pp. 119-128.

Fyson, W. K., 1964. Folds in the Carboniferous rocks near Walton, Nova Scotia. Am. J. Sci., 262, pp. 513-522.

Fyson, W. K., 1966. Structures in the lower Paleozoic Meguma Group, Nova Scotia. Bull. Geol. Soc. Am., 77, pp. 931-944.

Fyson, W. K., 1967. Gravity sliding and cross folding in Carboniferous rocks, Nova Scotia. Am. J. Sci., 265, pp. 1-11.

Gibbons, R. V., 1969. Geology of the Moreton's Harbour area, Newfoundland with emphasis on the environment and mode of formation of the arseno-pyrite veins. Unpubl. M.Sc. thesis, Memorial University of Newfoundland, St. John's, Newfoundland.

Goldthwaite, J. W., 1924. Physiography of Nova Scotia. Geol. Surv. Can., Mem. 140, 179 p.

Gretener, P. E., 1969. Fluid pressure in porous media - its importance in geology: a review. Bull. Can. Petrol. Geol., 17, pp. 255-295.

Griffith, A. .A, 1921. The phenomena of rupture and flow in solids. Roy. Soc. London Phil. Trans., Series A, 221, pp. 163-198.

Griffith, A. A., 1925. The theory of rupture. International Congress Applied Mechanics, First, Delft 1924 Proc., pp. 55-63.

Groves, D. I. and Solomon, M., 1969. Fluid inclusion studies at Mount Bischoff, Tasmania. Trans. Inst. Mining Met., Bull. 747, 78, pp. B1-B11.

Haas, J. L., Jr., 1971. The effect of salinity on the maximum thermal gradient of a hydrothermal system at hydrostatic pressure. Econ. Geol., 66, pp. 940-946.

Hall, W. E. and Friedman, I., 1963. Composition of fluid inclusions, Cave-in-Rock Fluorite district, Illinois, and Upper Mississippi Valley zinc-lead district. Econ. Geol., 58, pp. 886-911.

Handin, J. H. and Hager, R. V., Jr., 1958. Experimental deformation of sedimentary rocks under confining pressure: tests at high temperature. Bull. Am. Assoc. Petrol. Geol., 42, pp. 2892-2934.

Handin, J. H., Hager, R. V., Jr., Friedman, M., and Feather, J. N., 1963. Experimental deformation of sediment rocks under confining pressure: pore pressure tests. Bull. Am. Assoc. Petrol. Geol., 47, pp. 717-755.

Handin, J. H., Friedman, M., Logan, J. M., Pattison, L. J., and Swolfs, H. S., 1972. Experimental folding of rocks under confining pressure: buckling of single-layer rock beams. Am. Geophys. Union, Geophys. Mon. 15, pp. 1-28.

Hanshaw, B. B. and Bredehoeft, J. D., 1968. On the maintenance of anomalous fluid pressures II. Source layer at depth. Bull. Geol. Soc. Am., 79, pp. 1107-1122.

Harrison, R. B., 1938. Paragenesis of minerals in Nova Scotia gold ores. N. S. Dept. Mines, Ann. Rept., part 2, pp. 5-11.

Healy, J. H., Rubey, W. W., Griggs, D. T. and Raleigh, C. B., 1968. The Denver earthquakes. Science, 161, pp. 1301-1310.

Heard, H. C. and Rubey, W. W., 1966. Tectonic implications of gypsum dehydration. Bull. Geol. Soc. Am., 77, pp. 741-760.

Helgeson, H. C. and Garrels, R. M., 1968. Hydrothermal transport and deposition of gold. Econ. Geol., 63, pp. 622-635.

Heyl, A. V., Landis, G. P., and Zartman, R. E., 1974. Isotopic evidence for the origin of MIssissippi Valley-type mineral deposits: a review. Econ. Geol., 69, pp. 992-1006.

Hobbs, B.E., McLaren, A. C., and Paterson, M. S., 1972. Plasticity of single crystals of synthetic quartz. Am. Geophys. Union, Geophys. Mon. 15, pp. 29-53.

Holland, H. D., 1965. Some applications of thermochemical data to problems of ore deposits. II. Mineral assemblages and the composition of ore forming fluids. Econ. Geol., 60, pp. 1101-1166.

Holser, W. T. and Kennedy, G. C., 1958. Properties of water. Part IV. Pressure-volume-temperature relations of water in the range 100-400°C and 100-1400 bars. Am. J. Sci., 256, pp. 744-754.

Holser, W. T. and Kennedy, G. C., 1959. Properties of water. Part V. Pressure-volume-temperature relations of water in the range 400-1000°C and 100-1400 bars. Am. J. Sci., 257, pp. 71-77.

Hubbert, M. K. and Rubey, W. W., 1959. Mechanics of fluid-filled porous solids and its application to overthrust faulting. Bull. Geol. Soc. Am., 70, pp. 115-166.

Jackson, C. T. and Alger, F., 1829. A description of the mineralogy and geology of a part of Nova Scotia. Am. J. Sci., 15, pp. 132-160, 201-217.

Jaeger, J. C., 1963. Extension failures in rocks subject to fluid pressure. J. Geophys. Res., 68, pp. 6066-6067.

Jameson, B., 1974. The granite contact near Uniacke, Nova Scotia. Unpubl. B.Sc. thesis, Dalhousie University, Halifax, Nova Scotia.

Jones, R. S., 1970. Gold content of water, plants, and animals. U. S. Geol. Surv. Circular 625, 15 p.

Kelley, D. G., 1967. Cobequid mountains. Geol. Surv. Can., Paper 67-1, Part A, pp. 175-176.

Kennedy, G. C., 1950a. A portion of the system silica-water. Econ. Geol., 45, pp. 629-653.

Kennedy, G. C., 1950b. Pressure-volume-temperature relations in water at elevated temperatures and pressures. Am. J. Sci., 248, pp. 540-564.

Kennedy, G. C., 1954. Pressure-volume-temperature relations in CO_2 at elevated temperatures and pressures. Am. J. Sci., 252, pp. 225-241.

Kennedy, G. C., 1957. Properties of water. Part I. Pressure-volume-temperature relations in steam to 1000°C and 100 bars pressure. Am. J. Sci., 255, pp. 724-730.

Kennedy, G. C., Knight, W. L., and Holser, W. T., 1958. Properties of water. Part III. Specific volume of liquid water to 100°C and 1400 bars. Am. J. Sci., 256, pp. 590-595.

Kennedy, G. C., Wasserburg, G. J., Heard, H. C., and Newton, R. C., 1962. The upper three-phase region in the system SiO_2-H_2O. Am. J. Sci., 260, pp. 501-521.

King, L. H., 1972. Relation of plate tectonics to the geomorphic evolution of the Canadian Atlantic provinces. Bull. Geol. Soc. Am., 83, pp. 3083-3090.

Klein, G. de V., 1962. Triassic sedimentation, Maritime provinces, Canada. Bull. Geol. Soc. Am., 73, pp. 1127-1146.

Klevtsov, P. V. and Lemmlein, G. G., 1959. P corrections to the homogenization temperatures of NaCl aqueous solutions. Dokl. Akad. Nauk. U.S.S.R., 128, pp. 1250-1253. Translated in Acad. Sci. U.S.S.R. Dokl., 128, numbers 1-6, pp. 995-997 (1960).

Krauskopf, K. B., 1951. The solubility of gold. Econ. Geol., 46, pp. 858-870.

Krauskopf, K. B., 1971. The source of ore minerals. Geochim. et. Cosmochim. Acta, 35, pp. 643-659.

Kretschmar, U., 1973. Phase relations involving arsenopyrite in the system Fe-As-S and their application. Unpubl. Ph.D. thesis, University of Toronto, Toronto, Ontario, 146 pp.

Kullerud, G., 1970. Sulfide phase relations. Mineral. Soc. Am. Spec. Paper 3, pp. 199-210.

Lambert, R. St. J., 1971. The pre-Pleistocene Phanerozoic time scale - a review. The Phanerozoic Time Scale - a supplement. Geol. Soc. (London), part I, pp. 9-31.

Landis, G. P. and Rye, R. O., 1974. Geologic, fluid inclusion, and stable isotope studies of the Pasto Buena tungsten-base metal ore deposit, northern Peru. Econ. Geol., 69, pp. 1025-1059.

Leith, C. K., 1905. Rock cleavage. U. S. Geol. Surv. Bull., 239, 216 pp.

Lemmlein, G. G., 1956. Formation of fluid inclusions in minerals and their use in geological thermometry. Translated in Geochemistry, number 6, pp. 630-642.

Levorsen, A. I., 1954. Geology of Petroleum. W. H. Freeman and Co., San Francisco, 703 pp.

Lin, C. L., 1971. Cretaceous deposits in the Musquodoboit river valley, Nova Scotia. Can. J. Earth Sci., 8, pp. 1152-1154.

Lindgren, W., 1933. Mineral Deposits, fourth edition. McGraw-Hill Co., Inc., New York, 930 pp.

MacDougall, J. I., Cann, D. B. and Hilchey, J. D., 1963. Soil survey of Halifax County, Nova Scotia. N. S. Soil Surv., Rept. Number 13.

Magara, K., 1973. Compaction and fluid migration in Cretaceous shales of western Canada. Geol. Surv. Can., Paper 72-18, 81 pp.

Magara, K., 1975. Re-evaluation of montmorillanite dehydration as a cause of abnormal pressure and hydrocarbon migration. Bull. Am. Assoc. Petrol. Geol., 59, pp. 292-302.

Magara, K., 1974. Aquathermal fluid migration. Bull. Am. Assoc. Petrol. Geol., 58, pp. 2513-2516.

Maier, S. and Franck, E. U., 1966. Die Dichte des Wassers von 200 bis 850°C and von 1000 bis 6000 bar. Ber. Bunsengesellschoft Phys. Chem., 70, pp. 639-645.

Malcolm, W., 1912. Gold fields of Nova Scotia. Geol. Surv. Can., Mem. 20-E, 331 pp.

Malcolm, W., 1929. Gold fields of Nova Scotia. Geol. Surv. Can., Mem. 156.

Manger, G. E., 1963. Porosity and bulk density of sedimentary rocks. U. S. Geol. Surv. Bull. 1144-E, pp. 34-40.

Maxwell, J. C., 1962. Origin of slaty and fracture cleavage in the Delaware Water Gap area, New Jersey and Pennsylvania. Petrol. Studies (Buddington Volume), Geol. Soc. Am., pp. 281-311.

McCartney, W. D., 1965. Metallogeny of post-preCambrian geosynclines. Geol. Surv. Can. Paper 65-6, pp. 28-32.

McCartney, W. D. and Potter, R. R., 1962. Mineralization as related to structural deformation, igneous activity, and sedimentation in folded geosynclines. Can. Mining J., 83, number 4, pp. 83-87.

McClintock, F. A. and Walsh, J. B., 1962. Fricton on Griffith cracks in rocks under pressure. Proc. U. S. Natl. Congr. Applied Mech., pp. 1015-1021.

McKenzie, C. B., 1974. Petrology of the South Mountain Batholith. Unpubl. M.Sc. thesis, Dalhousie University, Halifax, Nova Scotia, 101 pp.

McKenzie, C. B. and Clarke, D. B., 1975. Petrology of the South Mountain Batholith, Nova Scotia. Can. J. Earth Sci., 12, pp. 1209-1218.

McKinstry, H. E., 1942a. Bendigo, Victoria, Australia. Ore Deposits as Related to Structural Features, W. H. Newhouse, editor, Princeton Univ. Press, Princeton, N. J., pp. 160-162.

McKinstry, H. E., 1942b. Ballarat, Victoria, Australia. Ore Deposits as Related to Structural Features, W. H. Newhouse, editor, Princeton Univ. Press, Princeton, N. J., pp. 162-163.

Miller, C. K., 1974. Scheelite mineralization in the region of the Moose River gold district, Halifax County, Nova Scotia. Unpubl. B.Sc. thesis, Dalhousie University, Halifax, Nova Scotia.

Money, P. L., 1967. Discussion: metamorphism of the Meguma Group of Nova Scotia, by F. C. Taylor and E. A. Schiller. Can. J. Earth Sci., 4, pp. 577-578.

Morimoto, N. and Clark, L. A., 1961. Arsenopyrite crystal-chemical relations. Am. Mineral., 46, pp. 1448-1469.

Mostofi, B. and Gansser, A., 1957. The story behind the 5 Alborz. Oil and Gas J., January, pp. 78-84.

Newhouse, W. H., 1936. A zonal gold mineralization in Nova Scotia. Econ. Geol., 31, pp. 805-831.

Nova Scotia Department of Mines Annual Report, 1964, Halifax, Nova Scotia.

Ode, H., 1960. Faulting as a velocity discontinuity in plastic deformation. Rock Deformation, Geol. Soc. Am., Mem. 79, pp. 293-321.

Onishi, H. and Sandell, E. B., 1955. Geochemistry of arsenic. Geochim. et Cosmochim. Acta, 7, pp. 1-33.

Parker, C. A., 1973. Geopressures in the deep Smackover of Mississippi. J. Petrol. Tech., 25, pp. 971-979.

Perry, E. A., Jr., 1972. Late-stage dehydration in deeply buried pelitic sediments. Bull. Am. Assoc. Petrol. Geol., 56, pp. 2013-2021.

Petrascheck, W. E., 1965. Typical features of metallogenic provinces. Econ. Geol., 60, pp. 1620-1634.

Phillips, W. J., 1972. Hydraulic fracturing and mineralization. J. Geol. Soc., 128, pp. 337-359.

Phinney, W. C., 1961. Possible turbidity-current deposit in Nova Scotia. Bull. Geol. Soc. Am., 72, pp. 1453-1454.

Platt, L. B., 1962. Fluid pressure in thrust faulting, a corollary. Am. J. Sci., 260, pp. 107-114.

Poole, W. H., 1971. Graptolites, copper, and K-Ar in Goldenville Formation, Nova Scotia. Geol. Surv. Can. Paper 71-1, part A, pp. 9-11.

Poole, W. H., 1973. Cleavage and orogeny. Geol. Surv. Can. Paper 74-1, part A, pp. 1-2.

Powell, C. McA., 1972. Tectonic dewatering and strain in the Michigamme slate, Michigan. Bull. Geol. Soc. Am., 83, pp. 2149-2158.

Powell, C. McA., 1974. Timing of slaty cleavage during folding of pre-Cambrian rocks, northwest Tasmania. Bull. Geol. Soc. Am., 85, pp. 1043-1060.

Powers, M. C., 1967. Fluid release mechanisms in compacting marine mud-rocks and their importance in oil exploration. Bull. Am. Assoc. Petrol. Geol., 51, pp. 1240-1253.

Price, M. J., 1969. A dynamic mechanism for the development of second order faults. Geol. Surv. Can. Paper 68-52, pp. 49-78.

Putnam, D. F., 1940. The climate of the Maritime provinces. Can. Geog. J.

Ramsay, J. G., 1967. Folding and Fracturing of Rocks. McGraw-Hill, New York, 568 p.

Raybould, J. G., 1974. Ore textures, paragenesis and zoning in the lead-zinc veins of mid-Wales. Trans. Inst. Mining Met., 83, pp. B112-B119.

Reynolds, P. H., Kublick, E. E., and Muecke, G. K., 1973. K-Ar dating of slates from the Meguma Group, Nova Scotia. Can. J. Earth Sci., 10, pp. 1059-1067.

Rodgers, J., 1967. Chronology of tectonic movements in the Appalachian region of eastern North America. Am. J. Sci., 265, pp. 408-427.

Rodgers, J., 1970. The Tectonics of the Appalachians. Wiley-Interscience, New York, Chapters 6 and 7.

Roedder, E., 1962a. Ancient fluids in crystals. Sci. Am., 207, October, pp. 38-47.

Roedder, E., 1962b. Studies of fluid inclusions. I: low temperature application of a dual-purpose freezing and heating stage. Econ. Geol., 57, pp. 1045-1061.

Roedder, E., 1963. Studies of fluid inclusions. II: freezing data and their interpretation. Econ. Geol., 58, pp. 167-211.

Roedder, E., 1967. Fluid inclusions as samples of ore fluids. Chapter 12 of Barnes, H. L., editor, Geochemistry of Hydrothermal Ore Deposits, Holt, Rinehart, and Winston, New York, pp. 515-574.

Roedder, E., 1971. Metastability in fluid inclusions. Soc. Mining Geol. Japan, Spec. Issue, 3, pp. 327-334.

Roedder, E., 1972. Composition of fluid inclusions. U. S. Geol. Surv., Profess. Paper 440-JJ, 164 p.

Roedder, E. and Skinner, B. J., 1968. Experimental evidence that fluid inclusions do not leak. Econ. Geol., 63, pp. 715-730.

Rose, E. R., 1970. In Chapter VII: Economic minerals of southeastern Canada. Geol. Surv. Can., Econ. Geol. Rept. 1, pp. 306-336.

Routhier, P., et al., 1973. Some major concepts of metallogeny (consanguinity, heritage, province) illustrated by examples. Mineral. Deposita, 8, pp. 237-258.

Rubey, W. W. and Hubbert, M. K., 1959. Role of fluid pressure in mechanics of overthrust faulting. II. Bull. Geol. Soc. Am., 70, pp. 167-206.

Rye, D. M. and Rye, R. O., 1974. Homestake gold mine, South Dakota: I. Stable isotope studies. Econ. Geol., 69, pp. 293-317.

Rye, D. M., Doe, B. R., and Delevaux, M. H., 1974. Homestake gold mine, South Dakota: II. Lead isotopes, mineralization ages, and source of lead in ores of the northern Black Hills. Econ. Geol., 69, pp. 814-822.

Rye, R. O. and O'Neill, J. R., 1968. The O^{18} content of water in primary fluid inclusions from Providencia, North-Central Mexico. Econ. Geol., 63, pp. 232-238.

Rye, R. O. and Sawkins, F. J., 1974. Fluid inclusion and stable isotope studies on the Casapalca Ag-Pb-Zn-Cu deposit, central Andes, Peru. Econ. Geol., 69, pp. 181-205.

Sawkins, F. J., 1964. Lead-zinc ore deposition in the light of fluid inclusion studies, Providencia mine, Zacatecas, Mexico. Econ. Geol., 59, pp. 883-919.

Sawkins, F. J., 1966. Ore genesis in the North Pennine orefield, in light of fluid inclusion studies. Econ. Geol., 61, pp. 385-401.

Schenk, P. E., 1970. Regional variation of the Flysch-like Meguma Group (Lower Paleozoic) of Nova Scotia, compared to Recent sedimentation off the Scotian Shelf. Geol. Assoc. Can., Spec. Paper 7, pp. 127-153.

Schenk, P. E., 1971. Southeastern Atlantic Canada, northwestern Africa, and continental drift. Can. J. Earth Sci., 8, pp. 1218-1251.

Schmidt, R. A., 1962. Temperatures of mineral formation in the Miami-Picher district as indicated by liquid inclusions. Econ. Geol., 57, pp. 1-20.

Schwartz, G. M., 1944. The host minerals of native gold. Econ. Geol., 39. pp. 371-411.

Schweigart, H., 1965. Solid solution of gold in sulfides. Econ. Geol., 60, pp. 1540-1542.

Secor, D. T., 1965. Role of fluid pressure in jointing. Am. J. Sci., 263, pp. 633-646.

Sharp, W. E., 1965. The deposition of hydrothermal quartz and calcite. Econ. Geol., 60, pp. 1635-1644.

Sharp, W. E. and Kennedy, G. C., 1965. The system $CuO-CO_2-H_2O$ in the two-phase region calcite + aqueous solution. J. Geol., 73, pp. 391-403.

Shcherbakov, Yu. G. and Perezhogin, G. A., 1964. Geochemistry of gold. Geokhimiya, number 6, pp. 518-528, translated in Geochem. Intern., 3, pp. 489-496.

Shearman, D. J., Mossop, G., Dunsmore, H., and Martin, M., 1972. Origin of gypsum veins by hydraulic fracture. Trans. Inst. Mining Met., 81, pp. B149-B155.

Shelley, D., 1968. Ptygma-like veins in graywacke, mudstone, and low grade schist from New Zealand. J. Geol., 76, pp. 692-701.

Shelley, D., 1975. Temperature and metamorphism during cleavage and fold formation of the Greenland Group, North of Greymouth. J. Roy. Soc. N.Z., 5, pp. 65-75.

Sheridan, R. E. and Drake, C. L., 1968. Seaward extension of the Canadian Appalachians. Can. J. Earth Sci., 5, pp. 337-373.

Shilo, N. A., 1971. The problems of the geology of gold. Earth-Sci. Rev., 7, pp. 215-225.

Siddans, A. W. B., 1972. Slaty-cleavage - a review since 1815. Earth-Sci. Rev., 8, pp. 205-232.

Smith, F. G., 1953. Historical Development of Inclusion Thermometry. Univ. of Toronto Press, Toronto, 149 pp.

Smitheringale, W. G., 1960. Geology of the Nictaux-Torbrook map-area, Annapolis and Kings Counties, Nova Scotia. Geol. Surv. Can., Paper 60-13, 32 pp.

Smitheringale, W. G., 1973. Geology of parts of Digby, Bridgetown, and Gaspereau Lake map-areas, Nova Scotia. Geol. Surv. Can., Mem. 375, 78 pp.

Sorby, H. C., 1858. On the microscopic structure of crystals indicating the origin of minerals and rocks. Geol. Soc. Lond. Quart. J., 14, part 1, pp. 453-500.

Sourijan, S. and Kennedy, G. C., 1962. The system H_2O-NaCl at elevated temperatures and pressures. Am. J. Sci., 260, pp. 115-141.

Stevenson, I. M., 1958. Truro map-area, Colchester and Hants Counties, Nova Scotia. Geol. Surv. Can., Mem. 297, 124 pp.

Stevenson, I. M., 1958. Shubenacadie and Kennetcook map-areas, Colchester, Hants, and Halifax Counties, Nova Scotia. Geol. Surv. Can., Mem. 302, 88 pp.

Stillwell, F. L., 1950. Origin of the Bendigo saddle reefs. Econ. Geol., 45, pp. 697-701.

Stoll, W. C., 1965. Metallogenic provinces of magmatic parentage. Mining Mag., 112, pp. 312-323, 394-405.

Takenouchi, S. and Kennedy, G. C., 1964. The binary system H_2O-CO_2 at high temperatures and pressures. Am. J. Sci., 262, pp. 1055-1074.

Takenouchi, S. and Kennedy, G. C., 1965. The solubility of carbon dioxide in NaCl solutions at high temperatures and pressures. Am. J. Sci., 263, pp. 445-454.

Taylor, F. C., 1965. Silurian stratigraphy and Ordovician-Silurian relationships in southwestern Nova Scotia. Geol. Surv. Can., Paper 64-13, 24 pp.

Taylor, F. C., 1967. Reconnaissance geology of Shelburne map-area, Queens, Shelburne, and Yarmouth Counties, Nova Scotia. Geol. Surv. Can., Mem. 349, 83 pp.

Taylor, F. C., 1969. Geology of the Annapolis-St. Mary's Bay map-area, Nova Scotia. Geol. Surv. Can., Mem. 358, 65 pp.

Taylor, F. C. and Schiller, E. A., 1966. Metamorphism of the Meguma Group of Nova Scotia. Can. J. Earth Sci., 3, pp. 959-974.

Terzaghi, K., 1936. Simple tests determine hydrostatic uplift. Engineering News Record, 116, pp. 872-875.

Tilling, R. I., Gottfried, D., and Rowe, J. J., 1973. Gold abundances in igneous rocks: bearing on gold mineralization. Econ. Geol., 68, pp. 168-186.

Tkhostov, B. A., 1963. Initial Rock Pressures in Oil and Gas Deposits. MacMillan, New York, 118 pp.

Todheide, K. and Franck, E. U., 1963. Das Zweiphasengebiet und die Kritische Kurve in System Kohlendioxid-Wasser bis zu Drucken von 3500 bar. Z. Phys. Chem., Neue Folge, 37, pp. 387-401.

Toulmin, P., III and Barton, P. B., 1964. A thermodynamic study of pyrite and pyrrhotite. Geochim. et Cosmochim. Acta, pp. 641-671.

Turner, F. J. and Verhoogen, J., 1960. Igneous and Metamorphic Petrology. McGraw-Hill, New York.

Vidale, R. J., 1974. Vein assemblages and metamorphism in Dutchess County, New York. Bull. Geol. Soc. Am., 85, pp. 303-306.

Viljoen, R. P., Saager, R., and Viljoen, M. J., 1970. Some thoughts on the processes responsible for the concentration of gold in the early pre Cambrian of southern Africa. Mineral. Deposita, 5, pp. 164-180.

Watts, E. V., 1948. Some aspects of high pressures in the D-7 zone of the Ventura Avenue field. Trans. Am. Inst. Mining Engineers, 174, pp. 191-205.

Weeks, L. J., 1954. Southeast Cape Breton Island, Nova Scotia. Geol. Surv. Can., Mem. 277, 112 pp.

Weiss, L. E., 1969. Flexural-slip folding of foliated model materials. Geol. Surv. Can., Paper 68-52, pp. 294-359.

Wilson, J. T., 1938. Drumlins of southwest Nova Scotia. Trans. Roy. Soc. Can., 3rd series, 32, section 4, pp. 41-47.

Winkler, H. G. F., 1974. Petrogenesis of Metamorphic Rocks, third edition. Springer-Verlag, New York, 320 pp.

Wood, D. S., 1974. Current views of the development of slaty cleavage. Ann. Rev. Earth Planetary Sci., 2, pp. 369-401.

Woodman, J. E., 1904. Nomenclature of the gold-bearing metamorphic series of Nova Scotia. Am. Geol., 33, pp. 364-370.

Woodman, J. E., 1899. Studies of the gold-bearing slates of Nova Scotia. Proc. Boston Soc. Nat. Hist., 28, #15, pp. 375-407.

Yermakov, N. P., et al., 1965. Research on the Nature of Mineral forming Solutions. Translated by V. P. Sokoloff, edited by E. Roedder, Pergamon Press, Oxford, 743 pp.

Zoback, M. D. and Byerlee, J. D., 1975. Permeability and effective stress. Bull. Am. Assoc. Petrol. Geol., 59, pp. 154-158.

APPENDIX I

Arsenopyrite analyses

TABLE 1

Mean arsenopyrite compositions from electron microprobe data as modified by EMPADR 7. (See Chapter III for discussion)

Comments column symbols: R = rim, C = centre, M = intermediate position of spot within grain, + = pyrite as adjacent grain, * = pyrrhotite as adjacent grain, ' = grain in country rock.

Sample Number	Spot Number	WT%				AT%			Comments
		As	Fe	S	total	As	Fe	S	
163-73	1	46.50	34.11	19.24	99.85	33.89	33.35	32.77	M+
	2	46.69	33.97	19.12	99.77	34.10	33.28	32.63	M+
	3	46.20	34.06	19.90	100.16	33.38	33.01	33.60	M+
	4	45.22	34.26	20.18	99.66	32.69	33.22	34.09	C*
	5	44.07	34.56	20.73	99.37	31.73	33.38	34.88	C
ZT03	1	44.22	34.55	20.75	99.52	31.80	33.33	34.87	M+
	2	45.40	34.54	20.18	100.13	32.69	33.36	33.95	R
	3	44.61	34.31	20.48	99.40	32.21	33.23	34.56	R
	4	44.86	34.41	20.09	99.36	32.52	33.46	34.03	R*
	5	43.42	34.60	20.69	98.71	31.42	33.59	34.99	M*
T03	1	43.62	34.43	20.35	98.40	31.76	33.62	34.62	M+
	2	45.14	34.18	20.36	99.69	32.58	33.09	34.34	R+
	3	42.97	34.93	20.75	98.65	31.07	33.88	35.06	M+
	4	44.02	34.50	20.52	99.04	31.84	33.48	34.68	M
	5	43.70	34.58	20.49	98.78	31.67	33.62	34.70	R+

Sample Number	Spot Number	WT%				AT%			Comments
		As	Fe	S	total	As	Fe	S	
ZT02	2	43.53	34.57	20.67	98.76	31.50	33.55	34.95	R+
173-73	1	43.29	34.55	20.92	98.76	31.25	33.46	35.29	M*
	2	43.69	34.38	20.84	98.91	31.54	33.30	35.16	M
	3	45.38	34.48	20.38	100.24	32.59	33.21	34.20	M
	4	46.65	33.57	19.32	99.54	34.09	32.91	33.00	R
	5	44.85	34.15	20.33	99.34	32.46	33.16	34.38	R
	6	44.38	33.87	19.93	98.18	32.54	33.31	34.15	M*
P1	1	43.61	34.35	20.99	98.96	31.43	33.21	35.35	
	2-1	44.86	34.66	21.23	100.74	31.82	32.98	35.19	
	2-2	44.46	34.49	21.09	100.05	31.75	33.04	35.20	
	3	43.08	34.99	22.10	100.17	30.41	33.13	36.46	
	4	44.04	34.50	21.22	99.77	31.48	33.08	35.44	
	5	44.27	34.51	20.95	99.73	31.73	33.18	35.09	
P2	2	46.80	34.38	19.78	100.97	33.63	33.14	33.22	
	5	45.44	34.70	20.71	100.86	32.37	33.16	34.47	
	3	45.47	34.71	20.61	100.79	32.43	33.21	34.35	
MC-170-73	1	46.16	34.19	20.46	100.80	33.01	32.80	34.19	R
	2	46.03	34.47	20.01	100.51	33.11	33.26	33.63	M+
	3	45.16	34.37	20.32	99.85	32.55	33.23	34.22	M+
	5	46.01	34.49	20.47	100.97	32.84	33.02	34.14	R
	8	45.52	34.54	20.39	100.45	32.63	33.21	34.16	R+

Sample Number	Spot Number	WT%				AT%			Comments
		As	Fe	S	total	As	Fe	S	
MC-170-73	11	46.92	33.89	19.24	100.05	34.16	33.10	32.74	R
	12	46.13	33.69	20.48	100.31	33.14	32.47	34.38	R'
CH4-1	2	45.79	34.46	20.53	100.78	32.71	33.02	34.27	R
ZLC-1	1	43.34	34.17	20.88	98.39	31.41	33.22	35.36	R'
	2	43.89	34.97	21.95	100.82	30.89	33.01	36.10	C'
	3	43.05	35.04	21.58	99.68	30.64	33.46	35.90	R'
	4	45.53	34.38	20.46	100.36	32.65	33.07	34.28	R'
	5	44.17	34.05	20.07	98.30	32.30	33.40	34.30	R'
	6	44.27	34.43	21.03	99.73	31.71	33.08	35.20	R
SR10	1	43.21	34.82	21.43	99.46	30.86	33.36	35.77	R
	2	42.94	35.02	21.73	99.68	30.52	33.39	36.09	C
	3	44.35	34.55	20.80	99.69	31.84	33.27	34.89	R
	4	45.43	34.01	20.05	99.50	32.94	33.08	33.98	M+*
WHT6	1	46.42	33.55	19.78	99.75	33.72	32.70	33.58	R'
	2	42.93	34.87	22.08	99.88	30.38	33.10	36.52	C
	3	45.18	34.35	20.61	100.14	32.40	33.05	34.54	R
	4	46.84	34.23	19.75	100.82	33.72	33.06	33.22	M'
MC-148-73	1	43.97	34.29	20.23	98.49	32.04	33.52	34.45	M
	2	44.06	34.52	20.46	99.04	31.89	33.51	34.60	R
MC-166-73	1	45.50	34.15	20.82	100.47	32.51	32.73	34.76	M
	2	46.25	33.90	19.70	99.85	33.57	33.01	33.42	R

Sample Number	Spot Number	WT%				AT%			Comments
		As	Fe	S	total	As	Fe	S	
GLD10	1	43.62	34.93	21.88	100.43	30.80	33.09	36.11	R
	3	44.54	34.79	21.57	100.91	31.45	32.95	35.59	R
	4	44.81	34.65	21.14	100.59	31.85	33.04	35.11	M
	5	43.59	35.05	21.60	100.14	30.90	33.33	35.78	R
15MS-11	1	44.78	34.14	20.39	99.31	32.40	33.13	34.47	M
	6	42.01	35.03	21.94	98.98	29.95	33.50	36.55	M
CHD10	1	45.55	34.34	19.87	99.76	33.00	33.37	33.64	R
	2	45.37	34.67	20.79	100.83	32.30	33.11	34.59	M
	3	44.00	34.75	20.95	99.70	31.52	33.40	35.08	M
	4	44.23	34.57	20.98	99.79	31.68	33.21	35.11	R
	5	45.47	34.24	19.77	99.47	33.04	33.38	33.58	M'
ZLT-1	3	44.28	35.29	21.19	100.76	31.37	33.54	35.08	R
1-C	1	44.75	34.68	20.89	100.31	31.94	33.21	34.85	M+*
	2	45.71	34.49	20.34	100.53	32.76	33.16	34.07	R+*
	3	45.46	34.46	20.76	100.69	32.42	32.97	34.60	M+*
KBDL2	1	44.47	35.09	21.33	100.89	31.45	33.29	35.25	C
	3	43.65	35.36	21.78	100.79	30.74	33.41	35.85	R
	5	44.48	35.07	21.23	100.77	31.52	33.33	35.15	M
GR10	2	43.60	34.79	21.31	99.70	31.13	33.32	35.55	C
ZLT-1	1	45.56	34.43	20.15	100.15	32.82	33.27	33.92	M+
	2	45.67	34.54	20.31	100.52	32.75	33.22	34.03	M
	3	44.75	34.57	20.48	99.80	32.20	33.37	34.44	M+

Sample Number	Spot Number	WT%				AT%			Comments
		As	Fe	S	total	As	Fe	S	
ZLT-1	6	46.35	34.47	20.08	100.90	33.22	33.14	33.63	M+
	8	44.13	34.91	21.27	100.32	31.37	33.29	35.34	R
	9	43.92	34.60	21.19	99.71	31.40	33.19	35.41	M
	10	44.95	34.22	20.56	99.74	32.36	33.05	34.59	C+
	11	44.76	34.76	21.25	100.78	31.73	33.06	35.21	C
CH4-2	1	45.62	34.35	20.47	100.44	32.69	33.02	34.28	M
	2	45.04	34.52	20.87	100.43	32.14	33.05	34.81	C
	3	45.48	34.39	20.33	100.20	32.69	33.16	34.15	R
	4	45.11	34.46	20.62	100.19	32.33	33.13	34.54	M
SR13	1	43.03	34.56	22.03	99.62	30.54	32.91	36.54	R
	2	42.58	34.59	22.03	99.20	30.31	33.03	36.65	M
	4	44.95	33.94	20.30	99.19	32.59	33.01	34.40	M
	5	44.83	34.03	20.25	99.11	32.53	33.13	34.34	M'
	6	45.38	34.09	20.21	99.68	32.80	33.06	34.14	M'
CH4-1	1	45.03	34.88	20.73	100.64	32.10	33.36	34.54	M*
	3	45.63	34.77	20.26	100.66	32.68	33.41	33.91	M
	4	45.55	34.70	20.54	100.79	32.51	33.22	34.26	M
Total	n=95	mean				32.11	33.21	34.68	
		1s.d.				0.91	0.22	0.86	

Sample Number	Spot Number	WT%				AT%			Comments
		As	Fe	S	total	As	Fe	S	
200	1	43.91	34.61	21.16	99.68	31.41	33.21	35.37	
	2	44.87	34.92	20.78	100.57	31.99	33.39	34.62	
	3	44.10	34.31	21.12	99.53	31.62	33.00	35.38	
	4	44.54	34.83	21.34	100.71	31.51	33.10	35.34	
	5	44.42	35.18	21.37	100.97	31.38	33.34	35.28	
	6	44.53	34.82	21.33	100.73	31.54	33.08	35.38	
	7	44.75	34.85	21.36	100.96	31.64	33.06	35.30	
	8	44.12	34.44	20.83	99.40	31.74	33.24	35.02	
	9	45.24	34.15	20.29	99.67	32.67	33.08	34.24	
	10	45.00	34.71	20.60	100.31	32.21	33.33	34.46	
	11	45.34	34.52	20.67	100.53	32.40	33.09	34.51	
	12	44.64	34.45	20.60	99.69	32.12	33.25	34.63	
	13	43.94	34.94	21.23	100.11	31.29	33.38	35.33	
	14	45.27	34.44	20.51	100.22	32.48	33.14	34.38	
	15	44.63	34.99	21.34	100.96	31.55	33.19	35.26	
	16	44.85	34.85	21.07	100.55	31.74	33.24	35.02	
	17	44.49	34.62	20.97	100.08	31.79	33.19	35.02	
	18	44.66	34.70	20.73	100.10	31.98	33.33	34.69	
	19	44.26	34.65	20.86	99.77	31.73	33.32	34.95	
	20	44.55	34.82	21.03	100.40	31.73	33.27	35.00	
	21	44.91	34.79	20.78	100.47	32.05	33.30	34.65	
Total	n=21	mean				31.84	33.22	34.94	
		1s.d.				0.37	0.12	0.38	

TABLE 2

Mean arsenopyrite compositions from electron microprobe data as modified by EMPADR 7 by sample. (See Chapter III for discussion)

Sample Number	n		WT%				AT%			Location
			Fe	As	S	total	Fe	As	S	
200	21	mean	44.61	34.69	20.95	100.25	31.84	33.22	34.94	
		ls.d.	0.41	0.25	0.32		0.37	0.12	0.38	
163-73	5	mean	45.74	34.19	19.83	99.76	33.16	33.25	33.59	Upper Seal Harbour
		s.d.	1.09	0.23	0.67		0.96	0.15	0.94	
ZT03	5	mean	44.50	34.48	20.44	99.42	32.13	33.39	34.48	The Ovens
		s.d.	0.74	0.12	0.30		0.52	0.14	0.47	
T03	5	mean	43.89	34.52	20.49	98.90	31.78	33.54	34.68	The Ovens
		s.d.	0.80	0.27	0.16		0.54	0.29	0.26	
ZT02	1		43.53	34.47	20.67	98.76	31.50	33.55	34.95	The Ovens
			-	-	-		-	-	-	
173-73	5	mean	44.77	34.23	20.36	99.36	-	-	-	Upper Seal Harbour
		s.d.	1.35	0.40	0.64		-	-	-	

Sample number	n		WT%				AT%			Location
			Fe	As	S	total	Fe	As	S	
173-73	6	mean	44.71	34.17	20.29	99.17	32.41	33.22	34.36	Upper Seal Harbour
		s.d.	1.22	0.38	0.60		1.00	0.18	0.83	
MC-170-73	7	mean	45.99	34.23	20.20	100.42	33.06	33.01	33.92	Upper Seal Harbour
		s.d.	0.55	0.33	0.45		0.53	0.29	0.57	
CH4-1	1		45.79	34.46	20.53	100.78	32.71	33.02	34.27	Cochrane Hill
			-	-	-		-	-	-	
ZLC-1	6	mean	44.04	34.51	21.00	99.55	31.60	33.21	35.19	Lake Catcha
		s.d.	0.87	0.41	0.69		0.78	0.19	0.77	
SR10	4	mean	43.98	34.60	21.00	99.58	31.54	33.28	35.18	Salmon River
		s.d.	1.14	0.44	0.74		1.09	0.14	0.95	
WHT6	4	mean	45.34	34.25	20.56	100.15	32.56	32.98	34.46	Whiteburne
		s.d.	1.76	0.54	1.09		1.58	0.19	1.48	
MC-148-73	2	mean	44.02	34.40	20.34	98.76	31.96	33.52	34.52	Isaac's Harbour
		s.d.	0.06	0.16	0.16		0.11	0.01	0.11	

Sample number	n		WT%				AT%			Location
			Fe	As	S	total	Fe	As	S	
MC-166-73	2	mean	45.88	34.02	20.26	100.16	33.04	32.87	34.09	Upper Seal Harbour
		s.d.	0.53	0.18	0.79		0.75	0.20	0.95	
GLD10	4	mean	44.14	34.86	21.55	100.55	31.25	33.10	36.65	Goldenville
		s.d.	0.63	0.17	0.30		0.49	0.16	0.42	
15MS-11	2	mean	43.40	34.58	21.16	99.14	31.18	33.32	35.51	15 Mile Stream
		s.d.	1.96	0.63	1.10		1.73	0.26	1.47	
CHD10	5	mean	44.92	34.51	20.47	99.90	32.31	33.29	34.40	Cranberry Head
		s.d.	0.74	0.22	0.60		0.71	0.13	0.75	
ZLT1	1		44.28	35.29	21.19	100.76	31.37	33.54	35.08	Lawrencetown
			-	-	-		-	-	-	
1-C	3	mean	45.31	34.54	20.66	100.51	32.37	33.11	34.51	Caribou
		s.d.	0.50	0.12	0.29		0.41	0.13	0.40	
KBDL2	3	mean	44.20	35.17	21.45	100.82	31.24	33.34	35.42	Killag
		s.d.	0.48	0.16	0.29		0.43	0.06	0.38	

Sample number	n		WT%				AT%			Location
			Fe	As	S	total	Fe	As	S	
GR10	1		43.60	34.79	21.31	99.70	31.13	33.32	35.55	Gold River
			-	-	-		-	-	-	
ZLT1	8	mean	45.01	34.56	20.66	100.23	32.23	33.20	34.57	Lawrencetown
		s.d.	0.81	0.21	0.50		0.69	0.11	0.69	
CH4-2	5	mean	45.92	34.18	20.09	100.19	33.12	33.05	33.83	Cochrane Hill
		s.d.	1.38	0.57	1.10		1.48	0.11	1.40	
SR13	5	mean	44.15	34.24	20.96	99.35	31.75	33.03	35.21	Salmon River
		s.d.	1.26	0.31	0.97		1.22	0.08	1.26	
CH4-1	3	mean	45.40	34.78	20.51	100.69	32.43	33.33	34.24	Cochrane Hill
		s.d.	0.32	0.09	0.24		0.30	0.10	0.32	
Total	n=95	mean					32.11	33.21	34.68	
		ls.d.					0.91	0.22	0.86	

TABLE 3

Mean arsenopyrite compositions from electron microprobe data as modified by EMPADR 7 by district. (See Chapter III for discussion)

Location	n		WT%				AT%			Sample Numbers
			As	Fe	S	total	As	Fe	S	
The Ovens	12	mean	44.15	34.51	20.52	99.18	31.90	33.45	34.65	ZT03, T03, ZT02, P1-5
		s.d.	0.74	0.18	0.25		0.50	0.22	0.38	
Seal Harbour &	23	mean	45.31	34.21	20.19	99.71	32.74	33.16	34.10	163-73, 173-73, P1-1,
Isaac's Hbr.		s.d.	1.12	0.29	0.56		0.86	0.26	0.79	170-73, 148-73, 166-73
Upper SealHbr.	13	mean	45.40	34.20	20.24	99.84	32.76	33.11	34.13	173-73, 170-73
Site #1		s.d.	1.10	0.34	0.50		0.82	0.26	0.71	
Upper Seal Hbr.	7	mean	45.78	34.14	19.96	99.88	33.12	33.14	33.74	163-73, 166-73
Site #2		s.d.	0.92	0.22	0.67		0.85	0.23	0.89	
Isaac's Hbr.	2	mean	44.02	34.40	20.34	98.76	31.96	33.52	34.52	148-73
		s.d.	0.06	0.16	0.16		0.11	0.01	0.11	
Molega	3	mean	44.45	34.55	21.18	100.18	31.68	33.03	35.28	P1-2-1, P1-2-2, P1-4
		s.d.	0.41	0.10	0.08		0.18	0.05	0.14	

Location	n		WT%				AT%			Sample Numbers
			As	Fe	S	total	As	Fe	S	
Lake Catcha	7	mean	43.90	34.58	21.15	99.63	31.43	33.20	35.37	ZLC-1, P1-3
		s.d.	0.87	0.42	0.76		0.84	0.17	0.85	
Cochrane Hill	10	mean	45.42	34.59	20.57	100.58	32.46	33.17	34.36	P2-5, P2-3, CH4-2, CH4-1
		s.d.	0.27	0.18	0.18		0.23	0.13	0.25	
Salmon River	9	mean	44.08	34.40	20.98	99.46	32.10	33.14	35.20	SR10, SR13
		s.d.	1.14	0.39	0.82		1.28	0.16	1.07	
Whiteburne	4	mean	45.34	34.25	20.56	100.15	32.56	32.98	34.46	WHT6
		s.d.	1.76	0.54	1.09		1.58	0.19	1.48	
Goldenville	4	mean	44.14	34.86	21.55	100.55	31.25	33.10	35.65	GLD10
		s.d.	0.63	0.17	0.30		0.49	0.16	0.42	
15 Mile Strean	2	mean	43.40	34.58	21.16	99.14	31.18	33.32	35.51	15MS-11
		s.d.	1.96	0.63	1.10		1.73	0.26	1.47	
Cranberry Head	5	mean	44.92	34.51	20.47	99.90	32.31	33.29	34.40	CHD10
		s.d.	0.74	0.22	0.60		0.71	0.13	0.75	
Lawrencetown	9	mean	44.93	34.64	20.72	100.92	32.14	33.24	34.63	ZLT-1
		s.d.	0.80	0.31	0.50		0.70	0.15	0.67	

Location	n		WT%				AT%			Sample Numbers
			As	Fe	S	total	As	Fe	S	
Caribou	3	mean	45.31	34.54	20.66	100.51	32.37	33.11	34.51	1-C
		s.d.	0.50	0.12	0.29		0.41	0.13	0.40	
Killag	3	mean	44.20	35.17	21.45	100.82	31.24	33.34	35.42	KBDL2
		s.d.	0.48	0.16	0.29		0.43	0.06	0.38	
Gold River	1		43.60	34.79	21.31	99.70	31.13	33.32	35.55	GR10
Total	n=95	mean					32.11	33.21	34.68	
		ls.d.					0.91	0.22	0.86	

APPENDIX II

Listing of gold district locations

Figure I.2. Province of Nova Scotia: numbers indicate location of gold districts where mining and/or prospecting activity has occurred since 1850. Numbers refer to index of gold districts found in Appendix II.

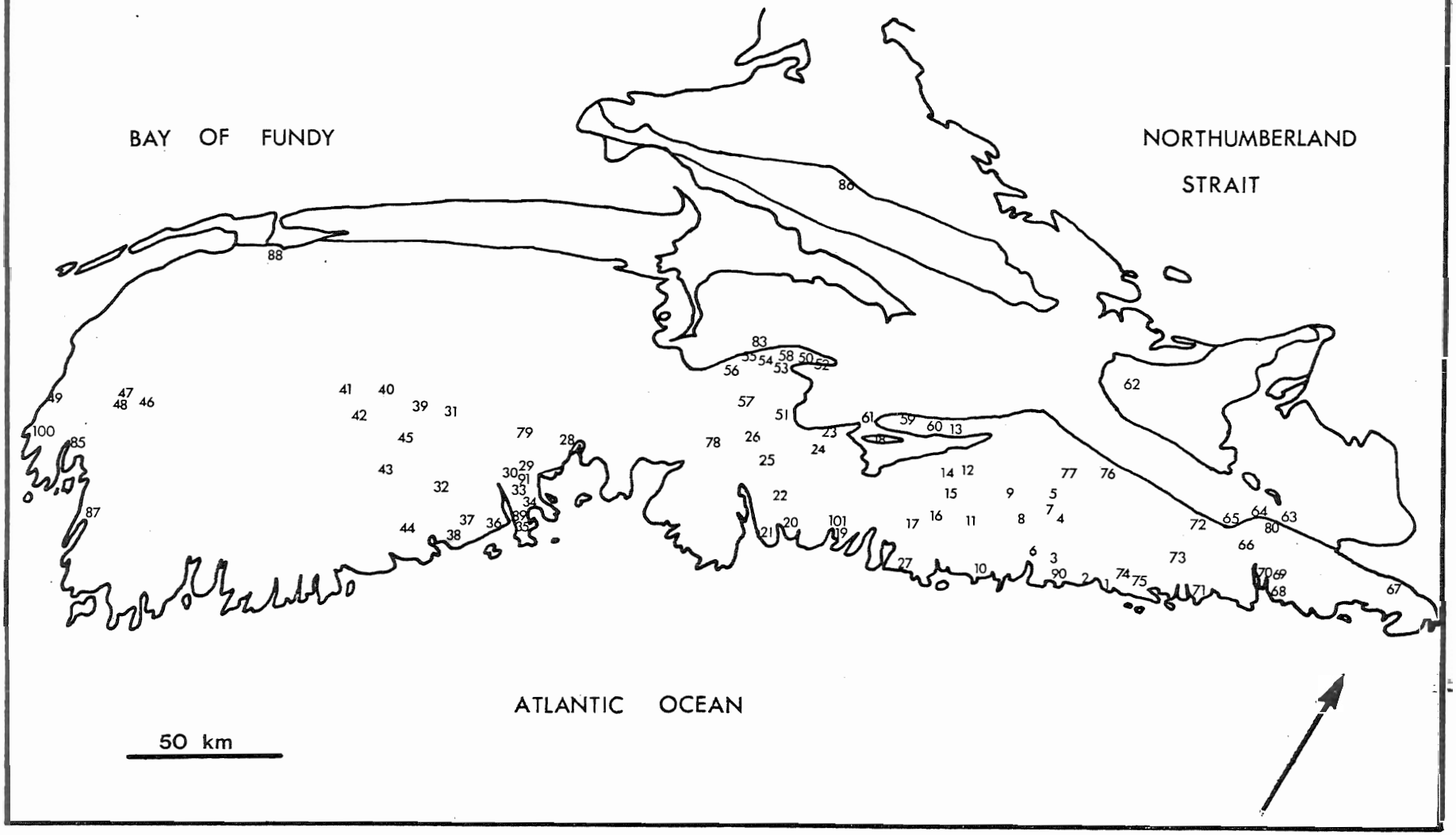

Notes to Appendix II -

- The reference number refers to index map.
- Interbedded veins are abbreviated as IV while crosscutting veins are abbreviated CV as discussed in Chapter II.
- Production history present three figures where available: total production to 1967 in ounces troy, percentage of total gold production of the province accounted for by any given district, and the rank of production of the district compared to others.
- Remarks column has been used to note when activity was carried on in any district.
- Information from Malcolm's (1912, 1929) two memoirs, Nova Scotia Department of Mines annual reports, and GSC annual reports.

GOLD

Reference Number	Name	NTS Map	Latitude	Longitude	County	Host Rock: age, formation and/or rock type	Geological character	Production History	Remarks
Au-1	Ecum Secum	11D/16	44°58'20"	62°11'	Halifax	Goldenville Fm.	IV w/one important CV on anticline & syncline 150 m apart	1,276 oz (.11%, #32)	1880's-1907
Au-2	Moosehead (Shrier's Point)	11D/16	44°57'	62°15'	Halifax	Goldenville Fm.	4IV's in so. limb of anticline	471 oz (.04 %; #41)	no mining since 1915
Au-3	Salmon River (Dufferin Mines) (Darrs Hill)	11D/16	44°57'30"	62°24'	Halifax	Halifax Fm.	IV's and saddles on so. most of 2 flexures at anticline crest	41649 oz (3.68%;#10)	1881-1900; drilling 1941-42
Au-4	Lochaber	11E/1	45°04'	62°28'40"	Halifax	Goldenville Fm.	IV pinching out in syncline	<5oz (#55)	prospecting 1882-1890,1934
Au-5	Fifteen Mile Stream	11E/2	45°08'	62°32'	Halifax	Goldenville Fm.	IV's in 3 minor folds on no. limb of anti-cline	19,741 oz (1.75%;#19)	1883-1941
Au-6	Sheet Harbour	11D/15	44°56'	62°30'	Halifax	Halifax Fm.	IV's - so. limb of anticline		drilling 1946
Au-7	Ragged Falls	11E/2	45°05'30"	62°34'	Halifax	Goldenville Fm.	IV's - so. limb of anticline		prospecting prior to 1928
Au-8	Killag (Black Duck Lake)	11E/2	45°01'15"	62°37'	Halifax	Goldenville Fm.	IV's on both limbs of an anticline close to axis; auriferous slate near one vein	3,584 oz (.32%;#30)	1869-1900, 1925, 26, 38-40, 1945-1951
Au-9	Beaver Dam	11E/2	45°04'	62°43'	Halifax	Goldenville Fm. - met qtz, garnet, olg, hb, ep, bt, ab, musc, chl, ap	IV in overturned anti-cline w/large slate + vein widths	966 oz (.08%; #35)	intermittant mining 1873-1931
Au-10	Tangier	11D/15	44°48'31"	62°41'20"	Halifax	Goldenville Fm. cut at right angles by 40' diorite dike	IV's around anticline dome - a well defined enrichment & widening zone diverges from dome	26,022 oz (2.30%;#15)	1860-1901, 1903-1919, 1926, 193[illegible]
Au-11	Mooseland	11D/15	44°56'25"	62°40'15"	Halifax	Goldenville Fm. granite to so. ~200 m	IV's on so. limb of anticline dome	471 oz (.04%;#41)	1866-1900, 1909-1914 intermet.; 1931-38 pros-pecting
Au-12	Caribou	11E/2	45°03'30"	62°56'30"	Halifax	Goldenville Fm. w/Halifax Fm. at periphery	IV's at anticline dome divergence from IV's as Hfx. Fm. is reached	91,352 (8.09%;#2)	1867-1947 con-tinuous, re-serves said exhausted, consolidated in 1908
Au-13	Benvie Brook	11E/3	45°07'20"	63°00'30"	Halifax	Halifax Fm.	no data	occurrence	
Au-14	Lake Lindsay	11E/3	45°02'	63°00'10"	Halifax	Halifax Fm.	IV on so. limb of anticline	prospect	

Au-15	Moose River	11D/15	44°58'45"	62°57'	Halifax	Goldenville Fm. large slate unit w/ thin qtzites.	IV's on no. limb & axis of four minor folds at anticline crest; zones of CV's common in thick slate unit	25,984 oz (2.30%;#16)	1876-1939, 1946 scheelite, rutile assemb- responsible for W production at edge of district
Au-16	Gold Lake (Scraggy Lake, Ship Hbr)	11D/15	45°55'	62°57'	Halifax	Goldenville Fm.	IV's on anticline	39 oz from prospect pits	and drift boulders
Au-17	Lake Charlotte	11D/15	44°52'	62°59'	Halifax	Goldenville Fm.	qtz. veins on so. limb of anticline near granite (<1 km)	38 oz in 1963	assoc. mins no, tellurides scheelite
Au-18	Ervin Brook	11E/13	45°02'	63°14'	Halifax	Goldenville Fm.	no data	occurrence	
Au-19	Lake Catcha	11D/11	44°44'30"	63°12'	Halifax	Goldenville Fm.	IV's on anticline dome; most on no. limb; 2CV's	17,954 oz (1.59%;#36)	1881-1902, 1911-1915, 1935-1939
Au-20	Lawrencetown	11D/11	44°41'30"	63°24'	Halifax	Goldenville Fm.	IV's on 2 converging anticlines - 500 m apart at most	867 oz (.08%;#38)	1866-70, 1875-1906 intermit., last reported prosp. 1934
Au-21	Cow Bay	11D/11	44°37'30"	63°24'	Halifax	Halifax-Golden-ville Fm contact	CV's in argillaceous qtzite. bed 30m x 6.5km heavily mineized w/po	1,243 oz	1895-1905
Au-22	Montague	11D/12	44°42'58"	63°31'	Halifax	Goldenville Fm.	IV's at anticlinal dome most on so. limb	68,139 oz (6.03%;#5)	1863-1901, 1911-1924, 1933-1939
Au-23	Elmsdale	11D/14	44°58'	63°28'	Halifax	Goldenville Fm.	qtz. veins probably IV's	1.4 oz re-ported pro-duction	no activity since 1890
Au-24	Oldham	11D/14	44°55'20"	63°29'30"	Halifax	Goldenville Fm.	IV's around anticline dome; 2 important CV's	85,295 oz (7.55%;#3)	1861-1929, 1935-1943 scheelite reported
Au-25	Waverly	11D/13	44°47'	63°36'	Halifax	Goldenville Fm.	IV's around anticline dome most important on no. limb	73,105 oz (6.47%;#4)	1862-1883, 1885-1903, 1933-1938 sch & wolf reported
Au-26	South Uniacke	11D/13	44°52'	63°41'30"	Halifax	Goldenville Fm.	IV's on no. limb	20,762 oz (1.84%;#18)	1889-1905; prosp. till 1947
Au-27	Clam Harbour	11D/10	44°44'25"	62°54'30"	Halifax	Goldenville Fm.	IV's at anticline crest richest ore in IV's where crossed by CV's	54 oz	last trenching in 1935
Au-28	Gold River	21A/19	44°34'30"	64°20'	Lunenburg	Goldenville Fm.	persistant IV's at dome	7,751 oz (.59%;#26)	1885-1915 inter-mit; 1930-1940
Au-29	Clearland	21A/8	44°29'	64°25'40"	Lunenburg	Halifax Fm.	qtz. veins along an anticline	prospect	
Au-30	Farmville	21A/8	44°28'	64°27'20"	Lunenburg	Halifax Fm.	qtz. veins along an anticline	prospect	
Au-31	Pleasant River Barrens	21A/7	44°27'	64°48'	Lunenburg	Goldenville Fm.	IV's in circular dome; 1 CV	112 oz. (.01%;#44)	1880's-1913 intermittant
Au-32	Leipsigate (Millipsigate)	21A/7	44°19'50"	64°35'30"	Lunenburg	Goldenville Fm.	IV's in eastern portion of a dome, important CV's rich where they cross IV's	12,084 oz (1.07%,#22) 1,521 oz Ag most from one CV	1883-84, 1888-92, 1895-1908, 1946-1949
Au-33	Rhodes Corner	21A/8	44°24'	64°24'	Lunenburg	Goldenville Fm.	IV's on w. plunge of a dome	prospect	

Au-34	Centre	21A/8	44°23'	64°22'	Lunenburg	Goldenville Fm.	gold-bearing drift boulders	occurrence	
Au-35	Ovens	21A/8	44°19'20"	64°15'30"	Lunenburg	Halifax Fm.	narrow IV's on anticline crest	541 oz (.05%;#39) mostly from beach places	1861-62; sporadic until 1896
Au-36	Oxner Brook	21A/8	44°16'05"	64°23'	Lunenburg	Halifax Fm.	one qtz. vein	occurrence	
Au-37	Somerset (Beach Hill)	21A/1	44°14'	64°30'	Lunenburg	Goldenville Fm.	gold-bearing qtz. boulders	occurrence	
Au-38	Vogler's Cove	21A/2	44°11'	64°31'30"	Lunenburg	Goldenville Fm.	CV on anticline flank some IV's also worked	43 oz	1893-1904; intermittant
Au-39	Brookfield	21A/7	44°25'	64°55'	Queen's	Goldenville Fm.	CV's most important; most poltn when intersect IV's or sulphide-rich slate; IV's imp. only when cut by angulars; anticline dome crest	43,041 oz (3.81%;#8)	1887-1891, 1895-1909
Au-40	Westfield	21A/6	44°25'	65°02'	Queen's	Halifax Fm.	thick IV's	prospect	pre-1890, 1934
Au-41	West Caledonia	21A/6	44°21'30"	65°10'30"	Queen's	Goldenville Fm.	IV's? on no. limb anticline	prospect (4 oz) probably from drift	1883, 1908-1909, 1933-1934
Au-42	Whiteburn	21A/6	44°18'45"	65°04'30"	Queen's	Goldenville Fm.	IV's on dome w/o slate	11,890 oz (1.06%;#23)	1885-1894, 1930-1940
Au-43	Fifteen Mile Brook	21A/2	44°14'15"	64°54'10"	Queen's	Goldenville Fm.	CV & IV most imp. was CV	880 oz (.08%;#36)	1901-1902, 1910-1914
Au-44	Mill Village	21A/2	44°09'30"	64°42'	Queen's	Goldenville Fm.	IV's on se anticline limb	910 oz (.08%;#35)	1899-1901, 1917-1919, 1929-1930
Au-45	Molega	21K/7	44°20'	64°54'	Queen's	Goldenville Fm.	disconnected IV's on dome	38,876 oz (3.09%;#12)	1887-1901, 1908-1928 intermit. 1938-1946 drilling 1961
Au-46	Kemptville	21A/4	44°03'20"	65°50'45"	Yarmouth	Goldenville Fm.	IV & irregular CV; richest at intersections	13,134 oz (.28%;#31)	1885-1919, 1927, 1935-1938
Au-47	Hilton	21A/4	44°01'20"	65°55'	Yarmouth	Goldenville Fm.	en échelon CV lenses oxidized appearance	gataspepy, cpy>sph	Ag & Au values reported prospecting till 1955
Au-48	Carleton	21A/4	44°00'20"	65°56'10"	Yarmouth	Goldenville Fm.	3 ll CV's in fault block	190 oz (.02%;#42)	1886-1911, 1914-15 intermit.
Au-49	Cranberry Head (Creampot)	20O/16	43°54'	66°10'10"	Yarmouth	Halifax Fm.	IV(?) boudinage	119 oz (.01%;#43)	1863-1875, prosp. until 1931
Au-50	Captain McPhee Brook	11E/4	45°05'20"	63°40'40"	Hants	Halifax Fm.	no data	occurrence	
Au-51	Renfrew	11E/4	45°00'03"	63°38'	Hants	Goldenville Fm.	IV's on flat dome	51,820 oz (4.59%;#7)	1862-1872, 1901-1905, 1911-1913, 1927-1932, 1954-1958 testing

Au-52	McLean Brook	11E/4	45°06'25"	63°45'	Hants	Halifax Fm.	no data	occurrence	
Au-53	East Rawdon	11E/4	45°03'	63°46'	Hants	Goldenville Fm.	IV's on north flank of anticline	13,495 oz (1.19%'#21)	1884-1887,1890-91, 1908,1931, 1942 (2 DDH's)
Au-54	Central Rawdon	11E/4	45°03'	63°50'45"	Hants	Halifax Fm.	3 CV's on anticline flank	6,745 oz (0.60%;#27)	1868-1897, 1904, 1923
Au-55	MacKay Settlement (Upper Newport)	11E/4	45°01'	63°56'	Hants	Halifax Fm.	IV's at anticline crest	14 oz (#50) some alluvial	production; 1868-1910 prospect
Au-56	Ardoise	11D/13	44°57'30"	63°55'	Hants	Halifax Fm.	narrow IV's, one CV on so. limb of syncline	7 oz (#53)	1868-1904; intermittant prospecting
Au-57	Mount Uniacke	11D/13	44°56'	63°48'	Hants	Goldenville Fm.	IV's at axis and on so. limb of anticline dome	27,740 oz (2.46%;#14)	1865-1870,1877-1885,1888-1908, sporadic until 1941
Au-58	Ralston Corner	11E/4	45°06'15"	63°38'	Hants	Halifax Fm.	no data	occurrence	
Au-59	Ervin Brook placer	11E/3	45°06'30"	63°14'	Colchester	Halifax Fm.	stream occurrence		
Au-60	South Branch Stewiacke	11E/3	45°07'20"	63°07'	Colchester	Halifax Fm.	IV's and small CV's	44 oz (#47)	1884,1906-1907
Au-61	Gay's River	11E/3	45°04'40"	63°18'30"	Colchester	Horton Group conglomerate over Halifax Fm.	Au highest at cong. base and in Hfx. Fm. paleosurface cracks	2,130 oz	1869-1880 intermit.; 1891-1901; last prospecting 1949
Au-62	Greenvale	11E/9	45°30'	62°29'	Pictou	E-O slates & qtzites.	qtz. vein	occurrence	1875
Au-63	North Ogden	11F/5	45°22'	61°41'	Guysborough	Horton-like quartzite in C terraine	quartzite bed about 30 m wide w/calcite and pyrite	occurrence	1943-44
Au-64	Salmon River Lake	11F/5	45°21'40"	61°43'	Guysborough	C conglomerate	dissem. in basal C cong.	bulk samples around 1948	
Au-65	Gunn Brook	11F/5	45°18'20"	61°51'	Guysborough	C conglomerate	dissem. in basal C cong.	occurrence	one non-bulk assay ~1947
Au-66	Country Harbour	11F/5	45°15'30"	61°49'	Guysborough	Goldenville Fm. cut by granitic dykes	IV's at anticline dome; x-cutting dykes do not effect gold values	9,960 oz (0.88%;#24)	1868-1873,1889-1902,1909-1911, prospecting until 1951 with DDH's
Au-67	Round Lake	11F/6	45°20'	61°13'	Guysborough	Goldenville Fm.	no data	occurrence	
Au-68	Lower Seal Harbour	11F/4	45°10'45"	61°36'50"	Guysborough	Goldenville Fm.	short IV's overlapping in a belt-considerable Au reported from country rock	34,235 oz (3.04%;#13)	1904-1915, 1934, 1936-1941
Au-69	Upper Seal Harbour	11F/4	45°12'30"	61°38'	Guysborough	Goldenville Fm.	IV's at anticline crest	57,830 oz (5.12%;#6)	1892-1912, 1926-1927
Au-70	Isaac's Harbour	11F/4	45°10'	61°34'20"	Guysborough	Goldenville Fm.	IV's on 3 small anticlines	39,552 oz (3.51%;#11) some alluvial production	1861-1916, 1938-1941

Au-71	Wine Harbour	11F/4	45°04'30"	61°51'	Guysborough	Goldenville Fm.	IV's on so. limb of anticline over 1 x 2.4 km area	42,726 oz (3.78%;#9) some alluvial production	1862-1882,1888-1889, 1891, 1896-1907
Au-72	Cochrane Hill (includes Crow's Nest Mines)	11E/17 (11E/1)	45°15'	62°03'	Guysborough	Goldenville Fm. w/granite dykes	IV's on so. limb of anticline within contact met. aureole of a (?D) granite	1,192 oz (0.10%;#34) scheelite reported	1868-1870; sporadic since DDH in 1934-35 & 1974-75
Au-73	Goldenville (Sherbrooke)	11E/1	45°07'30"	62°01'	Guysborough	Goldenville Fm.	IV's at anticline dome slate also Au-bearing	210,153 oz (18.60%;#1) scheelite reported	1861-1910,1912-1931,1934-1942
Au-74	Liscomb Mills	11E/1	45°01'	62°06'	Guysborough	Goldenville Fm.	IV on anticline flank	no data; prospect	
Au-75	Miller Lake	11E/1	45°02'30"	62°08'15"	Guysborough	Goldenville Fm.	IV's on anticline crest around a dome	539 oz (0.05%;#40)	1900-1905,1937-1941,1948-1950
Au-76	Little Liscomb Lake	11E/1	45°14'40"	62°27'	Guysborough	Goldenville Fm.	IV's on anticline limb	52 oz (#46)	prospect until 1941
Au-77	Cameron Dam (seventeen Mile Str.)	11E/2	45°12'	62°32'	Guysborough	Goldenville Fm.	IV's on anticline	prospect	
Au-78	Pcokwock Lake	11D/13	44°45'	63°51'	Halifax	Goldenville Fm.	no data	occurrence	
Au-79	Mushamush Lake	21A/9	44°30'	64°30'	Lunenburg	Halifax Fm.	no data	occurrence	
Au-80	Forest Hill	11E/5	45°18'	61°46'	Guysborough	Goldenville Fm. w/granite dikes	IV's on so. limb of anticline within contact met. aureole of (D?) granite	25,102 oz (2.22%;#17)	1894-1900,1937-1939,1947-1957
Au-81	Crow's Nest	see number Au-72 - Cochrane Hill							
Au-82	Goldboro	11F/5	45°11'	61°39'	Guysborough	Goldenville Fm.	no data	no data	reported as a district in Newhouse (1932)
Au-83	West Gore	11E/4	45°05'	63°47'30"	Hants	Halifax Fm.	vertical cross veins with Au-asp-py-cpy-sph-ga-po-cbt-stib-val-Sb-kermesite assemb.	primarily an Sb mine w/Au and Ag production	
Au-84	Middlefield	21A/2	44°02'	64°52'	Queen's	Halifax Fm.	no data	could be same as Fifteen Mile Brook (Au-43)	
Au-85	Tusket River (Dominique)	20O/16	43°50'	66°03'	Yarmouth	Goldenville Fm.	veins - no data	prospect	ga-rich drift
Au-86	Williamsdale (Farmington)	11E/12W	45°36'	63°54'	Cumberland	S & D sediments	asp-Au-py-obt in qtz. veins	prospect	~1909, assays 1923, 1931
Au-87	Pubnico	20O/12	43°43'	65°48'	Yarmouth	Halifax Fm.	no data	occurrence	
Au-88	Joggin Bridge-Digby	21A/5, 12	44°36'	65°46'	Digby	Goldenville Fm.	IV's	occurrence	
Au-89	Indian Path	21A/8W	44°20'	64°25'	Lunenburg	Halifax Fm.	IV's w/scheelite	50 oz - by-product of tungsten production	

Au-90	Harrigan Cove	11D/16W	44°56'	62°18'	Halifax	Goldenville Fm.	IV's at anticline dome	7,944 oz (0.70%;#25)	1872, 1899-1907 DDH 1936
Au-91	Blockhouse	21A/8W	44°23'	64°18'	Lunenburg	Goldenville Fm.	CV - ore shoot ll strata - minor IV's in anticline dome	3,588 oz (0.32%;#29)	1896,1898-1902, 1936-1938
Au-92	Barachois River	11K/7	46°22'20"	60°36'20"	Victoria	granite	vein w/qtz, cbt, py, cpy,Au	prospect - low assays	1910,1933-1940
Au-92a	Mouth Barachois River	11K/7	46°21'	60°32'	Victoria	granite	vein w/qtz, cbt, cpy, py, bn, cc, Au	prospect -	
Au-93	Middle River (Gold Brook, Wagamatcook)	11K/2	46°14'30"	60°54'	Victoria	George River Series interbedded metaseds.(argill.) & volcs.	IV's w/asp-py-Au & minor cpy, po, etc - assays show Ag and a trace of Ni	1,440 oz - some alluvial production	1907-1911,1914-1916, 1955 has been drilled for base metals
Au-94	Barachois Harbour	11K/1	46°09'	60°25'	Cape Breton	(D?) granite	vein w/Au & Ag values	prospect	
Au-95	Northeast Margaree River	11K/7	46°27'	60°55'30"	Inverness	stream sands	Tertiary-Recent placer	no data	over C rocks
Au-96	Whycocomagh	11F/14	46°59'	60°06'30"	Inverness	stream gravels	placer	no data	over George River rocks
Au-97	Clyburn Brook	11K/9	46°39'30"	60°27'45"	Victoria	gneiss	interbanded qtz-py and gneiss - assoc. lamprophyre dike	prospect	1910-1915
Au-98	Tarbot	11K/7	46°20'30"	60°34'10"	Victoria	hornblende granite	2 veins w/cpy, py, malach.	prospect w/ Au values	
Au-99	Stirling (Mindamar)				Richmond	seds. & rocks	interbedded massive sulphide deposit	16,718 oz as byproduct of major Zn-Pb Cu production	see other files
Au-100	Chegogin	200/16	43°52'	66°10'10"	Yarmouth	Goldenville Fm.	"very large qtz. masses" (IV's)		1890
Au-101	Chezzetcook				Halifax	Goldenville Fm.	IV's on so. limb of anticline	no data - prospect (>10 oz)	
Au-102	Gegoggin				Guysborough	Goldenville Fm.	IV's at anticline dome	prospect	1914